Functional characterization of the immune receptor RLP32 and its ligand IF1

Dissertation

der Mathematisch-Naturwissenschaftlichen Fakultät
der Eberhard Karls Universität Tübingen
zur Erlangung des Grades eines
Doktors der Naturwissenschaften
(Dr. rer. nat.)

vorgelegt von
Katja Fröhlich
aus Burg bei Magdeburg

Tübingen
2020

Gedruckt mit Genehmigung der Mathematisch-Naturwissenschaftlichen Fakultät der Eberhard Karls Universität Tübingen.

Tag der mündlichen Qualifikation:	20.08.2020
Dekan:	Prof. Dr. Wolfgang Rosenstiel
1. Berichterstatter:	Prof. Dr. Thorsten Nürnberger
2. Berichterstatter:	Prof. Dr. Georg Felix

Table of Contents

List of Tables

List of Figures

1 Introduction

1.1 Crop plants and impact of infectious diseases

A growing world population in combination with a changing climate puts increasing pressure on agriculture to produce sufficient crop yields. The nutrition of the world's population is already a very complex problem, and it is going to get exceedingly harder in the future. By 2050 the world's population is predicted to reach 9.3-10.6 billion people, who will require 3.6 billion tons of food each year (Dunwell, 2013). The majority of the population growth is predicted to happen in developing countries in Sub-Saharan Africa and South Asia, notably India, where access to a balanced diet is already a challenge (OECD *et al.*, 2019). Population growth and climate change will put major constraints on agriculture, as access to water and arable will decrease (Dunwell, 2013).

Plants constantly interact with surrounding organisms, like insects, nematodes, bacteria, fungi, oomycetes. Microorganisms can positively influence plant growth, general plant performance, germination and plant health (Bloemberg and Lugtenberg, 2001; Weller *et al.*, 2002; Raaijmakers *et al.*, 2009). However, a few microbes, namely pathogenic fungi, oomycetes and bacteria cause diseases presenting enormous challenges for food security. Every year 11–30% of crop harvest is lost to diseases and pests (Oerke and Dehne, 2004; Savary *et al.*, 2019).

Extreme weather changes and a rising temperature favour proliferation of pathogenic microbes and pests putting increasing abiotic and biotic stresses on crop plants. Continuous development of cultural controls, agrochemical use, plant breeding and agricultural practices reduce theses losses. Plants recognize and respond and limit the growth of invading pathogens. However, pathogenic microbes and insects can adapt to pesticides and overcome resistance in plants. The selective pressure on both ends leads to the establishment and maintenance of the long-standing host-pathogen co-evolutionary arms race (Jackson, 2009).

1.2 Layers of plant immunity

The first layer of defense is a physical and chemical barrier to prevent pathogens from entering the plant. The physical barrier is composed of the cuticle, mainly composed of cutin and wax; and the cell wall, which is composed of cellulose microfibrils, pectin, hemicelluloses, proteins, and, in certain cases, lignin (Vorwerk *et al.*, 2004; Malinovsky *et al.*, 2014; Miedes *et al.*, 2014; Serrano *et al.*, 2014). As chemical barriers a multitude of toxic metabolites like alkaloids, phenolics and terpenes as well as anti-microbial enzymes provide a layer of constitutive defense (Morrissey and Osbourn, 1999; Nürnberger *et al.*, 2004; Freeman and Beattie, 2008). Some pathogens can break those barriers by mechanical forces and production of enzymes, or they can enter the plant via pre-existing openings like stomata or wounds (Melotto *et al.*, 2008).

In addition to constitutive defenses, plants have evolved mechanisms to detect and respond to pathogenic challenges. Unlike animals, plants have not evolved an immune system that relies on circulating cells to defend themselves against microbes (Iwasaki and Medzhitov, 2015). Instead, the plant relies solely on an innate immune system, in which each individual cell has the ability to detect molecular patterns as endogenous self- and exogenous non-self danger signals in their direct environment by a multilayered interface of pattern recognition receptors (PRRs), which in turn activate an immune response (Smakowska *et al.*, 2016; Teixeira *et al.*, 2019). While plants and animal share the ability to recognize molecular patterns of pathogens via PRRs (Medzhitov and Janeway, 1997), the specific perception systems seem to rather be a case of convergent evolution (Ausubel, 2005; Zipfel and Felix, 2005).

1.2.1 Models of plant immunity - from zig-zag model to invasion model and danger model

1.2.1.1 The zig-zag model and its limitations

Several models have been proposed to describe the basic concepts of plant immunity. The most prominent of these, the zig-zag model (Jones and Dangl, 2006), describes two distinct staggered phases of plant innate immunity. A first layer of PRRs is located in the plasma membrane and perceives the presence of extracellular molecules, which are often conserved across whole classes of microbes (e.g. fungal chitin or bacterial flagellin), and are thus known as pathogen or microbe-associated molecular patterns (PAMPs or MAMPs) (Medzhitov and Janeway, 1997; Nürnberger and Brunner, 2002; Nürnberger *et*

al., 2004; Zipfel and Felix, 2005; Boller and Felix, 2009), later additional extracellular molecules derived from other organisms have been discovered, namely nematodes (nematode associated molecular patterns (NAMPs) (Manosalva *et al.*, 2015), herbivores (herbivore associated molecular patterns (HAMPs) (Mithöfer and Boland, 2008)), and parasitic plants (parasitic plant associated molecular patterns (ParAMPs) (Kaiser *et al.*, 2015; Hegenauer *et al.*, 2016).

In addition to exogenous danger signals, endogenous molecules of the plant itself can be recognized by PRRs. These so-called damage associated molecular patterns (DAMPs) (Rubartelli and Lotze, 2007) are passively released into the apoplast through damage of the host cells caused by microbial hydrolases or toxins or upon injury. Recognition of these patterns induces an immune response known as pattern or PAMP/MAMP-triggered immunity (PTI or MTI). PTI is sufficient to slow down or stop the proliferation of most microbes.

Pathogenic bacteria can adapt to the host by injecting effector molecules via their Type III secretion system into the host (Bent and Mackey, 2007; Boller and Felix, 2009). Some of these effectors suppress PTI leading to effector-triggered susceptibility (ETS). Similarly, fungi and oomycetes produce specialized structures, called haustoria to establish a very close connection with the host to exchange molecules, but haustoria never penetrate the plant cell membrane.

In turn, plants deploy a second level of receptors to counteract adapted pathogens via resistance (R) proteins. R proteins can either directly recognize the effectors, or indirectly guard the host virulence target (VT) of the effector. The cytoplasmatic R proteins belong to the family of nucleotide-binding leucine-rich repeat (NLR) proteins and function as intracellular receptors that recognize the presence of specific effector proteins. Direct or indirect perception of pathogen effectors by a correspondingly specific host NLR protein activates the effector-triggered immunity (ETI) (Jones and Dangl, 2006; van der Hoorn and Kamoun, 2008; Dodds and Rathjen, 2010; Cesari *et al.*, 2014). Contrary to PAMPs, effectors are typically variable and dispensable. In comparison with PTI, ETI is qualitatively stronger, more rapid, more robust and often result in a hypersensitive response (HR) and systemic defense signaling (systemic acquired resistance (SAR)) in the host (Tao *et al.*, 2003; Jones and Dangl, 2006; Tsuda and Katagiri, 2010; Wang *et al.*, 2013). The continuing evolutionary arms race between host and pathogen drives pathogens to shed or diversify the recognized effector gene or acquire additional effectors that suppress ETI.

In turn, the plant hosts develop new receptors recognizing the new effectors (Jones and Dangl, 2006).

The clear dichotomy between extracellular MAMPS and intracellular effectors and, in conclusion, the distinction between PTI and ETI, is however increasingly blurred as the number of “exceptions to the rule” increases over time (Thomma *et al.*, 2011). The detection of effectors is not limited to the intracellular space as for example the tomato receptor like proteins, *Cf*-2, *Cf*-4, *Cf*-5 and *Cf*-9 respond specifically to extracellular effectors produced by *Cladosporium fulvum* (Rivas and Thomas, 2005). Likewise, bacterial harpins are classified as effectors, even though they are perceived extracellularly leading to a typical ETI response. They are also widely conserved between bacterial clades (Tampakaki and Panopoulos, 2000; Chang and Nick, 2012; Choi *et al.*, 2013).

To address the limitations and inconsistences of the ETI/PTI model new models propose that the plant immune system is a general means to cope with invasion or danger (Boller and Felix, 2009; Thomma *et al.*, 2011; Gust *et al.*, 2017). Replacing the discrimination between PAMPS and effectors, different terms have been suggested to confer a more holistic view on the immune system of the plant.

1.2.1.2 The invasion model

In the invasion, model microbial invasion is recognized via invasion patterns (IPs) that include all microbe-derived or plant-derived molecules (Cook *et al.*, 2015; Kanyuka and Rudd, 2019). IPs therefore include MAMPs, effectors (both apoplastic and cytosolic) and DAMPs, as well as any other microbe-derived or plant-derived evolutionary conserved or variable molecules that signal the pathogen invasion and trigger an immune response (Kanyuka and Rudd, 2019). In this model, IPs are sensed by IP receptors (IPRs). In the most recent model, IPRs are divided either in cell surface immune receptors (CSIRs) synonymous to PRRs that include receptor like kinases (RLK) and receptor like proteins (RLPs) or intracellular immune receptors (IIRs), mainly synonymous to NLRs (Kanyuka and Rudd, 2019).

1.2.1.3 The danger model

The danger model, according to Gust *et al.* 2017 emphasizes eukaryotic immunity concepts that are shared in plants and metazoans. The danger model proposes the term danger signals (Chen and Nuñez, 2010), which can be categorized in exogenous danger signals and endogenous danger signals. Exogenous danger signals include all PAMPs,

HAMPs, NAMPs, ParAMPs and effectors. Endogenous danger signals are subdivided into I) primary endogenous danger signals, which include DAMPs directly caused by mechanical damage and are released passively into the apoplast (cellobiose, eATP (Choi *et al.*, 2014; de Azevedo Souza *et al.*, 2017)), and II) secondary endogenous danger signals (also phytocytokines), which are actively proteolytically processed and released by the host upon tissue damage, e.g. systemin which is proteolytically processed and released by the plant upon herbivore attack or wounding (Pearce *et al.*, 1991; McGurl *et al.*, 1992) or rapid alkalization factors *At*RALF17 (Stegmann *et al.*, 2017).

The term phytocytokines is derived from metazoan cytokines, which are a large group of peptides that are produced by immune cells in response to PAMPs or primary endogenous danger signals (Gust *et al.*, 2017). They are proteolytically processed and secreted actively by immune cells and recognized by specific receptors. There are proinflammatory and anti-inflammatory cytokines regulating the immune response (Banchereau *et al.*, 2012).

The danger model proposes that the immune system responds to PAMPs in the context of additional signals derived from common patterns of pathogenesis that only occur upon infection (Gust *et al.*, 2017). This could be an explanation how the plant differentiates between friend and foe, as many microbes live in a symbiotic relationship with the plant despite having a large number MAMPs/PAMPs. (He *et al.*, 2007; Boller and Felix, 2009).

We still need to build an in depth understanding how plants interact with the organisms in their environment. The strategies that evolved in different plant species, resulting in resistance and adaptation to the environment can be integrated into crop plants using modern breeding techniques (Wan *et al.*, 2019).

1.2.2 Pattern recognition in the apoplast

In animals, PAMPs are recognized as non-self signals by evolutionarily conserved PRRs (Girardin *et al.*, 2002; Medzhitov and Janeway, 2002). Toll-like receptors (TLRs) have been identified in *Drosophila* and mammals to detect extracellular microbes and trigger immune cascades (Aderem and Ulevitch, 2000; Medzhitov and Janeway, 2002; Cook *et al.*, 2004). TLRs are members of the type 1 membrane receptors family, which is characterized by an extracellular leucine-rich repeat (LRR) domain, that recognizes a PAMP; and an intracellular Toll-IL-(interleukin)-1 receptor (TIR) domain, that transduces

the signal into the cell (Underhill and Ozinsky, 2002; Bell *et al.*, 2003; Cook *et al.*, 2004; O'Neill and Bowie, 2007).

In plants, two types of PRRs exist in the plasma membrane: receptor like kinases (RLK) and receptor like proteins (RLP) (Couto and Zipfel, 2016; Boutrot and Zipfel, 2017), which are functionally like TLRs (Mogensen, 2009). RLKs consist of a highly variable ectodomain that detects a ligand, a single transmembrane region (TM), and an intracellular kinase domain required for response activation. RLPs share RLK's conformation but lack an intracellular signalling domain; thus, RLPs form complexes together with co-receptors to mediate signal transduction (Liebrand *et al.*, 2013; Gust and Felix, 2014). A variety of ectodomains with different properties enables the detection of PAMPs deriving from several macromolecules. The various downstream outputs play a central role in plant growth, development, immunity, and stress adaptation (Shiu and Bleecker, 2003; Belkhadir *et al.*, 2014).

In the *Arabidopsis* genome 600 RLKs and RLPs have been identified. 200 RLKs and RLPs have an LRR ectodomain (Shiu and Bleecker, 2003). Ectodomains containing leucine-rich-repeat (LRR) motifs recognize mainly proteinaceous components (Boutrot and Zipfel, 2017). The best characterized LRR-RLK FLAGELLIN-SENSING 2 (FLS2), is the receptor of flg22, a 22 amino acid peptide of the bacterial flagellin (Felix *et al.*, 1999; Gómez-Gómez *et al.*, 1999; Gómez-Gómez and Boller, 2000). Plant enzymes like the galactosidase *At*BGAL1 deglycosylates flagellin, making it susceptible to proteolytic degradation exposing the immunogenic epitope flg22 (Buscaill *et al.*, 2019). Another example for a LRR-RLK, the ELONGATION FACTOR (EF)-Tu RECEPTOR (EFR) recognizes a N-acetylated 18 aa peptide (elf18) of bacterial elongation factor Tu (EF-Tu) (Kunze *et al.*, 2004; Zipfel *et al.*, 2006). Endogenous peptides like *At*Pep1-8 peptides are perceived by the LRR RLK AtPEP RECEPTOR (*At*PEPR1 and 2) (Yamaguchi *et al.*, 2006; Krol *et al.*, 2010; Yamaguchi *et al.*, 2010). Some receptors like FLS2 are conserved across land plant families (Albert *et al.*, 2010), while others are only found in some members of the same family. In rice (*Oryza sativa*), LRR-RLK XA21 recognizes RaxX, a highly conserved protein in many Xanthomonas species, to trigger immune responses. RaxX21-sY, a sulfated, 21-amino acid synthetic peptide derived from RaxX, is sufficient for XA21 activation (Pruitt *et al.*, 2015).

Ectodomains with lysin motifs (LysM) interact with N-acetylglucosamine (GlcNAc)-containing glycans. In Arabidopsis, fungal chitin is recognized by complex of LysM-RLKs

comprising LysM CONTAINING RECEPTOR-LIKE KINASE 4 and 5 (*At*LYK4, *At*LYK5), and CHITIN ELICITOR RECEPTOR KINASE1 (*At*CERK1) (Miya *et al.*, 2007; Cao *et al.*, 2014; Schlöffel *et al.*, 2019; Xue *et al.*, 2019). The chitin fragments are liberated by the actions of exochitinases, which reside within the apoplastic space and actively generate the signal to initiate the plant defense program (Mott *et al.*, 2014). Another polysaccharide, bacterial peptidoglycan (PGN) is perceived by a receptor complex of *At*LYM1 and *At*LYM3 with *At*CERK1 (Willmann *et al.*, 2011; Boutrot and Zipfel, 2017; Schlöffel *et al.*, 2019).

Several non-proteinaceous elicitors are detected by lectin-type RLKs (Albert *et al.*, 2020). The lectin-type RLK DOES NOT RESPOND TO NUCLEOTIDES 1 (DORN1) binds extracellular ATP (Choi *et al.*, 2014). The lectin S-domain RLK LIPOOLIGOSACCHARIDE-SPECIFIC REDUCED ELICITATION (LORE) recognizes a bacterial medium-chain 3-hydroxy fatty acid metabolite (Kutschera *et al.*, 2019). The malectin-like-domain RLK FERONIA (*At*FER) detects RALFs which act as phytocytokines influencing plant stress response and plant development (Stegmann *et al.*, 2017). *At*FER constitutively associates with the co-receptor GPI-anchored *At*LLG1, both directly interact with *At*RALF23 (Xiao *et al.*, 2019).

PRRs with epidermal growth factor (EGF)-like ectodomains, for example WALL-ASSOCIATED KINASE 1 (*At*WAK1), recognize plant cell-wall derived oligogalacturonides (OGs) (Brutus *et al.*, 2010).

RLPs also have a role in plant immunity and plant development. LRR-RLPs display genus- or subgenus-specific distribution. Among the 57 LRR-RLPs encoded by the Arabidopsis genome (Wang *et al.*, 2008), LRR-RLPs *At*RLP1/ReMAX has been described to bind an enigmatic PAMP from *Xanthomonas* spp. (eMAX) (Jehle *et al.*, 2013); *At*RLP23 recognizes Nep1-like proteins (NLPs) from various bacteria, oomycetes, and fungi (Ottmann *et al.*, 2009; Albert *et al.*, 2015; Lenarčič *et al.*, 2017), *At*RLP30 recognizes the enigmatic *Sclerotinia sclerotiorum* filtrate elicitor 1 (SCFE1) (Zhang *et al.*, 2013) and *At*RLP42/RBPG1 recognizes fungal polygalacturonases (Zhang *et al.*, 2014).

Additional LRR-RLP/PAMP pairs have been identified in various plant species. In *Solanum lycopersicum*, CUSCUTA RECEPTOR 1 (*Sl*CuRe1) detects a proteinaceous pattern from *Cuscuta reflexa* and represents the first receptor implicated in defense against parasitic plants (Hegenauer *et al.*, 2016). *Sl*Cf4/9 recognize the *Cladosporium fulvum* effectors Avr4/Avr9. *Sl*Ve1 recognizes the effector Ave1 from *Verticillium dahliae* (Kawchuk *et al.*, 2001; de Jonge *et al.*, 2012; Postma *et al.*, 2016). Ethylene-inducing xylanase (Teixeira *et*

al., 2019) is recognized in tomato via the LRR-RLPs ETHYLENE INDUCING XYLANASE 2 (Eix2 and Eix1) (Ron and Avni, 2004). In *Solanum microdontum*, ELICITIN RESPONSE protein (*Sm*ELR) recognizes *Phytophthora*-derived elicitin INF1 (Du *et al.*, 2015; Domazakis *et al.*, 2018). In *Solanum lycopersicum*, the RLK SYSTEMIN RECEPTOR 1 (*Sl*SYR1) recognizes the peptide hormone systemin, an 18-amino acid peptide derived from a larger precursor protein (McGurl *et al.*, 1992; Wang *et al.*, 2018). The RLK COLD SHOCK PROTEIN RECEPTOR (*Sl*CORE) recognizes a 22 aa PAMP from bacterial cold shock protein, csp22 (Wang *et al.*, 2016), in *Nicotiana benthamiana* csp22 recognized by the LRR-RLP RECEPTOR-LIKE PROTEIN REQUIRED FOR CSP22 RESPONSIVENESS *Nb*CSPR (Saur *et al.*, 2016).

Different epitopes derived from the same molecule can be detected in by receptors that evolved independently in different organisms. TLR5 from mammals and FLS2 in plants are functional homologues, however they do not share similar amino acid sequence and recognize conserved epitopes of flagellin which are structurally distinct from each other (Felix *et al.*, 1999; Smith *et al.*, 2003). FLS2 in plants and TLR5 in animals, they have evolved convergently (Smith *et al.*, 2003). Tomato perceives yet another epitope of flagellin (flgII-28) with the LRR-RLK FLS3 (Hind *et al.*, 2016).

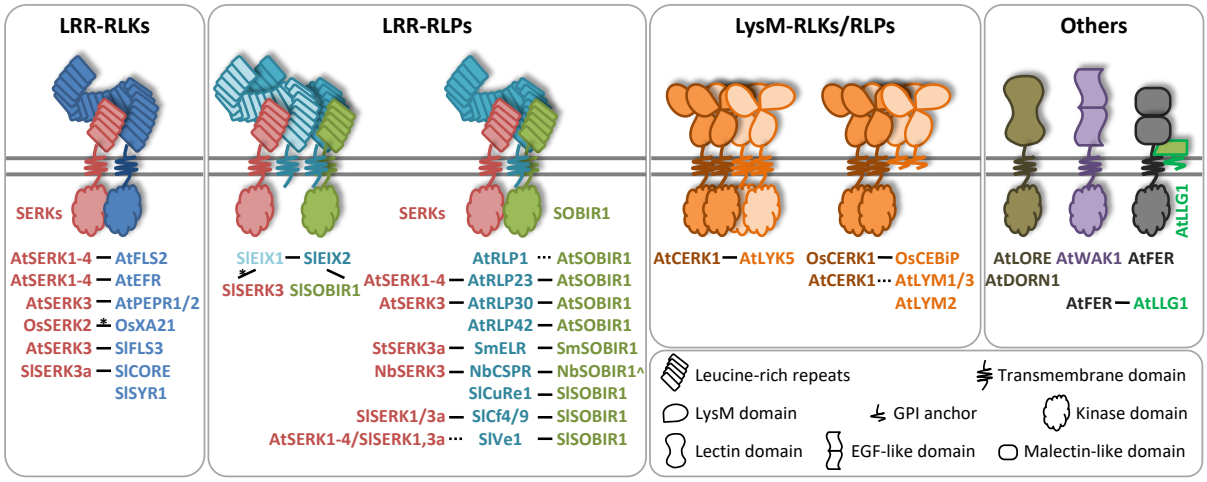

Figure 1: Plant plasma membrane immune receptors and co-receptors.
Only those ligand-perception receptors are shown for which the molecular nature of the ligand is known (see text). LRR-RLK and LRR-RLP-type immune receptors recognize proteinaceous patterns. LRR-RLK-type immune receptors often form heterodimeric complexes with one or several members of the LRR-RLK SERK family in a ligand-dependent manner. LRR-RLP-type immune receptors usually form complexes with LRR-RK SOBIR1 in a ligand-independent manner and with SERKs in a ligand-dependent manner. LysM-domain immune receptors recognize GlcNAc-containing ligands. LysM-type immune receptors, either LysM-RLK or LysM-RLPs are ligand-binding proteins that form heteromeric complexes with LysM-RLK-type receptors for signaling. The malectin-like domain RLK AtFER constitutively associates with the co-receptor GPI-anchored AtLLG1. Solid black lines indicate demonstrated association of receptors with SERKs, SOBIR1 or CERK1. Solid lines with an asterisk indicate constitutive association with SERKs in the absence of ligand. Dashed lines indicate demonstrated genetic relation without evidence of biochemical interaction. (Wan *et al.*, 2019)

1.2.3 Apoplastic PRRs form complexes with co-receptors for downstream signaling

1.2.3.1 SOBIR1

As RLPs lack a cytoplasmatic kinase domain, they rely on co-receptors for signal transduction. The LRR-RLK SUPPRESSOR OF BIR1 (BAK1-INTERACTING RECEPTOR-LIKE KINASE 1) SOBIR1/EVR (EVERSHED) was identified as an adaptor kinase for plant LRR-RLPs first in *Solanum lycopersicum* (Gao *et al.*, 2009; Leslie *et al.*, 2010) and later in *Arabidopsis thaliana* (Zhang *et al.*, 2013; Bi *et al.*, 2014; Zhang *et al.*, 2014), *Nicotiana benthamiana* (Liebrand *et al.*, 2013) and *Solanum microdontum* (Gust and Felix, 2014; Liebrand *et al.*, 2014; Du *et al.*, 2015). The interaction between RLPs and SOBIR1 is ligand independent. Both RLK and RLP receptor complexes mediate plant resistance to microbial infections (Zipfel *et al.*, 2004; Albert *et al.*, 2015). It was suggested that these proteins would function in a virtually identical manner and that LRR-RLP/SOBIR1 complexes constitute 'bimolecular receptor kinase' (Gust and Felix, 2014),

but recent studies revealed there are significant differences in the response patterns and composition of signaling cascades mediated by either LRR-RLP- or LRR-RLK (Wan *et al.*, 2019).

All SOBIR1 homologs have five predicted LRRs, a single TM domain and a cytoplasmic kinase domain (Gao *et al.*, 2009; Leslie *et al.*, 2010; Liebrand *et al.*, 2013). The single transmembrane spanning domains of LRR-RLPs as well as SOBIR1 commonly have one or several GxxxG motifs in a series for transmembrane helix–helix interactions (Gust and Felix, 2014; Albert *et al.*, 2019). SOBIR1 and RLPs exhibit complementary characteristics that could allow physical interaction via their LRR domains including opposite charges in their apoplastic juxtamembrane domains and helix–helix interaction of their transmembrane domains (Gust and Felix, 2014; Albert *et al.*, 2019). The intracellular kinase domain of the various SOBIR1 homologues is highly conserved. SOBIR1 is functionally required for all RLPs mediating immunity, additionally SOBIR1 interacts with the RLP CLAVATA2 (CLV2) involved in development (Jehle *et al.*, 2013; Liebrand *et al.*, 2013; Zhang *et al.*, 2013; Böhm *et al.*, 2014; Zhang *et al.*, 2014; Albert *et al.*, 2015; Hegenauer *et al.*, 2016).

1.2.3.2 BAK1

Upon recognition of their cognate ligands, many RLKs and RLP/SOBIR1 heterodimers recruit the LRR-RLK somatic embryogenesis receptor 3/BRI1-associated kinase 1 (SERK3/BAK1) into a heteromeric complex (Li *et al.*, 2002; Nam and Li, 2002; Chinchilla *et al.*, 2009; Albert *et al.*, 2015). BAK1 consists of a small extracellular LRR domain with repeats followed by a serine and proline rich region (SPP motif), a transmembrane domain and a cytoplasmic kinase domain. In total, there are 5 members of the SERK protein family in Arabidopsis; the other four are close homologs of BAK1 (Chinchilla *et al.*, 2009). The RLK brassinosteroid (BR) receptor BRASSINOSTEROID INSENSITIVE 1 (BRI1) was the first receptor described to form a complex with BAK1 (Li *et al.*, 2002; Nam and Li, 2002; Santiago *et al.*, 2013). BRI1 exists as homodimers at the plasma membrane. Binding of BRs results in hetero-oligomerization with BAK1, transphosphorylation, and activation of BR-signaling (Wang *et al.*, 2005). The ligand induced BRI1/BAK1 complex undergoes sequential mutual transphosphorylation of both partners (Wang *et al.*, 2008; Oh *et al.*, 2009; Oh *et al.*, 2010). BRI1 also interacts with other SERK protein family members including SERK1 and SERK4/BKK1 (BAK1-like kinase 1) (Kinoshita *et al.*, 2005). Thus, SERKs appear to function as a shared signaling node that connects complex signaling

networks via association with various RLKs and RLPs and modulates distinct cellular responses in plant immunity (Chinchilla *et al.*, 2009; Li, 2010; Liebrand *et al.*, 2014). Additionally, BAK1 functions in light signaling and the regulation of cell death (Whippo and Hangarter, 2005; Kemmerling *et al.*, 2007). Upon binding of flg22, BAK1 is recruited to FLS2 (Chinchilla *et al.*, 2007; Heese *et al.*, 2007). The C-terminus of the flg22 fragment is bound by both FLS2 and BAK1, thereby facilitating complex formation and induction of downstream signaling (Chinchilla *et al.*, 2006; Sun *et al.*, 2013). Cells transfected with FLS2 plus BAK1 were ~300 times more sensitive than cells transfected with FLS2 alone and showed half-maximal response (EC_{50}) at a concentration of ~1 nM flg22 (Albert *et al.*, 2013).

RLPs also interact with BAK1, but also with other SERKs and in a ligand dependent manner. This has been shown for RLP23 (Albert *et al.*, 2015); ELR (Domazakis *et al.*, 2018); *Cf*-4 (Postma *et al.*, 2016), and RLP30 (Zhang *et al.*, 2013). While BAK1 is recruited to RLKs and RLPs upon ligand recognition, recent studies showed that are significant differences in the signaling between both receptor types (Wan *et al.*, 2019).

1.2.3.3 BIR2/3- negative regulators

Two BAK1-interacting LRR-RLKs, BIR2 and BIR3 are unidirectionally phosphorylated by BAK1. The constitutive interaction between BAK1 and BIR2/3 is kinase-activity dependent and prevents interaction with the ligand-binding LRR-RLK FLS2. BIR2 and BIR3 act as a negative regulators of PAMP-triggered immunity by limiting BAK1-receptor complex formation in the absence of ligands (Halter *et al.*, 2014). PAMP perception leads to BIR2/3 release from the BAK1 complex and enables the recruitment of BAK1 into the FLS2 complex (Halter *et al.*, 2014; Imkampe *et al.*, 2017). BIR2 affects flg22- and elf18-induced signaling, as well as cell death control, but not BR signaling (Halter *et al.*, 2014). BIR2 and BIR3 have partially redundant functions, but BIR3 is not involved in cell death regulation (Imkampe *et al.*, 2017). BIR3 not only interacts with BAK1 but also shows direct interaction with the ligand-binding receptor BRI1 (Imkampe *et al.*, 2017). BIR3 stabilizes BAK1 and other SERK proteins (Imkampe *et al.*, 2017).

1.2.4 After pattern recognition: Signaling in the cytoplasm

FLS2 and BAK1 constitutively interact with soluble receptor-like cytoplasmic kinases (RLCKs) including BIK1 (*Botrytis*-induced kinase 1) and the paralogous proteins PBS1, PBL1 (PBS1-like kinase 1) and PBL2 which have a positive regulatory function in immunity

(Lu *et al.*, 2010; Zhang and Zhou, 2010; Monaghan and Zipfel, 2012). BAK1 phosphorylates BIK1 upon flg22 binding, and BIK1 subsequently transphosphorylates FLS2 and BAK1 (Lu *et al.*, 2010; Zhang and Zhou, 2010). Recent studies revealed that BIK1 acts as a negative regulator in RLP mediated signaling (Wan *et al.*, 2019).

Similarly to FLS2, ligand-induced complex formation of BAK1 with EFR and PEPR1 has also been found to coincide with de-novo phosphorylations of the complex partners *in vivo* (Schulze *et al.*, 2010; Schwessinger *et al.*, 2011). One of the earliest immune responses, occurring 30-60 seconds after ligand perception, is the depolarization of the cell membrane. This is marked by an influx of Ca^{2+}- and H^{+}- ions and a simultaneous efflux of K^{+}-, Cl^{-}- and NO^{3-}-ions leading to alkalization in the apoplast (Jabs *et al.*, 1997; Zimmermann *et al.*, 1997; Felix *et al.*, 1999; Wendehenne *et al.*, 2002; Kunze *et al.*, 2004; Garcia-Brugger *et al.*, 2006). Both flg22 and nlp20 induced similar depolarization patterns (Wan *et al.*, 2019). Activated BIK1 has several functions including the phosphorylation of the NADPH oxidase RESPIRATORY BURST OXIDASE HOMOLOG PROTEIN D) (RbohD) (Kadota *et al.*, 2014; Li *et al.*, 2014), Regulator of G protein signaling 1 (RGS1) (Liang *et al.*, 2018), WRKY transcription factors (Lal *et al.*, 2018) and cyclic nucleotide-gated channel (CNGC2) (Tian *et al.*, 2019), and the activation of mitogen-activated protein kinases (MAP kinases) (Lu *et al.*, 2010). Phosphorylation of RbohD leads to the production of reactive oxygen species (ROS), the oxidative burst. Peroxidases rapidly convert membrane-impermeant superoxide (O_2^{-}•), produced in the apoplast by NADPH oxidases, into H_2O_2, which can enter cytosol and nucleus to execute intracellular functions as a secondary stress signal, but also can act antibiotic agents directly (Torres *et al.*, 2006; Boller and Felix, 2009). Both ROS production and the phosphorylation of MAPKs are induced by flg22 and nlp20, but the response resulting from flg22 is stronger and faster than after nlp20 recognition (Wan *et al.*, 2019). The increased intracellular Ca^{2+}-levels function as second messenger. Ca^{2+} are monitored by calcium-dependent protein kinases (CDPKs), which mediate further signaling steps (Blume *et al.*, 2000; Hrabak *et al.*, 2003; Romeis and Herde, 2014).

MAPK cascades are combinatorial modules consisting of an upstream MAPK kinase kinase (MAP3K) that activates MAPK kinases (MKKs) by phosphorylation, while MKKs further activate MAPKs via dual phosphorylation of a conserved T-D/E-Y motif (Nühse *et al.*, 2000; Asai *et al.*, 2002). The activation of the MAP kinase cascade leads to phosphorylation of WRKY (N-terminal "WRKY" motif) transcription factors. The activated

WRKY transcription factors are translocalized into the nucleus where they induce immunity defense genes (Mao *et al.*, 2011). These events lead to a variety of transcriptional adaptation and metabolic changes. The plant produces phytohormones (e.g. ethylene, salicylic acid, jasmonic acid) and synthesizes antimicrobial compounds, (e.g. phytoalexin like camalexin) (Glawischnig, 2007; Boller and Felix, 2009; Tena *et al.*, 2011; Yamaguchi and Huffaker, 2011; Böhm *et al.*, 2014; Zheng *et al.*, 2015; de Torres Zabala *et al.*, 2016; Saijo *et al.*, 2018; Noman *et al.*, 2019). Compared to flg22, nlp20 can induce higher levels of the phytohormones ethylene and salicylic acid (Wan *et al.*, 2019). Only nlp20, but not flg22 stimulates the accumulation of the phytoalexin camalexin (Wan *et al.*, 2019). In response to pathogens the plant also deposits callose at the cell wall, closes its stomata and reduces its growth via downregulation of auxin-responsive genes (Melotto *et al.*, 2006; Navarro *et al.*, 2006; Ellinger and Voigt, 2014). Arabidopsis produces callose upon flg22 and nlp20 perception (Wan *et al.*, 2019). Both flg22 and nlp20 treatments cause massive transcriptional reprograming. Whereas most genes responsive to nlp20 are also up- or downregulated in flg22 samples, flg22 treatment causes differential regulation of an additional set of genes (Wan *et al.*, 2019).

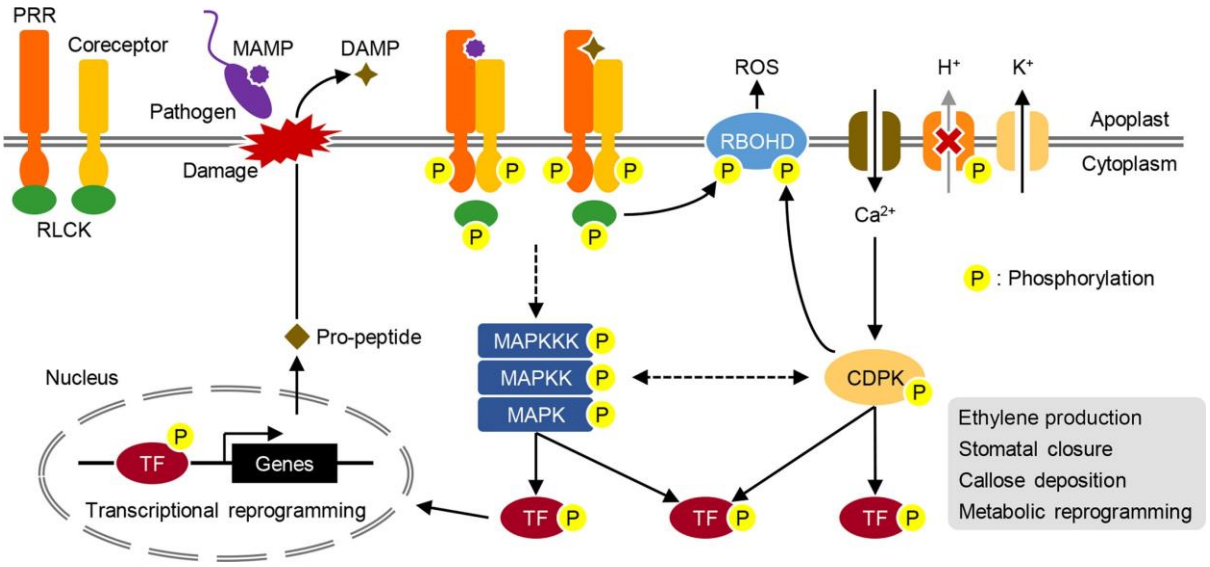

Figure 2: Perception of exogenous danger signals
Microbe-/damage-associated molecular patterns (MAMPs/DAMPs, respectively) by cognate pattern recognition receptors (PRRs) involves dynamic association/dissociation with co-receptors and receptor-like cytoplasmic kinases (RLCKs), and transphosphorylation within the PRR complexes to initiate the downstream signaling. PRR-derived signals are transmitted via further phosphorylation cascades including mitogen-activated protein kinases (MAPKs) and calcium-dependent protein kinases (CDPKs) to the downstream targets such as the NADPH oxidase RBOHD, the plasma membrane (PM)-resident H^+-ATPases and transcriptional factors (TFs) during PTI. (Saijo *et al.*, 2018)

1.3 Translation in prokaryotes

Translation is the process that translates the sequence of a messenger RNA (mRNA) molecule to a sequence of amino acids during protein synthesis. Translation involves three stages: initiation, elongation and termination. Translation initiation is a crucial step of protein synthesis which largely defines how the composition of the cellular transcriptome is converted to the proteome and controls the response and adaptation to environmental stimuli. During initiation, the mRNA–ribosome complex is formed and the first codon (always AUG) binds the first aminoacyl tRNA (initiator tRNA). During the elongation phase, the other codons are read sequentially and the polypeptide grows from the N-terminus by addition of amino acids to its C-terminal end. This process continues until a termination codon (Stop codon) is reached, which does not have a corresponding aminoacyl-tRNA. At this point, protein synthesis terminates (termination phase) and the finished polypeptide is released from the ribosome (Milón *et al.*, 2012; Voet *et al.*, 2013).

1.4 Function of IF1 in bacterial translation initiation

Translation initiation involves three phases. In the first phase the initiator tRNA has a special amino acyl residue, the methionine residue is N-formylated. The initiator tRNA interacts with the initiation codon of an mRNA bound to the surface of the small 30S ribosomal unit forming the 30S preinitiation complex (30S PIC). Three initiation factors; IF1, IF2, and IF3 promote the assembly of the ribosomal subunits and deliver the initiator tRNA (Gualerzi and Pon, 1990). IF1 binds at the A site of the 30S subunit and 16S rRNA (Carter *et al.*, 2001), where it might prevent the inappropriate binding of tRNA. IF1 stabilizes the binding of IF2 and IF3 to the 30S subunit and modulates the selection of mRNA and fMet-tRNA$_f^{Met}$ by controlling the conformational dynamics of the 30S subunit (Gualerzi *et al.*, 1977; Milon *et al.*, 2008; Milon *et al.*, 2010).

IF2 binds GTP and fMet-tRNA$_f^{Met}$ in a ternary complex, thereby ensuring that the tRNA bound to the 30S subunit is the initiator tRNA.

IF3 plays several roles in the initiation process. The ribosome remains in an inactive 70S state after a cycle of polypeptide synthesis is completed; IF3 promotes the dissociation of the 30S and the 50S subunits binding to the 30S subunit. IF3 also promotes the selection of the initiator tRNA by monitoring the tRNA anticodon stem-loop region and the correctness of the anticodon-initiator codon interaction on the ribosome (Voet *et al.*, 2013).

The 30S PIC is converted to a functional 30S initiation complex (30S IC) when the interaction between the start codon and the anticodon of fMet-tRNA$_f^{Met}$ in the P site is established. At the last phase, IF1 and IF3 are released and the large (50S) ribosomal subunit joins the 30S IC forming the 70S initiation complex (70S IC) in a manner that stimulates IF2 to hydrolyze its bound GTP. The resulting conformational rearrangement of the 30S subunit leads to the release of IF2 (Myasnikov *et al.*, 2005; Grigoriadou *et al.*, 2007). In the 70S IC the fMet-tRNA$_f^{Met}$ occupies the P site, while the A site is poised to accept an incoming aminoacyl tRNA.

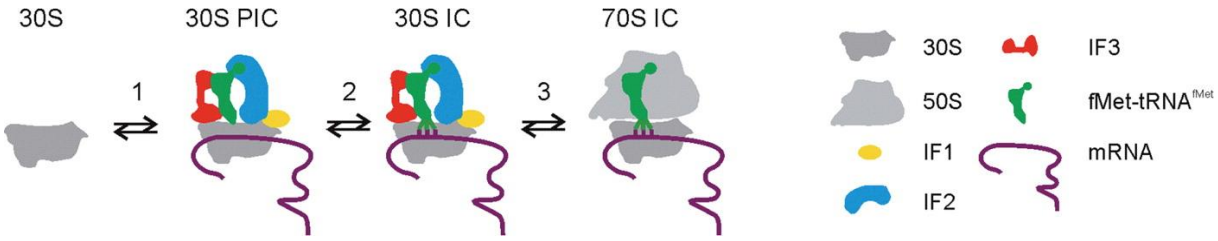

Figure 3: Schematic of the three main phases of translation initiation.
Phase 1: Assembly of the 30S PIC upon recruitment of initiation factors, mRNA, and fMet-tRNA$_f^{Met}$ to the 30S subunit. Phase 2: Conversion of 30S PIC to 30S IC after start codon recognition by fMet-tRNA$_f^{Met}$. Phase 3: Formation of the 70S IC following 50S subunit joining and release of initiation factors. (Milón *et al.*, 2012)

1.4.1 Comparison of IF1 structure to other proteins

IF1 is a small (71 amino acid residues) basic protein. The structure of IF1 in solution has been determined by NMR spectroscopy, it is comprised of a single domain that is formed by a 5- stranded beta-barrel with the loop between strands 3 and 4, the loop connecting strands 3 and 4 contains a short 3_{10} helix capping one end of the barrel. IF1 belongs to the oligo-nucleotide binding fold (OB) family of proteins (Sette *et al.*, 1997). Other examples of bacterial OB fold proteins are the cold shock proteins CspA and CspB (Bycroft *et al.*, 1997), with CspA and IF1 sharing the highest homology. Interestingly, the loop in CspA does not form a helix (Sette *et al.*, 1997). Cellular defects resulting from a double deletion in the genes encoding cold shock proteins CspB and CspC in *Bacillus subtilis* can be complemented by heterologous expression of *E. coli* IF1 (Weber *et al.*, 2001). This confirms the structural resemblance and functionality between IF1 and the cold shock proteins. Structures of the archaeal and eukaryotic IF1 homologues (aIF1A and eIF1A) have also been determined (Battiste *et al.*, 2000; Boelens and Gualerzi, 2002). These structures are highly similar with respect to the OB fold. The C-terminus, however,

contains-helical structures that are important for the archaeal and eukaryotic scanning mechanism and interactions with the small ribosomal subunit (Laursen *et al.*, 2005).

1.5 Aims of this thesis

Prior to this study, Dr. Li Fan identified a novel plant immune receptor, RLP32, in *A. thaliana.* RLP32 recognizes a PAMP that is present in *R. solanacearum* as well as in *E. coli* (Fan, 2015). Dr. Eric Melzer purified the translation initiation factor 1, IF1, from *E. coli* bacterial extract (Melzer, 2013). IF1 showed RLP32-dependent induction of ethylene. The hypothesis of this study is that IF1 is the ligand of RLP32. To that end, IF1 and RLP32 are characterized and binding studies are conducted. As IF1 recognition leads to activation of numerous immunity-associated immune responses, this study further investigates if IF1 recognition leads to RLP32-dependent resistance against proteobacterial pathogens.

2 Materials and Methods

2.1 Materials

2.1.1 Chemicals

Chemicals were purchased in standard purity from Sigma-Aldrich (Taufkirchen), Carl Roth (Karlsruhe), Merck (Darmstadt), Qiagen (Hilden), Invitrogen (Karlsruhe), Duchefa (Haarlem, The Netherlands), Molecular Probes (Leiden, The Netherlands), Fluka (Buchs, Switzerland) and BD (Sparks, USA). Restriction enzymes, ligase and DNA modification enzymes were purchased from Thermo Fisher Scientific (St. Leon-Rot) and New England Biolabs (Beverly, USA). Oligonucleotides were received from Eurofins MWG Operon (Ebersberg). All solutions and media have been prepared with deionized water from a MilliQ machine (Millipore, Schwalbach).

Primary antibodies were purchased from Sigma-Aldrich (α-Myc, α-HA), Sicgen (α-GFP) and Roche (Streptavidin-AP), abcam (α-6x His). Alkaline phosphatase conjugated secondary antibodies α-rabbit IgG, α-goat IgG and α-mouse IgG were purchased from Sigma-Aldrich.

Synthetic peptides were purchased from Genscript Inc. (nlp20, IF1 full length and shorter peptides), Biomatik (flg22, IF1), KE Biochem (IF1), nlp20 was dissolved in 100 % DMSO as 10mM stock solution and working dilutions thereof were prepared with water prior to use. Flg22 was dissolved in 0,1% BSA+0,1M NaCl as 1µM stock solution. IF1 full length was dissolved in sterile filtered 10 mM MES pH 5,7 as a 100µM stock solution, IF1 (30 aa long) was dissolved in 100%DMSO as a 10 mM stock solution. IF1 A1-S36 was dissolved in 3% ammonium water as a 1 mM stock solution, IF1 G37-R71 and IF1 N27-R71 were dissolved in MilliQ water as 1 mM stock solutions.

2.1.2 Media and Antibiotics

Table 1 Antibiotics

Antibiotic	Stock solution in mg/ml	Final concentration in µg/ml
Cycloheximide	12,5	50
Rifampicin	100	100
Kanamycin	50	50
Carbenicillin	50	50
Chloramphenicol	34	34
Spectinomycin	100	100
Gentamycin	40	40

LB Medium (10 g/l Bacto-Tryptone, 5 g/l Yeast extract, 5g/l NaCl, pH 7.0)

King's B Medium (20 g/l Glycerol, 40 g/l Proteose Peptone No. 3) after autoclavation 10 ml/l 10% K_2HPO_4 (sterile filtered) and 10 ml/l 10% $MgSO_4$ (sterile filtered) have been added.

½ MS (2.2g/l MS (Sigma), adjust pH 5.7 with KOH. Add water to 1 l, add 0,8% Select-agar.

2.1.3 Vectors and constructs

All constructs have been cloned first into the entry vector pCR™8/GW/TOPO

Table 2: Constructs used for protein expression

Constructs	received from:
p19	Dr. Eric Melzer
pB7FWG2 35S:RLP32-GFP	Dr. Eric Melzer
pGW14 35S:SOBIR1-3x HA	Dr. Eric Melzer
pGWB17 35S:SERK1-4x Myc	Dr. Eric Melzer
pGWB17 35S:SERK2-4x Myc	Dr. Eric Melzer
pGWB17 35S:SERK3-4xMyc (BAK1)	Dr. Eric Melzer
pGWB17 35S:SERK4-4x Myc	Dr. Eric Melzer
pGWB17 35S:SERK5-4x Myc	Dr. Eric Melzer
pK7FWG2 35S::GFP	Dr. Isabell Albert
pGWB1 Prom2::RLP32 stop	
pGWB4 Prom2:RLP32-GFP	
pET DEST42 T7::IF1 *E. coli*-6x His (1)	
pET pDEDST42 T7::IF1 stop	
pET pDEST42 T7::(-1 Cys) IF1 *E. coli* -6xHis	
pET pDEST42 T7::IF1 I6-R71 *E. coli*-6xHis	
pET pDEST42 T7::IF1 A1-I66 *E. coli*-6xHis	
pET pDEST42 T7::IF1 *A. tumefaciens*-6xHis	
pET pDEST42 T7::IF1 *P. syringae*-6x His	
pET pDEST42 T7::IF1 R69A *E. coli*-6x His	
pET pDEST42 T7::IF1 R69E *E. coli*-6x His	
pET pDEST42 T7::IF1 R69K *E. coli*-6x His	

2.2 Organisms

2.2.1 Bacteria

Escherichia coli

Were grown at 37°C or during protein expression at 17°C in LB-medium for liquid culture or LB agar plates for solid culture with corresponding selective antibiotics overnight.

Escherischa coli One Shot™ Mach1™ T1 Phage-Resistant Chemically Competent cells (Genotype F-φ80(lacZ)ΔM15 ΔlacX74 hsdR($r_{K-}m_{K+}$) ΔrecA1398 endA1 tonA)

Escherischa coli One Shot™ TOP10 Chemically Competent cells (Genotype: F- *mcrA* Δ (*mrr-hsd*RMS-*mcr*BC) Φ80*lac*ZΔM15 Δ *lac*X74 *rec*A1 *ara*D139 Δ(*araleu*)7697 *gal*U *gal*K *rps*L (StrR) *end*A1 *nup*G)

Eschrischia coli BL21AI (Genotype F-*omp*T *hsd*S_B (r_B- m_B-) *gal dcm ara*B::T7RNAP-*tet*A)

Agrobacterium tumefaciens GV3101 (rif^r, $gent^r$)

Were grown at 30°C in LB-medium for liquid culture and LB agar plates for solid culture with corresponding selective antibiotics for 2 days.

Pseudomonas syringae pv. *tomato* strain DC3000 (rif^r) or hrcC- (rif^r, kan^r) were grown for 24-48 h at 28°C on LB medium plates or King's B medium at 180 rpm. For the determination of bacterial growth, the *Pseudomonas* strains were reisolated from plant material (see 2.3.x) and dilution series thereof plated on LB-plates containing. cycloheximide (50 µg/ml) and rifampicin (100 µg/ml).

2.2.2 Plants

2.2.2.1 *Arabidopsis thaliana*

Ecotypes: Col-0, ICE73

Mutant lines: *rlp32* (SM3.33902) (12bp downstream of start codon, Col-0 Background)(Fan, 2015), *rlp32* (SM3.15851) (487bp downstream of start codon, Col-0 Background)(Fan, 2015), *rlp23* (Albert *et al.*, 2015), *efr fls2* (SAIL_691C4, SALK_044334) (Zipfel *et al.*, 2004; Zipfel *et al.*, 2006; Zhang *et al.*, 2013), *sobir1-12* (SALK_050715) (Col-0 Background)

All plants were grown on GS90 soil with Confidor under standard conditions (8 h light 150µmol/cm^2s light, 40-60 % humidity, 22°C) and used for the experiments at an age of 5-6 weeks.

Plants used for infection assays with *Pseudomonas syringae* strain DC3000 were grown under a translucent cover.

After stable transformation surface sterilized seeds were planted on ½ MS agar and then transplanted on GS90 soil with Confidor under standard conditions (8h light 150µmol/cm^2s light, 40-60 % humidity, 22°C) and used for the experiments at an age of 5-6 weeks.

2.2.2.2 *Nicotiana benthamiana*

Nicotiana benthamiana wildtype plants

Nicotiana benthamiana 35S::RLP32-GFP T2 (1.2.1, 3.0.2, 3.0.4)

Plants were grown in the green house (16 h light, 22°C)

Plants used for infection assays with *Pseudomonas syringae* strain DC3000 hrcC- were grown on GS90 soil with Confidor under standard conditions (8h light 150µmol/cm^{2}s light, 40-60 % humidity, 22°C) and used for the experiments at an age of 5-6 weeks.

Plants used for transient transformation were grown in the greenhouse (16 h light, 22°C) for 3-4 weeks.

2.2.2.3 *Solanum lycopersicum*, *Solanum pennellii*, Introgression lines

Solanum lycopersicum, *Solanum pennellii* and Introgression lines (Chitwood *et al.*, 2013) were grown in the greenhouse (16 h light, 22°C) for 5-6 weeks and used in ethylene assays. The material was developed by and/or obtained from the UC Davis/C.M. Rick Tomato Genetics Resource Center and maintained by the Department of Plant Sciences, University of California, Davis, CA 95616.

2.2.2.4 Other plants

Capsella rubella, Brassica napus, Brassica oleracea, Brassica oleracea var. botrytis, Arabis alpina, Thellungiella halophila Commelina communis Solenostemon scutellarioides, Cucumis sativus, Cucumis melo, Medicago truncatula, Trifolium, Solanum pennellii, Solanum lycopersicum, Capsicum annuum were grown on GS90 soil with Confidor under standard conditions (8h light 150µmol/cm^{2}s light, 40-60 % humidity, 22°C)

Nicotiana tabacum, Solanum pennellii, Solanum lycopersicum were grown in the greenhouse (16 h light, 22°C).

2.3 Methods

2.3.1 General molecular biology methods

2.3.1.1 Plant genomic DNA isolation

For cloning, genomic DNA was extracted from leave tissue according to protocol using Edwards buffer (Edwards *et al.*, 1991). One leaf piece was crunched in a 1.5 ml Eppendorf tube with a blue pestle. 200 µl Edwards buffer (200mM Tris/HCl, pH 7.5, 250 mM NaCl, 25 mM EDTA pH 8.0, 0,5% (w/v) SDS) was added and samples were completely homogenized at room temperature. After centrifugation for 5 min at 13000 rpm the supernatant was transferred to a fresh tube and 200 µl isopropanol (2-propanol) were added and thoroughly mixed. DNA was precipitated at RT for 5 min (large leaf piece) up to 45 min (small leaf piece). After another round of centrifugation for 10 min at 4°C with 14000 rpm the supernatant was discarded, and the pellet was washed with 200 µl 70% (v/v) EtOH and incubated for 5 min at RT. The pellet was centrifuged for 5 min at RT with 13000 rpm. After removing the supernatant, the pellet was air dried. Finally, the DNA pellet was dissolved in 50 µl (small leaf piece) or 100 µl (large leaf piece) ddH2O overnight at 4°C or alternatively heated for 10 min at 65°C. Alternatively, the "Phire Plant Direct PCR Kit" (Thermo Fisher Scientific) was used according to the manufacturer's protocol for genotyping.

2.3.1.2 Bacterial DNA isolation

Genomic DNA from *Agrobacterium tumefaciens* GV3101 and *Pseudomonas syringae* DC3000 was extracted from 3 ml (*A. tumefaciens* was grown in LB Medium overnight at 28°C, *P. syringae* was grown in King's B medium overnight at 28°C). Bacteria were pelleted by centrifugation at 2000× g for 20 min and resuspended in 80 µL sonication buffer (50 mM Tris and 10 mM EDTA, pH 7.5, with optional 100 ng/µL RNase A). The suspension was transferred to a 1.5-mL thin tube, then the bacteria was sonicated. Six treatments of 1 min each at an amplitude setting of 6 for Gram negative bacteria (M72: 65% 3 s pause 3 s impulse, 0,2 kJ) were performed. The disrupted cells were then brought down to the bottom of the tube by centrifugation at 2500× g for 20 min. The tube/plate was then incubated at 98°C for 5 min to precipitate out the proteins in the supernatant by denaturation. After centrifugation at 2500× g for 20 min, approximately 50 µL clean DNA, already broken down to small fragments, were transferred to a new tube (Zhang *et al.*, 2005).

2.3.1.3 Polymerase chain reaction (PCR)

For cloning, recombinant Phusion High-Fidelity DNA Polymerase (Thermo Scientific Fisher) with proofreading function was used according to manufacturer's protocol. To analyze the correct insertion of a PCR fragment into the vector backbone, colony PCR was performed after the construct was transformed into *E. coli* Top10 or Mach1T1 cells. Successfully transformed bacteria were selected according to gained vector specific resistance to antibiotics according to manufacturers protocol. For colony PCR reactions were performed using a home-made Taq DNA polymerase using its corresponding buffer (67 mM Tris pH 8.8, 16 mM $(NH_4)_2SO_4$, 2.5 mM $MgCl_2$, 0.01 % Tween-20). For genotyping Phire Plant Direct PCR Kit (Thermo Fisher Scientific).

Table 3: PCR for cloning (Phusion High Fidelity (Thermo scientific))

	1x
10x HF Buffer+ $MgCl_2$	5 µl
10mM dNTPs	1 µl
10µM Insert-specific primer forward	2.5 µl
10µM Insert-specific Primer reverse	2.5 µl
genomic DNA	2 µl
Phusion DNA Polymerase (2U/µl)	0.5 µl
optional: DMSO	1.5 µl
MilliQ	add to 50 µl

	Temperature	Time	cycle
Initial Denaturation	98°C	30 s	1
Denaturation	**98°C**	**10 s**	**35**
Annealing	**Tm calculator Thermo scientific**	**30 s**	
Extension	**72°C**	**15-30 s/kb**	
Final Extension	72°C	10 min	1
	12°C forever		

Table 4: Primers used for cloning

Cloning	RLP32 endogenous promotor [-1597 bp] forward	5'-GATTGCTTTGTGGAGTGGACTG-3'
Cloning	RLP32 stop reverse	5'-TTATTGCTTTCTCCTCAATCTTTTTTCATGTGC-3'
Cloning	RLP32 no stop reverse	5'-TTGCTTTCTCCTCAATCTTTTTTCATGTGC-3'
Cloning	IF1 *E. coli* start forward	5'-ATGGCCAAAGAAGACAATATTGAAATGCAAGG-3'
Cloning	IF1 *E. coli* start 2	5'-ATGGCCAAAGAAGACAATATTGAAAT-3'
Cloning	IF1 *E. coli* stop reverse	5'-TCAGCGACTACGGAAGACAATGCGG-3'
Cloning	IF1 *E. coli* no stop reverse	5'-GCGACTACGGAAGACAATGCGG-3'
Cloning	IF1 *E. coli* no stop 2 reverse	5'-GCGACTACGGAAGACAATGC-3'
Cloning	IF1 *E. coli* I6-R71 forward	5'-ATGATTGAAATGCAAGGTACCGTTC-3'
Cloning	IF1 *E. coli* A1-I66 reverse	5'-AATGCGGCCTTTGCTCAG-3'
Cloning	IF1 *E. coli* +Cys N-terminal forward	5'-ATGTGCGCCAAAGAAGACAATATTG-3'
Cloning	IF1 *A. tumefaciens* C58 forward	5'-ATGTGCCGGGATTGTGTAG-3'
Cloning	IF1 *A. tumefaciens* C58 no stop reverse	5'-CTTGAAGCGATAGGTGATGC-3'
Cloning	IF1 *P. syringae* DC3000 forward	5'-ATGTCGAAAGAAGACAGCTTCGAAA-3'
Cloning	IF1 *P. syringae* DC3000 no stop reverse	5'-ACGAGCGCGGTAGGTGAT-3'
Cloning	IF1 *E. coli* R69A reverse	5'-GCGACTTGCGAAGACAAT-3'
Cloning	IF1 *E. coli* R69E reverse	5'-GCGACTTTCGAAGACAAT-3'
Cloning	IF1 *E. coli* R69K reverse	5'-GCGACTTTTGAAGACAAT-3'

Table 5: Colony PCR

	1x
Taq buffer	2 µl
10 mM dNTP	1 µl
10 µM Vector-specific primer forward	0.5 µl
10 µM Insert- specific Primer reverse	0.5 µl
Bacteria dissolved in 10µl MilliQ water	1 µl
Taq	0.5 µl
MilliQ water	add to 20 µl

	Temperature	Time	Number of cycles
Initial Denaturation	96°C	2 min	1
Denaturation	**96°C**	**10 s**	**35**
Annealing	**Tm-5°C**	**10 s**	
Extension	**72°C**	**4min**	
Final Extension	72°C	10 min	1
	12°C	forever	

Table 6: Primer used for colony PCR

Colony PCR	35S promotor forward	5'-GACGCACAATCCCACTATCCTTCG-3'
Colony PCR	GFP reverse	5'-GGTAGCGGCTGAAGCACTGCAC-3'
Colony PCR	M13 FP	5'-CCCAGTCACGACGTTGTAAAACG-3'
Colony PCR	M13 RP	5'-AGCGGATAACAATTTCACACAGG-3'
Colony PCR	M13 fwd	5'-GTAAAACGACGGCCAG-3'
Colony PCR	M13 rev	5'-CAGGAAACAGCTATGAC-3'
Colony PCR	T7 promotor forward	5'-TAATACGACTCACTATAGGG-3'
Colony PCR	T7 terminator reverse	5'-CTAGTTATTGCTCAGCGGT-3'

2.3.1.4 Genotyping of *A. thaliana* T-DNA insertion lines, Transposon lines

To confirm homozygosity of the Transposon line rlp32 (SM3.3902) and the T-DNA insertion line *sobir1-12* (SALK _050715) genomic DNA was extracted from leave tissue using Phire Plant Direct PCR Kit (Thermo Fisher Scientific) following two PCRs according to the manufacturer's protocol. PCR 1 amplifies a region spanning the insertion region; a primer pair is used that binds outside 5' of the insertion region (right primer (RP)-and outside 3' of the insertion left primer (LP)). PCR 2 amplifies a region from outside the insertion to inside of the insertion in which one primer binds outside of the insertion region (right primer (RP))- and a second primer binds inside of the insertion region (left border of the insertion (LB)). Only if there is no PCR product after PCR 1, but a PCR product after PCR 2, the plant is homozygous for the mutated gene. In wildtype plants the results are reversed.

Table 7: Primers for genotyping

Genotyping	*rlp32* (SM 3.3902) LB	5'-TACGAATAAGAGCGTCCATTTTAGAGTGA-3'
Genotyping	*rlp32* (SM 3.3902) LP	5'-CAGATTGAGTAGGGAAAGGGG-3'
Genotyping	*rlp32* (SM 3.3902) RP	5'-AATTGTTCAAAACCGGTTGTG-3'
Genotyping	*sobir1-12* (SALK_050715) LB	5'-TGGTTCACGTAGTGGGCCATCG-3'
Genotyping	*sobir1-12* (SALK_050715) LP	5'-GGAGCCATAGGAGGAACAATC-3'
Genotyping	*sobir1-12* (SALK_050715) RP	5'-TGACATCTTTACTGTTCGGCC-3'

Table 8:Genotyping PCR (Phire Plant Direct (Thermo scientific))

	1x
2x Phire Plant Direct PCR Mastermix	10 µl
Primer RP	1 µl
Primer LB or LP	1 µl
genomic DNA in Dilution buffer	1 µl
MilliQ water	add to 20 µl

	Temperature	Time	Number of cycles
Initial Denaturation	98°C	5min	1
Denaturation	**98°C**	**5 s**	**40x**
Annealing	**Tm calculator Thermo scientific**	**5 s**	
Extension	**72°C**	**20 s**	
Final Extension	72°C	1 min	1
	4°C	forever	

2.3.1.5 Agarose gel electrophoresis

PCR products were separated horizontally using agarose gel electrophoresis with a 1-2% agarose gel containing 0,5 µg/ml ethidium bromide or peqGREEN in 1x TAE buffer (4 mM Tris/acetate, 1 mM EDTA pH 8,0). Samples were mixed with 6x loading dye (Thermo Fisher Scientific) and loaded next to GeneRuler 1kb (Thermo Fisher Scientific) used as a size marker. Electrophoresis was performed at an electric field strength of 5 V/cm. DNA fragments were visualized in a UV-transilluminator (Infinity-3026 WL/26 Mx, Peqlab) with the software InfinityCapt 14.2 (Peqlab).

2.3.1.6 DNA purification from agarose gel

DNA purification from agarose gels was performed with the GeneJet Gel Extraction Kit (Thermo Fisher Scientific) according to manufacturer's protocol. Nucleic acid concentrations were determined with a NanoDrop 2000 spectrophotometer (Thermo Fisher Scientific) at 220-340 nm and evaluated with the NanDrop Software. Sequencing of plasmid DNA was performed by GATC (Konstanz) and prepared according to the company's instructions

2.3.1.7 Cloning

The pCR8/GW/TOPO Cloning kit (Invitrogen) was used for cloning of PCR products into the pCR8-vector with a polyA-overhang to generate an entry clone for the Gateway system according to the manufacturer's instructions. For adding the polyA-overhang to the PCR product, 2.4 µl of 10x Taq buffer (100 mM Tris-HCl, 500 mM KCl, and 15 mM $MgCl_2$, pH 8.3), 1 µl 10 mM dATP, 1 µl homemade Taq-Polymerase (Inoue *et al.*, 1990) and 20 µl of the purified PCR product was incubated for 30 min at 72°C. 4 µl of this reaction was afterwards used, together with 1 µl provided salt solution (1.2 M NaCl, 0.06 M $MgCl_2$) from the pCR8/GW/TOPO Cloning kit (Invitrogen) and 1 µl of the pCR™8 /GW/TOPO® vector (TOPO®-adapted). For transferring the fragment of interest into the gene expression vector, an LR reaction between the entry clone and a Gateway destination vector was performed using the Gateway® LR Clonase® II Enzyme Mix (Invitrogen) according to the manufacturer's recommended protocol. (Karimi *et al.*, 2002)

2.3.1.8 Transformation of bacteria

2.3.1.8.1 Chemically competent *Escherichia coli*

200 µl of chemically competent *E. coli* BL21 AI (homemade according (Inoue *et al.*, 1990) or *E. coli* TOP10 or Mach1T1 (commercial, Invitrogen) cells were thawed on ice. 5-20 µl of plasmid DNA were added to the cells and incubated for 30 min on ice. After a 30 s heat-incubation step at 42°C the cells were immediately transferred on ice again for 2 min. 600 µl of LB-medium was added and the *E. coli* cells were incubated for 1 h at 37°C with 220 rpm shaking to allow expression of plasmid-borne resistance markers. Depending on the transformed construct, 5 µl (retransformation of plasmid) or up to all cells (ligation) were plated on selective LB-agar-plates containing the appropriate selection marker and incubated at 37°C overnight until colonies were visible.

2.3.1.8.2 Electro-competent *Agrobacterium tumefaciens*

For the transformation of electro-competent *A. tumefaciens* cells GV3101 40 µl of cells were thawed on ice, mixed with 100 ng of plasmid DNA and stored on ice in a pre-cooled electroporation cuvette (1mm electrode distance) for 30 min. The cells were pulsed one time with 1800V for 5 ms using an Electroporator2510 (Eppendorf) and 600 µl LB-medium was directly added to the cuvette. The cells were carefully transferred to an Eppendorf-tube and incubated for 4 h at 28°C with 180 rpm shaking, before they were plated on selective LB-agar-plates and incubated for 48 h at 28°C until colonies were visible.

2.3.1.9 Plasmid purification

Plasmids were extracted from *E. coli* using the GenJET Plasmid Miniprep Kit (Thermo Fisher Scientific) according to the manual. Nucleic acid concentrations were determined with a NanoDrop 2000 spectrophotometer (Thermo Fisher Scientific) at 220-340 nm and evaluated with the NanDrop Software.

2.3.1.10 Sequencing

Sequencing of plasmid DNA was performed by GATC (Konstanz) and prepared according to the company's instructions. Sequences were analyzed using the CLC Main Workbench (Qiagen).

2.3.1.11 Stable transformation of plants

2.3.1.11.1 Stable transformation of *N. benthamiana*

Stable transformation of *N. benthamiana* was performed by Caterina Brancato. *N. benthamiana* leaf pieces were incubated in *Agrobacterium* cell suspensions (grown as described in 2.2.2.2 and resuspended in LB medium without antibiotics for 3 minutes, transferred to MS medium with 2% sucrose and incubated for 48 h in the dark. Transgenic calli were selected on MS medium containing BASTA. For transformation of *S. lycopersicum*, cotyledons were incubated in *A. tumefaciens* suspension for 2 days at room temperature in the dark and transferred to selection medium containing BASTA.

2.3.1.11.2 Stable transformation of *Arabidopsis thaliana*.

Agrobacteria were harvested and resuspended in 5% (w/v) sucrose, 10 mM MgSO4 and 0.01 % (v/v) Silwet and the buds of 6 to 8-week-old *rlp32* mutant plants or accessions ICE73. The T1 generation was selected with ½ MS Agar with kanamycin as a selective antibiotic according to (Barik, 2013)

2.3.1.12 Seed surface sterilization

An appropriate number of seeds were filled into a 1,5 ml tube. The open tube was placed in a desiccator under the hood. A flask with 50ml Sodium-hypochlorite solution was also placed into the desiccator, 2ml 37% HCl were added to the hypochlorite solution and quickly close the desiccator. The chlorine gas generated. The seeds were incubating for four hours or overnight. The desiccator was opened, and the tubes closed. The tubes were opened again in the sterile bench for thirty minutes.

2.3.1.13 Selection of stably transformed plants

Successfully transformed *A. thaliana* were sowed on ½ MS agar with selective antibiotics (Kanamycin) and grown in a dark-light rhythm described in (Harrison *et al.*, 2006).

2.3.1.14 Transient transformation of *N. benthamiana*

Agrobacterium tumefaciens-mediated transient transformation of *N. benthamiana* was used for transient protein expression. The bacterial strains carrying the appropriate expression constructs were grown in LB medium with selective antibiotics for 2 days. After harvesting the cells by centrifugation for 10 min at 2000 g, the pellet was washed for two times with 10 mM $MgCl_2$. The density of the culture was adjusted to an OD_{600} of 1 in 10 mM

$MgCl_2$ and 150 µM acetosyringone. The bacterial suspension was then incubated at RT for 2 hours. Afterwards, the bacteria were mixed 1:1 with a suspension of bacteria carrying an p19 expression construct (Voinnet *et al.* 2003) and adjusted to an OD_{600} of 0,2. The mixture was infiltrated into the leaves of 3-week-old tobacco plants and the leaf tissue was analyzed 2-3 days post infection for the presence of the protein.

2.3.1.15 Protein extraction from plant tissue

For Coimmunoprecipitation of RLP32 with co-receptors total protein was extracted from 200 mg of frozen leaf material and solubilized with 0.6 ml of solubilization buffer (25 mM Tris-HCl pH 8.0, 150 mM NaCl, 1% (v/v) NP40, 0,5% (w/v) DOC, 2 mM DTT, 6 µl plant protease inhibitor cocktail (PPI, Sigma-Aldrich) per 200 mg leaf material). After grinding in liquid nitrogen another 0.3 ml solubilization buffer were added to wash the pistil.

For Immunoprecipitation of RLP32 with chemically crosslinked ligand total protein was extracted from 300 mg of frozen leaf material and solubilized with 0.65 ml of solubilization buffer (25 mM Tris-HCl pH 8.0, 150 mM NaCl, 1% (v/v) NP40, 0,5% (w/v) DOC, 2 mM DTT, cOmplete™ ULTRA tablets (Ailloud *et al.*) Protease inhibitor) per 300 mg leaf material). After grinding in liquid nitrogen another 0.65 ml solubilization buffer were added to wash the pistil.

The samples were solubilized for 1 h at 4°C by overhead shaking (5-7 rpm). Centrifugation for 1 h at 4°C and 20000 g separated the soluble proteins from the cell debris and could be used for further analysis.

2.3.1.16 Immunoprecipitation on GFP-trap beads

For co-immunoprecipitation of RLP32 and co-receptors, leaves of transiently transformed *N. benthamiana* were harvested 5 min after infiltration of IF1 or 10 mM $MgCl_2$ as negative control. 200 mg ground leaf material from *N. benthamiana* was used per sample.

For Immunoprecipitation of RLP32 with chemically crosslinked ligand as described in 2.3.2.6 300 mg ground leaf material from *N. benthamiana* was used.

GFP-Trap beads (ChromoTek) were prewashed and equilibrated in solubilization buffer. Membrane proteins were solubilized as described 2.3.1.15. For protein input analysis 150µl of the extracted protein was added to 50 µl 5xSDS-buffer and boiled for 10 min at 95°C. The rest of the extracted Protein was used for immunoprecipitation of the GFP-tag to GFP-Trap beads. The protein extracts were incubated with the beads for 1-2 h at 4°C

in an overhead rotator (5-7 rpm). By carefully sedimenting the beads (1000 g, 4°C, 1 min) they were washed two times with solubilization buffer and two times with washing buffer (25 mM Tris-HCl pH 8.0, 150 mM NaCl) and boiled with SDS loading buffer for 10 min at 95°C. After sedimenting the beads at 1000 g, the samples were subjected to SDS-PAGE (2.3.2.8) and Western blot analysis (2.3.2.12).

2.3.2 Biochemical methods

2.3.2.1 Recombinant protein expression

For IF1 *E. coli*-6xHis, IF1 *A. tumefaciens*-6xHis, IF1 *P. syringae*-6x His, IF1 I6-R71-6xHis and IF1 A1-I66-6xHis, IF1 R69A-6xHis, IF1 R69E-6xHis, IF1 R69K-6xHis 5 ml LB medium containing 50 µg/ml Carbenicillin per construct were inoculated with *E. coli* BL21AI transformed with the respective construct and incubated overnight at 37°C.
The overnight cultures were used to inoculate 250 ml fresh LB medium containing 50 µg/ml Carbenicillin in baffled flasks to an OD_{600} of 0.05–0.1. This dilution allowed the cells to quickly return to logarithmic growth and reach the appropriate cell density. The cultures were grown at 37°C 220 rpm until they reached mid-log phase (OD_{600}~0.4; 2 to 3 hours). Protein expression was induced in the cultures by adding L-arabinose to a final concentration of 0.2% and IPTG to a final concentration of 1 mM. The cultures were incubated for an additional 4.5 hours at 37°C 220 rpm. To harvest the cells, the culture was centrifuged at 90000 rpm for 30 min. The cell pellet was stored at -20°C.

For IF1 -6x His+ N-terminal cysteine: 60 ml LB medium containing 50µg/ml Carbenicillin were inoculated with *E. coli* BL21AI transformed with the IF1 -6x His+ N-terminal cysteine construct and incubated over night at 37°C. 6 l in 500 ml fresh LB medium containing 50 µg/ml Carbenicillin in baffled flasks were inoculated with 5 ml overnight culture per flask to an OD_{600} of 0.05–0.1. The culture was grown until they reach mid-log phase (OD_{600}~0.4; 2 to 3 hours). Protein expression was induced in the cultures by adding L-arabinose to a final concentration of 0.2% and IPTG to a final concentration of 1 mM. The cultures were incubated for an additional 24 hours at 17°C 220 rpm. To harvest the cells, the culture was centrifuged at 90000 rpm for 30 min. The cell pellet was stored at -20°C.

2.3.2.2 Protein purification of IF1-6x His +/- N terminal cysteine

2.3.2.2.1 Purification of IF1 *E. coli*-6xHis, IF1 *A. tumefaciens*-6xHis, IF1 *P. syringae*-6x His, IF1 I6-R71-6xHis and IF1 A1-I66-6xHis, IF1 R69A-6xHis, IF1 R69E-6xHis and IF1 R69K-6xHis

Cell Lysis

The frozen bacterial pellets were resuspended in 40 ml binding buffer for the HisTrapFF column ((20 mM KPi (from 0.1 M KPi pH 7.6); 500 mM KCl; 50 mM imidazole pH 7.4). 20 ml aliquots of the resuspended bacteria were lysed via sonification (3s Puls, 3s Pause bei 65%) until 2 kJ were reached.

Immobilized metal ion affinity chromatography (IMAC)

The extracts were purified using IMAC via a 1 ml HisTrapFF column, binding the 6xHis-tag. The column was washed and equilibrated with 5 column volumes (CVs) HisTrap FF binding buffer, 5 CV HisTrapFF elution buffer (((20 mM KPi (from 0.1 M KPi pH 7.6); 500 mM KCl;500 mM imidazole pH 7.4) and again with 5 CV binding buffer.

The bacterial extract was loaded on the column, the glow through was collected separately. the columns binding the IF1-6xHis constructs was washed using 10 CV binding buffer then the IF1-6xHis constructs were eluted with 10 CV of increasing elution buffer in 10 min (1 ml/min, 0-100%) 1 ml fractions were collected.

The presence and activity of the different IF1 constructs was determined by elicitation of *efr fls2* and *rlp32* leaf pieces with different dilutions of the eluted fractions for 4 h as described in 2.3.4. The protein concentration of the purified constructs was determined as described in 2.3.2.5. 100 ng of each construct was separated on a Tricine SDS-PAGE as described in 2.3.2.9 , the gel was stained with Coomassie brilliant blue according to 2.3.2.10 to determine the purity of the preparations.

2.3.2.2.2 Purification of IF1 -6x His+ N-terminal cysteine

Cell Lysis

The frozen bacterial pellet was resuspended in 200 ml binding buffer for the HisTrapFF column. The resuspended cell pellet was incubated with 1 mg/ml Lysozyme (Sigma 62970-5G-F) + 1U/ml DNase1 Sigma (DN25-100MG) at 4°C for 1 hour while stirring. The cells were lysed using a liquid nitrogen bomb according to manufactures protocol. The

bacterial extract was separated from the cell debris by centrifugation. To make sure that no residual solid particles remained in the bacterial extract, the extract was filtrated through Whatman filter paper.

Immobilized metal ion affinity chromatography (IMAC)

The bacterial extract was loaded onto the column, the glow through was collected separately. the columns binding the IF1-6xHis constructs was washed using 10 CV binding buffer then the IF1-6xHis constructs were eluted with 10 CV of increasing elution buffer in 10 min (1 ml /min, 0-100%) 1 ml fractions were collected. The collected flow through was loaded to the same column again after an empty run to purify residual IF1 that could not bind to the HisTrapFF column due to overloading. The presence and activity of IF1 was determined by elicitation of *efr fls2* and *rlp32* leaf pieces with different dilutions of the eluted fractions for 4 h as described in 2.3.4.

Reversed phase chromatography

The fractions obtained from IMAC, inducing ethylene production at the 10^{-3} dilution were pooled and further purified by reversed-phase chromatography (C8 column). The C8 column was washed and equilibrated with 10 ml MilliQ +0,25% trifluoroacetic acid (TFA), 10 ml 100% acetonitirl+0,25% TFA, 10 ml MilliQ water +0,25% TFA. The pooled active fractions were loaded on the C8 column, the flow through was collected. The C8 column was washed with 10 ml MilliQ water+0,25% TFA. IF1 was eluted from the C8 column with 10 ml 50% Acetonitril +0,25% TFA and then 10 ml 100% Acetonitirl+0,25% TFA. The column was washed with 10 ml MilliQ water+0,25% TFA, then the flow through was loaded on the column. The wash and elution steps were repeated. The fractions containing IF1 were determined again by elicitation of ethylene production in *efr fls2*. These fractions were combined. Acetonitrile was removed using vacuum concentration.

Size exclusion chromatography for buffer exchange

At this point the buffer was exchanged to 1x PBS pH 7.4 for IF1-6xHis+N-terminal cysteine using size-exclusion chromatography (PD10 desalting columns). The PD10 column was equilibrated with 5 CV 1x PBS pH 7.4. 2.5 ml IF1 was loaded on the PD10 column, then IF1 was eluted with 1x PBS pH 7.4. The protein concentration of IF1-6x His +N-terminal cysteine was determined as described in 2.3.2.5. The activity of the IF1 preparation was

determined in an ethylene assay as described in 2.3.4. *efr fls2* leaves were elicited with different dilutions of IF1-6x His+N-terminal cysteine.

2.3.2.3 Biotinylation of IF1-6x His +N-terminal cysteine

The purified protein IF1-6x His +N-terminal cysteine preparation (2.3.2.2.2) was used to biotinylate the added cysteine at the N-terminus using EZ-Link BMCC-Biotin (Thermo scientific) according to manufacturer's recommendations. The reagent was warmed up at RT 30 min before usage.2.1 mg BMCC-biotin was dissolved in 500 µl DMSO to prepare an 8 mM stock solution. 10 mmol BMCC-biotin per 1 mmol IF1 was added to IF1 in 1xPBS pH 7.4. The reaction was incubated on ice overnight.

2.3.2.4 Purification of biotinylated IF1-6xHis +N-terminal cysteine

The biotinylated IF1 was separated from free biotin by an additional size-exclusion chromatography step (PD10 column) as described in, the buffer was exchanged to MilliQ water as described in 2.3.2.2.2. The activity of the biotinylated IF1 was determined again in an ethylene assay as described in 2.3.4. *efr fls2* leaves were elicited with different concentrations of biotinylated IF1. The protein concentration was determined as described in 2.3.2.5. The biotinylated IF1 in MilliQ was used in experiments.

Affinity chromatography (Streptavidin 1 ml column)

Biotinylated IF1 was separated from unbiotinylated IF1 using affinity chromatography. For this step the buffer was exchanged to binding buffer for Streptavidin HP column ((20 mM KPi buffer+ 0.15 mM KCl pH 7.5) instead of water after biotinylation. An aliquot of the desalted biotinylation reaction was kept before it was loaded onto the column to compare the activity of IF1 before and after the affinity chromatography. The preparation was loaded onto the equilibrated 1 ml Streptavidin column. The flow through containing the unbiotinylated IF1 was collected. Biotinylated IF1 was eluted from the column with increasing concentration of elution buffer (8 M urea pH 1.5) 1ml/min 0-100% in 10 min.

The flow through was tested for residual unbiotinylated IF in an ethylene assay 2.3.4. *Efr fls2* leaves were elicited with different concentrations of biotinylated IF1 before loading on the Streptavidin column, the flow through of the column and the eluted fractions from the column. The purity and identity of biotinylated IF1-6xHis + N-terminal cysteine was determined by separation on a Tricine SDS-PAGE 2.3.2.9 and subsequent silver staining 2.3.2.11, and Western blot analysis using αHis antibody or Streptavidin-AP 2.3.2.12.

2.3.2.5 Determination of protein concentration

The protein concentration was determined after the Bradford method (Bradford 1976) using Roti-Quant solution (Carl Roth). A standard curve was calculated with bovine serum albumin (BSA).

2.3.2.6 *In vivo* cross-linking

For in vivo cross-linking of IF1-biotion (2.3.2.4) to RLP32 to RLP23 leaves of *N. benthamiana* expressing 35S::RLP32–GFP, or control as a control 35S::RLP23–GFP or p19 (2.3.1.14), were infiltrated with 100 nM biotinylated IF1, 100 nM nlp24-biotin or 10 mM $MgCl_2$ with or without 10µM unlabeled synthesized IF1 as competitor. 5 min after peptide treatment 2 mM EGS (ethylene glycol bis (succinimidyl succinate); initially solved in a small volume of DMSO, further diluted in 25 mM HEPES buffer, pH 7.5) was infiltrated into the same leaves for cross-linking of peptides to the receptor proteins. 15 min after cross-linking, leaf samples were harvested and frozen in liquid nitrogen. 300 mg of the sample was used for protein extraction 2.3.1.15 and immunoprecipitation 2.3.1.16.

2.3.2.7 *In vitro* transcription and translation (TnT)

pET PDEST42 T7::IF1 without tag was used for in vitro transcription and translation in rabbit reticulocyte lysate using TnT® Quick Coupled Transcription/ Translation Systems Promega from T7 sample kit according the manufacturers protocol. As a control the provided Luciferase construct was used. 40 µl T_NT®Quick Master mix, 1 µl 1 mM methionine 2 µl 0.5 µg/µl plasmid DNA template and MilliQ water was added to 50 µl. The reaction was incubated for 2h at RT. The immunogenic activity of IF1 T_NT determined in an ethylene assay 2.3.4. *efr fls2*, *rlp32* and *rlp23* leaves were elicited with IF1 T_NT, Luciferase, T_NT®Quick Master mix as a negative control.

2.3.2.8 SDS-PAGE

SDS polyacrylamide gel electrophoresis was performed using the protocol of (Laemmli, 1970) by the method of (Sambrook and Russell, 2001). The acrylamide bisacrylamid mixture (37,5:1) was purchased as Rotiphorese Gel 30 (Carl Roth). Separating gels of 8%, 10% or 12% were used with 5% stacking gels in the gel chamber system of BioRad. Protein separation was performed at 20 mA and the prestained PageRulerTM protein ladder mix (Fermentas) was used as a protein marker.

2.3.2.9 Tricine SDS-PAGE

Tricine SDS PAGE was used to separate small proteins below 20 Da according to the protocol established by Schägger and Jagow (1987). For this study a 16% separating and a 4% stacking gel was used. A constant current of 30mA per gel was used to separate the proteins. 0.2 µl of the prestained PageRuler™ protein ladder mix (Thermo Fisher Scientific) was used as a protein marker.

2.3.2.10 Coomassie blue stain

Non-specific staining of proteins after SDS-PAGE was done using a Coomassie staining solution containing 0.125% (w/v) Coomassie brilliant blue R-250, 50% (v/v) MeOH and 10% (v/v) acetic acid. The solution was heated up and shaken with the gel for 30 min. For destaining of the gel the solution was exchanged by 10% (v/v) acetic acid, heated up and shaken until excess stain was removed.

2.3.2.11 Silver stain

Tricine SDS-PAGE gels were incubated in fixing solution (50% (v/v) methanol, 12% (v/v) acetic acid and 0.5% (v/v) 37% formaldehyde) for at least one hour or overnight at RT. After three times washing for 20 min with 50% (v/v) ethanol the gels were pretreated with fresh 0.02% (w/v) $Na_2S_2O_3*5H_2O$ for 1 min. The gels were then rinsed three times for 20 s with ddH_2O and then impregnated with 0.2% (w/v) $AgNO_3$ and 0.75% (v/v) 37% formaldehyde for one hour. After quickly rinsing the gels two times in ddH2O, the gels were developed with 6% (w/v) Na_2CO_3, 0.5% (v/v) 37% formaldehyde and 4 mg/l $Na_2S_2O_3$. The developing process was stopped after 5 – 10 min (or when the signal was strong enough), first with rinsing the gels two times with ddH_2O and then with a solution of 50% (v/v) methanol and 12% (v/v) acetic acid. The gels were scanned for later documentation.

2.3.2.12 Western blot analysis

Western blotting was performed in a PerfectBlue semi-dry-blotting gadget (PeqLab, Erlangen). The SDS polyacrylamide gel was sandwiched together with a nitrocellulose Hybond ECL- Membrane (GE Healthcare) between three layers of whatman paper after all components were equilibrated in blotting buffer (25 mM Tris-HCl pH 8.3, 192 mM glycine, 20% (v/v) MeOH). Blotting was performed for 1 h at 1 mA/cm^2 and stained with Ponceau-S (0.1% (w/v) Ponceau-S, 5% (v/v) acetic acid) to control blotting efficiency and evenness. The membrane was blocked for 1-2 h in 5% (w/v) BSA in TBS-T

(20 mM Tris-HCl pH 7.5, 150 mM NaCl, 0.1 % (v/v) Tween-20). The membrane was then incubated with the first antibody in 5% BSA in TBS-T overnight at 4°C, washed with TBS-T (3 x 5 min) and incubated in the second antibody in 5% BSA in TBS-T for 2 h. After three washing steps the membrane was equilibrated in alkaline phosphatase buffer (AP-buffer, 150 mM Tris-HCl pH 9.5, 100 mM NaCl, 5 mM $MgCl_2$) and detected using either the substrates NBT (100 µg/ml) and BCIP (50 µg/ml) or by chemiluminescence using nitroblock solution (1:20 in AP, Thermo Fisher Scientific) to enhance the alkaline phosphatase signal and CDP Star (0.25 mM in AP). The chemiluminescent signal was detected with a CCD camera (Viber Louromat, PeqLAB).

2.3.3 Bioassays

2.3.3.1 Priming of *Arabidopsis thaliana* plants

Eight 6-week-old plants (Col-0, rlp32 (SM3.33902), (SM3.15851)) were primed by leaf infiltration with a needleless syringe with either 1 µM nlp20, 1 µM IF1 or 10mM Mg_2Cl 24h prior to infection with *Pseudomonas syringae* pv. *tomato* strain DC3000 (Pst).

2.3.3.2 Infection with *Pseudomonas syringae* pv. *tomato* DC3000 or hrcC-

25 ml King's B Medium containing 100 µg/ml rifampicin) were inoculated with *Pseudomonas syringae* pv. *tomato* DC3000 or *Pseudomonas syringae* pv. *tomato* DC3000 hrcC- from bacterial colonies grown on LB-Plates for 2 days at 28°C. The inoculum was grown for 24h at 28°C at 180 rpm. At the day of infection, the bacteria were harvested by centrifugation at 3500 rpm for 10 min at room temperature. The bacterial pellet was resuspended in 25 ml sterile 10 mM Mg_2Cl and centrifuged again for 10 min at 3500 rpm at room temperature. The pellet was resuspended in 15 ml and diluted to a final cell density of 10^4 cfu/ml. Two leaves per plant (middle age, already serrated) were infiltrated with a needleless syringe. At the day of infection two infected plants were picked, the infected leaves were cut off and surface sterilized by washing them in 70% ethanol for 1 min. The leaves were dried and washed again in sterile water for 1 min ad dried. Two leaf disks (5 mm diameter) per leaf were cut with a cork borer, transferred to a 1,5 ml tube filled with 100 µl 10 mM Mg_2Cl and homogenized with a mortar attached to a drill. The residual plant material at the mortar was rinsed of with 100 µl 10 mM Mg_2Cl and added to the tube. 10 µl of the homogenized plant material were plated on LB agar plates containing rifampicin (100 µg/ml) and cycloheximide (50 µg/ml) in case of infection of *A. thaliana* the

procedure was repeated three days after infection with 6 plants per line that have been primed 24h prior to infection (2.3.3.1). Until the harvest of the plant material the plants were kept under a translucent lid to keep a humid environment. The homogenized plant material was diluted serially 1:10 with 10 mM Mg_2Cl. 10 µl of each dilution were plated on LB agar plates containing rifampicin (100 µg/ml) and cycloheximide (50 µg/ml). After 2 days incubation at 28°C colonies were counted.

In case of infection of *N. benthamiana* with *Pseudomonas syringae* pv*. tomato* DC3000 hrcC-, the bacteria were always grown in media containing rifampicin (100 µg/ml), kanamycin (50µg/ml) and on agar cycloheximide (50 µg/ml). The 5th leaf (0 dpi) and the 7th leaf (4 dpi) of 8 plants were infected with and original density of $2*10^4$cfu. The samples were collected in a similar way as the *A. thaliana* samples, but four days after infection instead of three. A week prior to the infection the transgenic *N. benthamiana* plants (T2) were checked for RLP32 expression via ethylene production after IF1 elicitation

2.3.4 Biosynthesis of ethylene

Middle aged plant leaves were cut in ca 4 mm x 4 mm squares. The leave pieces were incubated overnight in MilliQ water. At the next day 6 ml-test tubes were filled with 400 µl 10 mM MES pH 5.7. Three leave pieces were placed on the surface of the buffer. For elicitation of ethylene production, reagents were added to the tube. A rubber plug was placed on top of the test tube. After 4 h incubation at 170 rpm 1 ml air from the test tube was injected with a syringe into a gas chromatograph (Shimadzu GC-14A) to measure ethylene production.

2.3.5 Statistical analysis

All statistical analyses were carried out with SAS jmp. At normal distribution data sets of the infection assays were evaluated using the post-hoc comparisons following one-way ANOVA (Tukey's test) multiple comparison analysis at a probability level of $p < 0.05$

EC_{50} values and curve fit were calculated using Logistic 3P or 4P Rodbard Model comparison (three parametric logistic regression)

2.3.6 Software and Online tools

CLC workbench, Pymol, jmp, BLASTn and Blastp, Easy Sequencing in PostScript 2.2, I-TASSER

3 Results

3.1 Identification of RLP32 and its ligand IF1

This research is focusing on the characterization of a novel pattern recognition receptor RLP32 and its ligand, the bacterial translation initiation factor 1 (IF1). Prior to this work Dr. Eric Melzer and Dr. Li Fan identified a novel PRR in *A. thaliana* that would recognize a PAMP from *Ralstonia solanacearum*. As *A. thaliana* is not a host to this pathogen, there must be a defense mechanism in place which detects *R. solanacearum*. Later, this plant defense-inducing activity was also found in the *E. coli* strain Rosetta.

3.1.1 IF1- a new PAMP

Dr. Eric Melzer identified candidate proteins for the RLP32-ligand, known as RsE (Melzer, 2013), by liquid chromatography mass spectrometry/ mass spectrometry (LC-MS/MS) analysis of purified bacterial extract. The bacterial cell pellet was heated at 85°C for 10 min and lysed by sonification. After centrifugation, the bacterial extract was fractionated using cation exchange chromatography. The eluted fractions were tested for induction of RLP32-dependent ethylene response. Active fractions were subsequently combined and subjected to anion exchange column. Flow through preparations were collected and further purified by reversed-phase chromatography (C18 column). The new PAMP was identified to be a proteinaceous, alkaline protein with a molecular size of around 10 kDa (Melzer, 2013).

To identify the proteins in the fractions inducing RLP32-dependent ethylene response, the samples were analyzed by mass spectrometry. More than 30 bacterial candidate proteins were identified, mostly proteins that are involved bacterial protein translation apparatus.

The cDNA's encoding 20 of these ligand candidates were recombinantly expressed as His-tagged proteins in *E. coli* and purified using immobilized metal affinity chromatography (IMAC). Of the purified proteins, only IF1 showed RLP32-dependent induction on ethylene biosynthesis after treating *efr fls2* and *rlp32* plants. *Efr fls2* plants were used instead of Col-0 plants to exclude the possibility of accidental co-purification of the known bacterial PAMPS flagellin and EF-Tu.

3.1.2 RLP32- a new PRR

In her dissertation Dr. Li Fan describes the identification of the presumptive receptor for IF1 (formerly known as RsE2) (Fan, 2015). She screened for IF1-induced/triggered ethylene response in multiple *Arabidopsis thaliana* ecotypes and conducted a genome wide associated study (GWAS). She developed a F2 mapping population of an insensitive ecotype (ICE73) and a sensitive ecotype (ICE153). Using a NGS-assisted (Next Generation Sequencing) QTL (Quantitative Trait Locus) mapping approach, she mapped IF1 sensitivity to an 1.1 Mb region on the third chromosome. In this region she identified four RLPs clustered into two groups, RLP30, RLP31, RLP32 and RLP33, one LRR containing protein and one disease related R protein, all the candidates were predicted to be trans-membrane proteins. Mutant plants lacking expression of those candidate receptors were treated with purified bacterial extract containing IF1. Only the knock-out mutant of RLP32 was insensitive to IF1, concluding that RLP32 is most likely the receptor recognizing IF1. Furthermore, she could show that RLP32-mediated IF1 perception was compromised in the *bak1/bkk1* double mutant or *sobir1* mutant (Figure 21: Supplement 1B).

3.2 Recombinant expression and purification of IF1 6xHis-tag ± biotinylated N-terminal cysteine

IF1 consists of 71 amino acids, it is part of the first step of the protein translation initiation in bacteria. In the first phase of initiation, IF1, IF2 (a GTP-binding protein), IF3, mRNA and the initiator fMet-tRNA$_f^{Met}$ bind to the 30S ribosomal subunit, forming the 30S initiation complex (Milón *et al.*, 2012). IF1 was cloned into pDEST42 to produce stable IF1 fused to 6x His-tag at the C-terminus under the control of the T7 promotor. Biotinylated IF1 was required to demonstrate specific interaction of IF1 and RLP32. Conventional biotinylation of IF1 lysine residues or at the N-terminus resulted in elicitor-inactive protein. Therefore, a cysteine biotinylation approach was devised using an engineered IF1. A single cysteine was cloned to the N-terminus of IF1, forming the final construct: IF1-6xHis+cysteine N-terminal. The native structure of IF1 derived from *E. coli* does not contain cysteine, so the additional cysteine at the N-terminus could be biotinylated without disrupting the immunogenic activity of the protein (Figure 4 B).

IF1-6xHis and IF1-6xHis+ N-terminal cysteine were recombinantly expressed in *E. coli* BL21AI and purified according to the purification protocol in material and methods (2.3.2.1, 2.3.2.2, 2.3.2.3, 2.3.2.4). First IF1-6xHis was purified from the bacterial extract with IMAC (Figure 4 A). The IF1-6xHis activity could be found in a very broad peak from 30-100% of the elution buffer. Active fractions were pooled and further purified with reversed phase chromatography (Figure 4 B). The purification process was monitored by separating the samples on a 16% SDS-PAGE and silver staining (Figure 4 C). IF1-6xHis was used in experiments. The additional N-terminal cysteine of IF1-6xHis was then biotinylated and further purified according to the protocol in Material and methods (2.3.2.3). A sample of the biotinylated IF1 and the flow through of the Streptavidin HP column were used in an ethylene assay with *efr fls2* plants (Figure 4 B) to check how efficient the biotinylation reaction has been. The flow through after the affinity chromatography was eliciting much less ethylene in *efr fls2* compared to the combined, desalted biotinylated IF1. The biotinylated IF1 bound to the column while unbiotinylated IF1 could be found in the flow through, indicating that almost all IF1 was successfully biotinylated. The biotinylation of cysteine did not influence the immunogenic activity of IF1, which could be observed by comparing the induction of ethylene in *efr fls2* before and after biotinylation (Figure 4 B).

The purification process was monitored by analyzing the fractions on SDS-PAGE (2.3.2.9) and either silver staining (2.3.2.11) or western blot (2.3.2.12) using antiserum against His-tag or streptavidin binding to biotin (Figure 4 C IF1-6xHis= 13.1 kDa, biotinylated IF1-6xHis= 13.6 kDa). The detection of biotinylated IF1 (0.576 pmol) via western blot is more sensitive than detection of IF1 via anti His-tag antibody (5.76 pmol). Biotinylated IF1-6xHis were used for binding studies, that require low concentration of the ligand to show specific binding to the receptor.

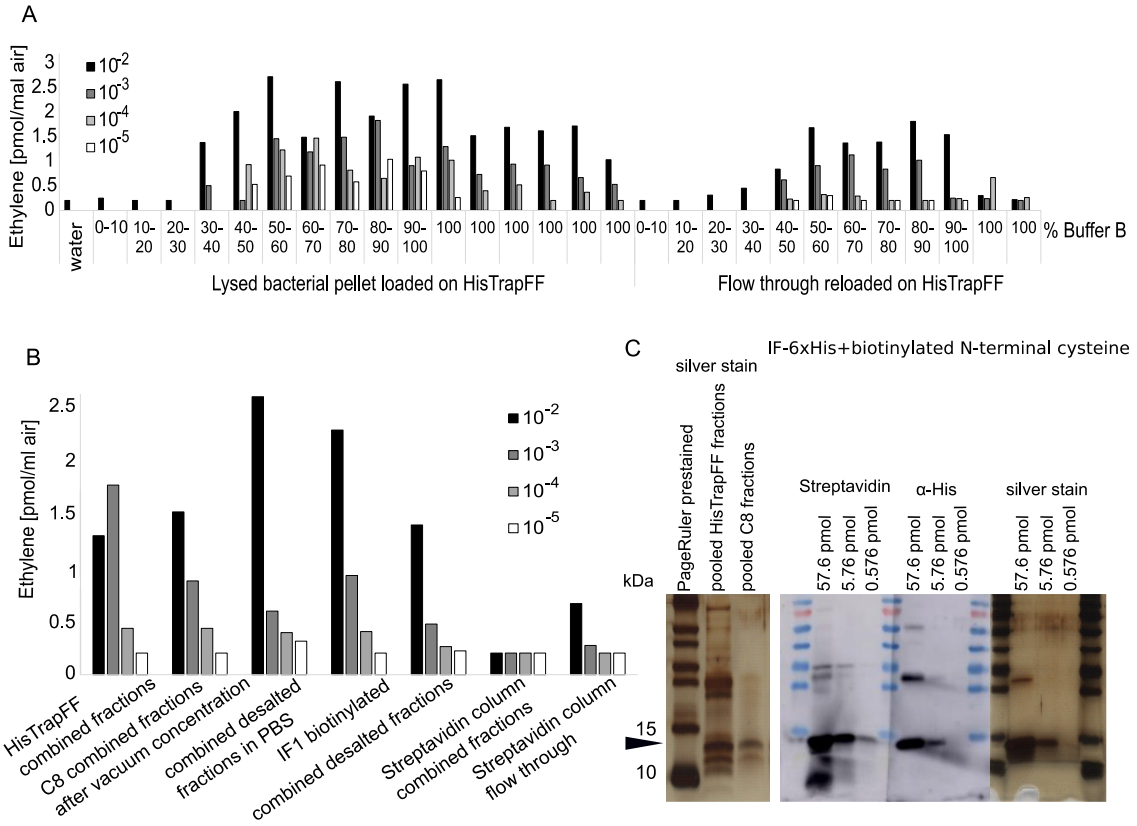

Figure 4: Purification of IF1-6xHis-tag ± biotinylated N-terminal cysteine
A) Induction of ethylene biosynthesis in *efr fls2*-plants in response to different dilutions of collected elution fractions from 1 ml HisTrapFF-column (n=1). 240 ml lysed bacterial pellet containing recombinantly expressed IF1-6xHis-tag+N-terminal cysteine was loaded onto the column. After the first elution from the column, the flow through was loaded on the same column to harvest the residual IF1-6xHis-tag+N-terminal cysteine. All fractions inducing ethylene production when diluted 10^{-3} were combined **B)** Induction of ethylene biosynthesis in *efr fls2* plants in response to different dilutions of IF1-6xHis-tag+N-terminal cysteine in different purification steps (n=1). **A)** and **B)** Leaf pieces from *efr fls2* plants were treated for 4 h. The experiment was performed three times with similar results. **C)** From left to right: Silver stained 16% SDS-PAGE of IF1-6xHis-tag+N-terminal cysteine after IMAC and reversed phase purification, Western Blot of different concentrations of IF1-6xHis-tag+biotinylated N-terminal cysteine after purification (stained with Streptavidin, anti-His-tag antibody), Silver stained 16% SDS-PAGE of different concentrations of purified IF1-6xHis-tag+biotinylated N-terminal cysteine. Black arrow indicates IF1-6xHis+N-terminal cysteine (13.1 kDa, + biotin=13.6 kDa)

3.3 Characterization of IF1

The immunogenic activity of recombinantly expressed IF1 is RLP32-dependent as it can induce ethylene biosynthesis in *efr fls2* and *rlp23,* but not in *rlp32* plants (Figure 5). Recombinantly expressed IF1 was purified from *E. coli*, a bacterium that also contains the ligand naturally. It was possible, that the elicitor was not IF1 but an interacting protein co-purified with IF1.

3.3.1 *In vitro* transcription and translation of IF1

To provide evidence that IF1 itself is the elicitor, it was produced using different techniques. To exclude the possibility of another bacterial protein being the ligand, IF1 was expressed *in vitro* using a coupled eukaryotic transcription and translation system (TnT), rabbit reticulocyte lysat. For this reaction, IF1 in pDEST42 is expressed under the control of the T7 promotor (2.3.2.7). The translated IF1 in the TnT master mix was used in an ethylene assay (Figure 5 and Figure 7). Like the *E. coli*-expressed recombinant IF1, *in vitro*-translated IF1 induced RLP32-dependent ethylene biosynthesis. As negative controls, *efr fls2*, *rlp23* and *rlp32* plants were treated with either MilliQ water, the TnT master mix and *in vitro*-translated Luciferase. None of these treatments elicited an ethylene response. As a positive control, the plants were treated with 1 µM nlp20, which elicited a RLP23-dependent ethylene response (Albert *et. al,* 2015).

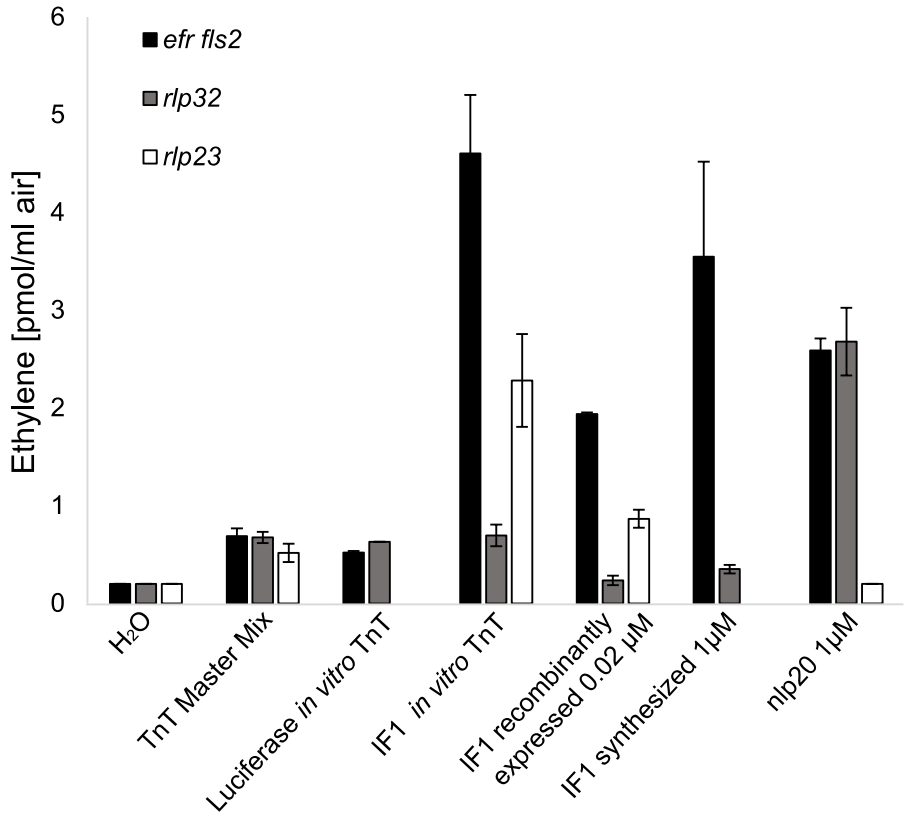

Figure 5: Characterization of IF1
Induction of ethylene biosynthesis in *efr fls2*, *rlp32* and *rlp23* plants in response to IF1 from various sources (*in vitro* transcribed and translated IF1, bacterially expressed recombinant IF1-6xHis-tag, and synthesized IF1). As negative controls, plants were treated with water, the master mix for the *in vitro* reaction and *in vitro* expressed luciferase. As a positive control, plants were treated with 1 µM nlp20. Bars represent average values ±S.D. (n=3). Leaf pieces from *efr fls2*, *rlp32* and *rlp23* plants were treated for 4 h. The experiment was performed twice.

3.3.2 Chemically synthesized IF1

As an additional approach to confirm the activity of IF1, we obtained full length IF1 produced by cell-free synthesis. The 72 amino acid protein (starting from methionine) was successfully synthesized by three companies: GenScript, Biomatik and KE biochem. Synthetic IF1 was dissolved in MilliQ water and used in an ethylene assay (Figure 5 and Figure 6 A and B). RLP32-dependent ethylene response could be observed for peptides obtained from all three companies. IF1 was therefore successfully produced using three different techniques (recombinant expression, *in vitro* translation and peptide synthesis). In addition, Dr. Isabell Albert was able to express active IF1 in *Pichia pastoris*. Altogether, IF1 preparations from different sources proved to be active in RLP32-dependent manner, indicating that IF1 cognate elicitor or RLP32.

3.3.3 Comparison of recombinantly expressed and synthesized IF1

Ethylene assays were further used to determine the EC_{50} concentration of IF1. *Efr fls2* plants were treated with different concentrations of IF1-6x His and synthesized full length IF1 (Figure 6 A). The EC_{50} values of the two IF1 preparations varied; the EC_{50} of the recombinantly expressed and purified IF1-6xHis is 0.55 nM whereas the EC_{50} of synthesized IF1 is 38.9 nM. The purity of the recombinantly expressed IF1 is very high (Figure 4 C and Figure 21: Supplement 1 A). During synthesis of full length IF1 shorter peptides can occur from aa chain breakage. It is likely that the concentration of synthesized active or full length IF1 is lower than calculated, because shorter, inactive peptides might also be present. This could lead to a skewed dose response curve and higher EC_{50} value.

IF1-6x His+N-terminal cysteine was produced in addition to IF1-6x His to serve as a ligand that could be biotinylated without losing its immunogenic activity. *Efr fls2* plants were treated with different concentrations of IF1-6x His and IF1-6x His+N-terminal cysteine (Figure 6 B) that were recombinantly expressed and purified in the same way (Figure 21: Supplement 1 A). The ethylene dose response curves resulting from the treatment with both IF1 versions overlap, indicating an identical immunogenic activity. The final concentration of both IF1 versions was too low to reach the saturated state of ethylene production, so the EC_{50} could not be calculated. IF1-6x His and IF1-6x His+N-terminal cysteine can be used interchangeably in experiments.

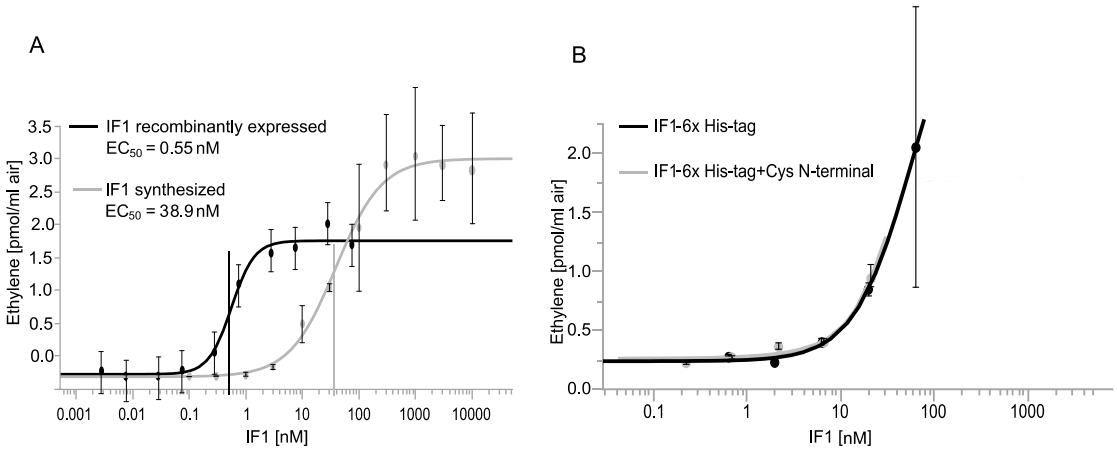

Figure 6: EC50 of IF1 synthesized and recombinantly expressed
A) Induction of ethylene biosynthesis in *efr fls2* plants in response to recombinantly expressed IF1-6xHis-tag or synthesized IF1. Each dot represents the average value ±S.D. (n=3). EC_{50} values and curve fit were calculated using Logistic 4P Rodbard Model comparison (four parametric logistic regression). **B)** Induction of ethylene biosynthesis in *efr fls2* plants in response to different concentrations of recombinantly expressed and purified IF1-6xHis-tag, IF1-6xHis-tag+N-terminal cysteine and synthesized native IF1. Each dot represents the average value ±S.D. (n=3). EC_{50} values and curve fit were calculated using Logistic 3P Rodbard Model comparison (three parametric logistic regression). Leaf pieces from *efr fls2* plants were treated for 4 h. The experiment was performed three times with similar results.

3.3.4 Effect of heat treatment and SDS-treatment on the immunogenic activity of IF1

When the native IF1 was purified from bacterial extract before its identification, a heat treatment was part of the purification procedure to inactivate proteases. After heat treatment, IF1 showed similar activity as untreated IF1 (Figure 7). This suggests that the secondary and tertiary structure of IF1 is not required for its immunogenic activity. In its native form, a globular protein is folded into a very compact, highly ordered configuration. The structure of proteins is disrupted by heat because the non-covalent bonds between amino acids are broken, reorganizing all levels of the protein structure (Tanford, 1970; Davis and Williams, 1998).

SDS also denatures proteins by covering the intrinsic charge of the protein (Tanford, 1970). Recombinantly expressed and purified IF1 was heated at 95°C with or without 0.5% SDS for 10 min to test the influence of denaturing conditions on the IF1 activity. *Efr fls2* plants were elicited with different concentrations of untreated, heat treated or heat and SDS-treated IF1 (Figure 7 A). As negative controls the plants were treated with either MilliQ water or SDS (Figure 1Figure 7 B).

The ethylene dose response curves resulting from the different treatments show that IF1 did not lose its immunogenic activity (Figure 7 A), but the curves of the treated IF1 both shifted (IF1 untreated EC_{50}=0.5 nM, IF1 95°C EC_{50}=1.2 nM, IF1 95°C + 0.5% SDS EC_{50}=5.5 nM), reaching the EC_{50} at around double to 10-fold higher concentrations compared to the untreated IF1 (Figure 7 A). *Pichia pastoris*-produced, purified IF1 was heated at 95°C. The EC_{50} of heat-treated IF1 (252.4 nM) was around 40 times higher than the EC_{50} of the untreated IF1 (5.5 nM) (data produced by Dr. Isabel Albert, personal conversation). This confirms the observation in this work, that the activity is lowered under the influence of heat. The shift of the dose response curves after heat treatment suggests that the structure of IF1 plays a role in the binding of the ligand to the receptor. IF1 might refold to a degree after cooling down or the structure might not have been completely denatured under the influence of high temperature as IF1 is a highly globular protein.

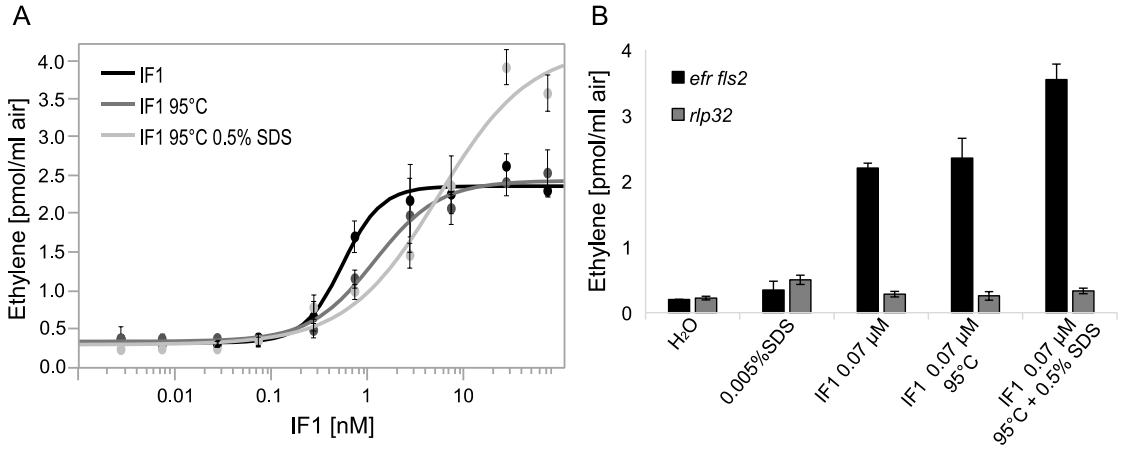

Figure 7: Effect of treatment with heat and SDS on IF1
A) Induction of ethylene biosynthesis in *efr fls2* plants in response to different concentrations of recombinantly expressed IF1-6xHis-tag, heat-treated IF1-6xHis-tag ± SDS-treatment. Each dot represents the average value ±S.D. (n=3). EC_{50} values and curve fit were calculated using Logistic 4P Rodbard Model comparison (four parametric logistic regression). **B)** Induction of ethylene biosynthesis in *efr fls2* and *rlp32* plants in response to IF1 recombinantly expressed IF1-6xHis-tag, IF1-6xHis-tag was also tested for immunogenicity following heat/SDS treatment. As negative controls, plants were treated with MilliQ water and the SDS in the same concentration, that was used for the treatment. Bars represent average values ±S.D. (n=3). Leaf pieces from *efr fls2* plants were treated for 4 h. The experiment was performed two times with similar results.

3.4 Attempt to identify the epitope of IF1 that is recognized by RLP32

Pattern recognition receptors (PRR) can bind to an array of substances derived from microorganisms. The recognized patterns do not necessarily need to be the complete molecule. Smaller epitopes are typically recognized by the receptor. For proteobacterial cold shock protein, a 22 aa fragment was identified as epitope recognized by CORE (Wang *et al.*, 2016). Likewise, a 20 aa long fragment is the immunogenic core of NEP-like protein recognized by RLP23 (Böhm *et al.*, 2014).

3.4.1 Immunogenic activity of IF1 peptides

Minimum immunogenic epitopes of proteinaceous PRR-ligands have been successfully identified in the past by investigation of overlapping shorter peptides. Eight overlapping 30 aa peptides as well as a 35 aa N-terminal peptide, a 37 aa C-terminal peptide and a 45 aa C-terminal peptide (N27-R71) were synthesized by GenScript (Figure 8 A). None of the peptides elicited ethylene biosynthesis in *efr fls2* or *rlp32* leaves treated with 1 µM of the peptides (Figure 8 B). These results further indicate that the structure of IF1 may be required for its immunogenic activity. The structure of *E. coli* IF1 was determined by (Sette *et al.*, 1997) using multidimensional NMR spectroscopy. IF1 is characterized by a five-stranded beta-barrel and a short 3_{10} alpha helix connecting beta strands 3 and 4, which shows higher flexibility than the beta barrel (Figure 11 E).

Five aa at the C-terminus and 5 aa at the N-terminus are not involved in the secondary structures (Figure 8 A). Peptides lacking either the first (I6-R71) or the last 5 aa (A1-I66) were recombinantly expressed with a C-terminal 6xHis-tag in *E. coli* BL21AI and purified as described above for full-length IF1 (2.3.2.2.1) (Figure 21 Supplement 1A). *Efr fls2* and *rlp32* plants were treated with 10 nM of the purified peptides and 20 nM full length recombinant IF1. Full length IF1 and N-terminally truncated IF1 I6-R71 induced RLP32-dependent ethylene biosynthesis, whereas C-terminally truncated IF1 A1-I66 did not (Figure 11 B).

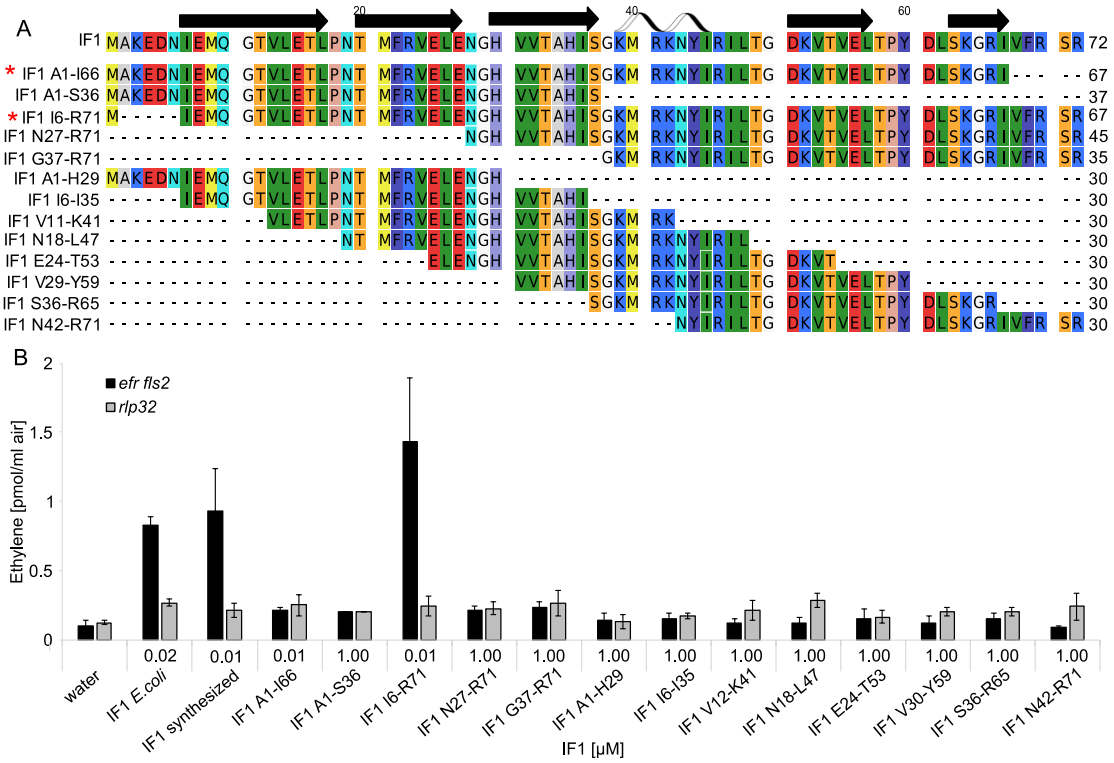

Figure 8: Near full length IF1 is required for the induction of immune response
A) Alignment of IF1 peptides. On top of the alignment, arrows (beta sheets) and a helix (alpha helix) indicate secondary structures. The red asterisks indicate IF1 peptides which were recombinantly expressed. The unmarked peptides were synthesized. **B)** Induction of ethylene biosynthesis in *efr fls2* and *rlp32* plants in response to IF1 peptides. Each bar represents the average value ±S.D. (n=3). Leaf pieces from different plant species were treated for 4 h. The experiment was performed two times with similar results.

3.4.2 Comparison between IF1 and IF1 I6-R71

The activities of IF1 and IF1 I6-R71 were compared in a dose response assay (Figure 9). The concentration of the peptides was not high enough to reach saturation in ethylene production in *efr fls2* plants, but lower concentrations of IF1 I6-R71 were needed to induce ethylene response compared to the full length IF1. These results above indicate that nearly the entire IF1 is needed to induce ethylene response.

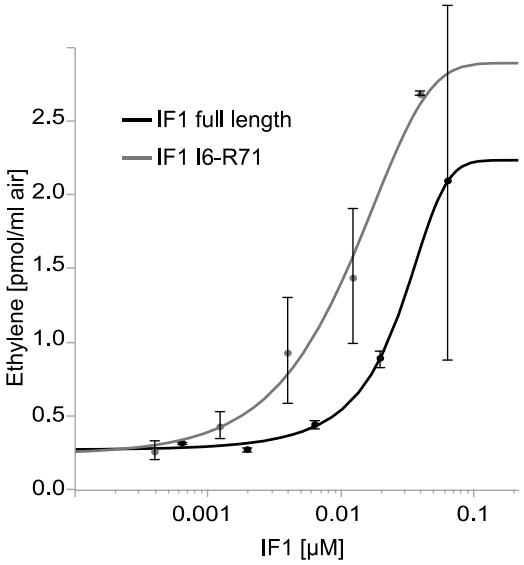

Figure 9: IF1 I6-R71 dose response curve
C) Induction of ethylene biosynthesis in *efr fls2* plants in response to different concentrations of recombinantly expressed IF1-6xHis-tag or IF1 (I6-R71)-6xHis-tag. Each dot represents the average value ±S.D. (n=3). Curve fits were calculated using Logistic 4P Rodbard Model comparison (four parametric logistic regression). Leaf pieces from *efr fls2* plants were treated for 4 h. The experiment was performed once.

3.4.3 Inhibitory effect of long peptides

It has been shown that shorter fragments of immunogenic peptides inhibit activation of plant responses by longer fragments derived from the same pattern. The peptide elf12 antagonizes elicitor activity of EF-Tu (Kunze *et al.*, 2004). A C-terminally truncated form of flg22 antagonizes its elicitor activity (Meindl *et al.*, 2000; Bauer *et al.*, 2001). It is possible, that shorter IF1 peptides bind to the receptor, but are not sufficient to lead to signal transduction and defense activation. To test if the shorter peptides have an inhibitory effect on the induction of the immune response by IF1, *efr fls2* plants were treated with 1 µM of synthesized peptide fragments mixed with 10 nM, 33.3 nM IF1 or MilliQ water. None of the peptides have an inhibitory effect on the induction of ethylene. On the contrary, N27-R71 enhances the IF1-induced ethylene response (Figure 10) for unknown reasons.

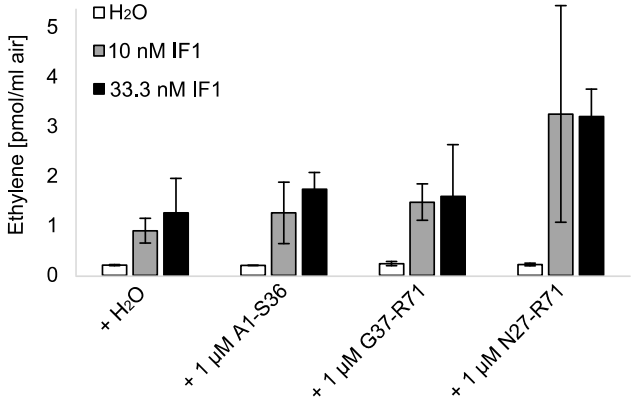

Figure 10: Inhibitory effect of synthetic peptide fragments
Induction of ethylene biosynthesis in *efr fls2* plants in response to either 0,03 µM or 0,01 µM IF1 6xHis-tag adding peptides. Each bar represents the average value ±S.D. (n=3). Leaf pieces from *efr fls2* plants were treated for 4 h. The experiment was performed two times with similar results.

3.5 IF1 is highly conserved in *Proteobacteria*

3.5.1 Analysis of conservation of IF1

IF1 plays an important role in bacterial biology, therefore it is conserved in prokaryotic translational apparatus. The inactivation of IF1 cannot be tolerated by the cell without loss of viability (Cummings and Hershey, 1994), indicating that the activity of IF1 must be essential for the cell. As most of the short peptide versions of IF1 were not immunogenically active, the IF1 sequence between organisms was compared via BLASTp to gain insight into a potential three-dimensional structured epitope that is recognized by RLP32. The amino acid sequence of IF1 is conserved amongst *Proteobacteria* (Figure 11 A). The closer the *Proteobacteria* are related to one another, the higher is the conservation of the IF1 amino acid sequence. IF1 from *Ralstonia solanacearum* and IF1 from *E. coli* share 75% of the amino acid sequence. Analyzing the conservation of the different IF1 sequences, no stretch longer than approximately 10 aa seems to be strictly conserved. It should be noted though, that primary sequence polymorphisms may not necessarily result in changes in the secondary or tertiary structure of IF1.

3.5.2 Immunogenic activity of IF1 derived from different *Proteobacteria*

To investigate the immunogenic activity of IF1 derived from other *Proteobacteria*, two other organisms, *A. tumefaciens* and *P. syringae*, that were not to closely related to *E. coli* and that were available in the lab, were picked as template organisms for cloning IF1 from their genomic DNA (Figure 11 A and B). *A. tumefaciens* and *E. coli* share around 60% of the amino acids, whereas 85% of the sequence of IF1 of *P. syringae* and *E. coli* are identical. IF1-6xHis *P. syringae* and *A. tumefaciens* were successfully expressed in BL21AI and purified as previously described for *E. coli* IF1 (2.3.2.2.1) (Figure 21 Supplement Figure 1 A). *Efr fls2* plants were treated with different concentrations of the IF1 from all three species. Although the necessary concentration to saturate ethylene biosynthesis was not reached, the dose response curves almost overlapped, suggesting similar immunogenic activities of IF1 from all species (Figure 11 C).

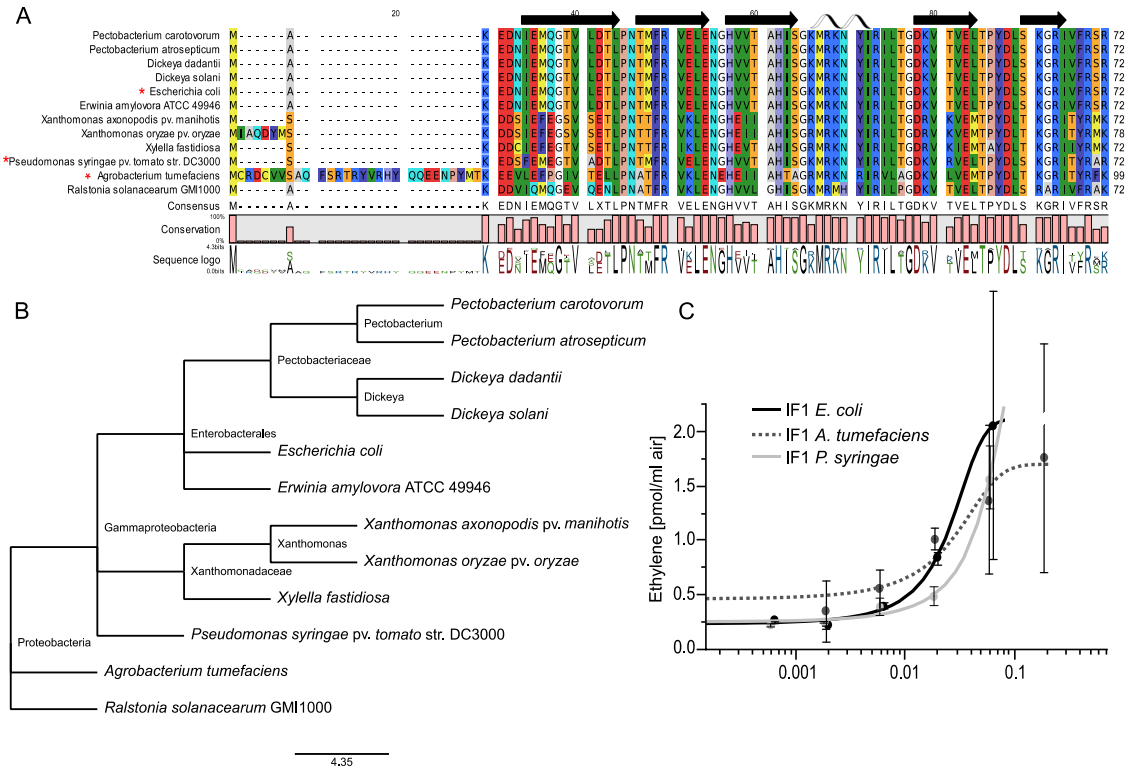

Figure 11: IF1 is highly conserved in *Proteobacteria*
A) Alignment of amino acid sequence of IF1 from different *Proteobacteria*. On top of the alignment arrows (beta sheets) and a helix (alpha helix) indicate which amino acids are forming the secondary structures. The red asterisks indicate the organisms from which the IF1 was cloned and recombinantly expressed. **B)** Common taxonomy tree (phylogenetic tree) of *Proteobacteria* was created using the NCBI Taxonomy common tree tool. **C)** Induction of ethylene biosynthesis in *efr fls2* plants in response to different concentrations of recombinantly expressed and purified IF1-6xHis-tag derived from *A. tumefaciens*, *E. coli* and *P. syringae*. Each dot represents the average value ±S.D. (n=3). Leaf pieces from *efr fls2* plants were treated for 4 h. Curve fits were calculated using Logistic 4P Rodbard Model comparison (four parametric logistic regression). The experiment was performed twice with similar results.

3.5.3 Tertiary structure prediction of IF1 derived from different *Proteobacteria*

The 3D structure of IF1 from *A. tumefaciens* and *P. syringae* were predicted with I-TASSER using the *E. coli* IF1 structure (Sette *et al.*, 1997) as a template. IF1 derived from *A. tumefaciens* has additional 22 aa at the N-terminus that do not seem to form secondary structures (Figure 12 A). All predicted 3D structures are very similar to the structure of IF1 derived from *E. coli* even though the amino acid sequences differ from one another (Figure 11 A). This is in agreement with RLP32-dependent immunogenic activities of these IF1 homologs.

All IF1 sequences of the different *Proteobacteria* shown in Figure 11 A and B were compared, and each residue was assigned a conservation score. These scores were mapped onto the structure of IF1 and displayed using a rainbow color code with red indicating high conservation and blue indicating low conservation. The alpha helix seems to be especially highly conserved (Figure 12 B). Parts of, but not entire, beta sheet are highly conserved.

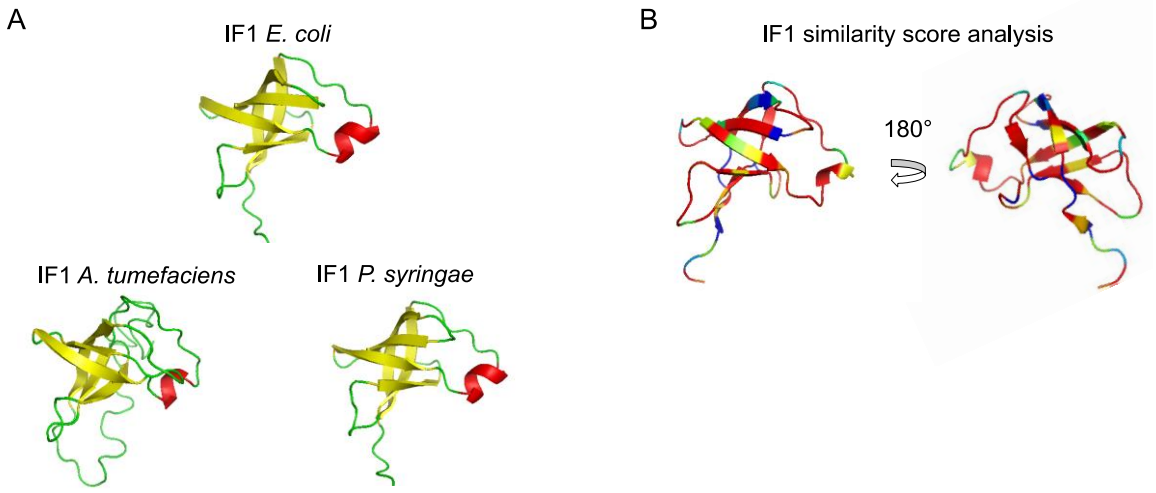

Figure 12: IF1 structure prediction
A) Iterative threading assembly refinement (I-TASSER) 3D structure prediction of IF1 derived from *E. coli, P. syringae* and *A. tumefaciens* as ribbon presentation (yellow=beta sheet, red=alpha helix). As a template, the NMR structure of IF1 derived from *E. coli* was used (Sette *et al.*, 1997).
B) Ribbon representation of IF1, colored by conservation (blue=low B-factors; red=high B-factors). Conservation scores for each amino acid were calculated and mapped onto the IF1 structure with Easy Sequencing in PostScript (ESPript 2.2). Ribbon presentation was done with PYMOL.

3.5.4 IF1 R69 mutations still induce ethylene biosynthesis

C-terminally truncated IF1 A1-I66 did not trigger ethylene response in *efr fls2* plants, indicating that one or more amino acids in this region are crucial for binding of IF1 to RLP32. Phylogenetic comparisons revealed that an arginine within this sequence, R69, is conserved among all *Proteobacteria* (Figure 11 A and Figure 12 B).

To test if R69 is essential for the binding of IF1 to the receptor, R69 was mutated to alanine, an uncharged amino acid; glutamate, a negatively charged amino acid and lysine, a positively charged amino acid. All IF1 mutations, as well as the native IF1 were recombinantly expressed in *E. coli* BL21AI and purified like IF1-6xHis (2.3.2.2.1). *Efr fls2* and *rlp32* plants were treated with the mutated versions of IF1 as well as the native version (Figure 21 Supplement 1 B). All mutations induced RLP32-dependent ethylene response (Figure 13) in a similar dose response as the native IF1. Thus, R69 is not crucial for the binding of IF1 to the receptor.

The amino acid at position 71 is either arginine or lysine, which are both positively charged and could be important for the binding of the ligand to the receptor. The R/K71 could be mutated, expressed and tested like the R69 mutations, for ethylene induction.

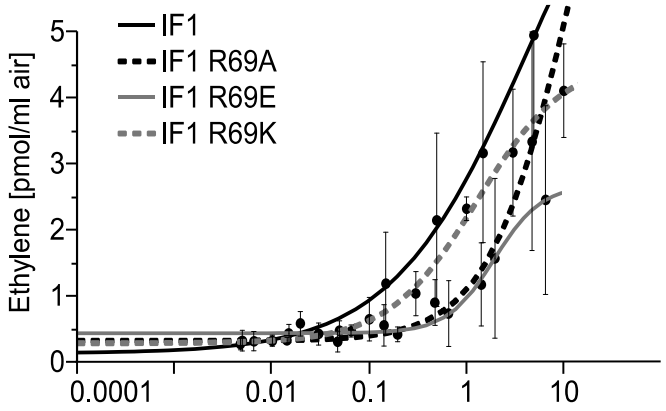

Figure 13: Point mutations of IF1
Induction of ethylene biosynthesis in *efr fls2* and *rlp32* plants in response to different concentrations of recombinantly expressed and purified IF1-6xHis-tag, and mutated IF1 (R69A/E/K)-6xHis-tag. Bars represent average value ±S.D. (n=4). Leaf pieces from *efr fls2* plants were treated for 4 h. Curve fits were calculated using Logistic 4P Rodbard Model comparison (four parametric logistic regression). The experiment was performed twice with similar results.

3.6 RLP32 binds IF1 with high specificity

PRRs physically interact with their ligands (Böhm *et al.*, 2014). A well-characterized receptor -ligand pair is RLP23 and nlp20 or nlp24 (Albert *et al.*, 2015), which serves as a positive control in the following assays.

To show direct and specific binding of IF1 to RLP32, RLP32-GFP was stably expressed and RLP23-GFP was transiently expressed in *N. benthamiana* (2.3.1.14). Both receptors were expressed under the control of the 35S promotor. IF1-6xHis + biotinylated cysteine was used as a ligand, because biotin is detectable at very low concentrations by protein blotting using Streptavidin-AP (Figure 4 C). IF1 biotinylated on the engineered N-terminal cysteine showed the same specific activity as IF1-6xHis in ethylene assays (Figure 4 B). Receptor-expressing plants were infiltrated with 100 nM of either biotinylated IF1 as a ligand for RLP32 or nlp24 as a ligand for RLP23 (Albert *et al.*, 2015). As a negative control, the plants were infiltrated with 10 mM $MgCl_2$. Five minutes after infiltration, the ligand was chemically crosslinked to the receptor and the leaves were harvested (2.3.2.6). The receptors were immunoprecipitated with anti-GFP agarose beads (2.3.1.15, 2.3.1.16). Binding of the ligand to the receptor could be confirmed in western blots with streptavidin. The receptor could be detected on the western blot using GFP-specific antiserum (2.3.2.12).

The western blot of the protein input before immunoprecipitation showed that a higher concentration of RLP23-GFP than of RLP32-GFP was expressed in *N. benthamiana* even though the gels were loaded with equal amount of total protein (Figure 14 A Ponceau). After the immunoprecipitation, RLP23-GFP was enriched in a higher concentration than RLP32-GFP. Likewise, the band representing biotinylated nlp24 is much stronger than the band representing biotinylated IF1 (Figure 14 A). However, IF1 was successfully pulled down together with RLP32 three times. This proves that RLP32 physically interacts with IF1.

To examine the specificity of the binding, 100 nM biotinylated IF1 was co-infiltrated with 10 µM of unlabeled synthesized IF1 to compete for binding of biotinylated ligand. The band representing IF1 is much weaker when unlabeled IF1 is added (Figure 14 B). As a positive control RLP32-GFP expressing *N. benthamiana* was infiltrated with 100 nM biotinylated nlp24 or 100 nM biotinylated IF1 and chemically crosslinked. Only biotinylated nlp24, but not biotinylated IF1, could be pulled down with RLP23-GFP. The result was

confirmed repeatedly by Dr. Isabel Albert. This suggests a specific interaction between IF1 and RLP32.

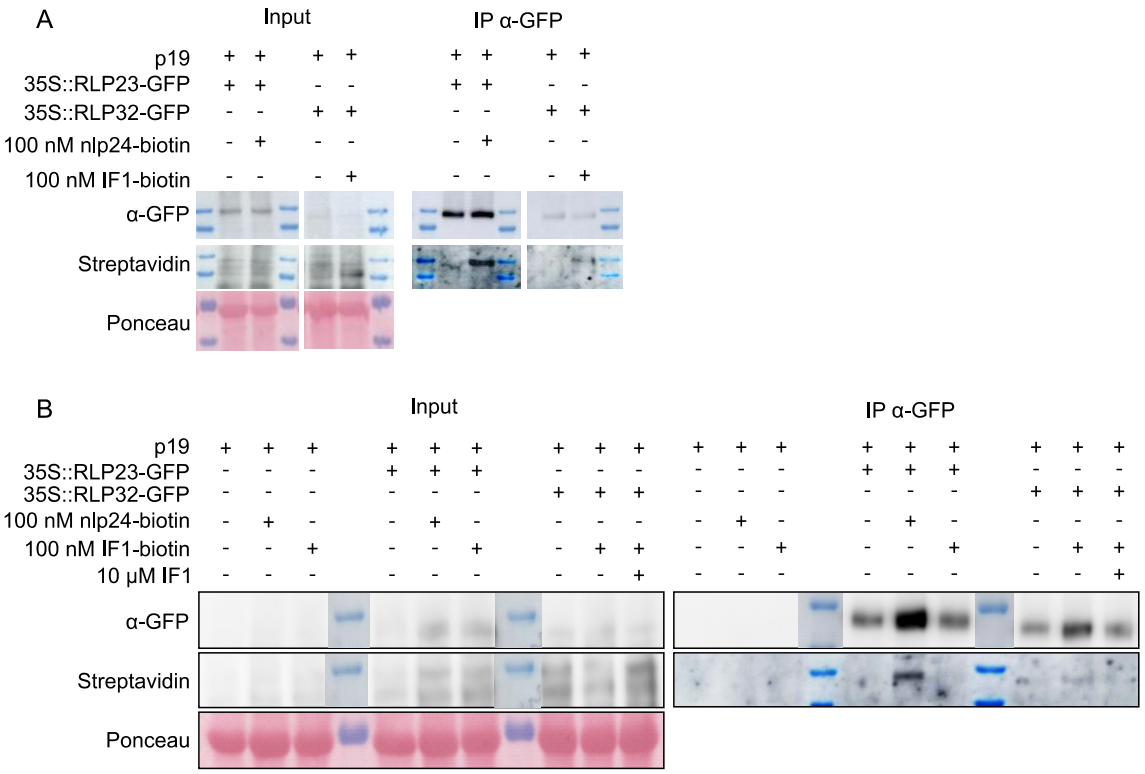

Figure 14: IF1 specifically binds to RLP32 *in planta*
A) Western Bot analysis of proteins obtained by crosslinking assays using RLP32-GFP as a receptor and 100 nM recombinant F1-6xHis-tag + biotinylated N-terminal cysteine as a ligand. As a positive control, RLP23–GFP was used as receptor and 100 nM synthesized biotinylated nlp24 (nlp24-bio) as ligand. As a negative control, 10 mM $MgCl_2$ was infiltrated instead of a ligand. The experiment was performed three times with similar results. **B)** 10 µM unlabeled IF1 was co-infiltrated with biotinylated IF1. The experiment was performed once. Dr. Isabel Albert repeated this experiment three times with synthetic biotinylated IF1 instead of purified biotinylated IF1 with similar results **A)** and **B)** *N. benthamiana* plants were either stably expressing RLP32-GFP or transiently expressing RLP23-GFP. The membranes were stained with Ponceau prior to western blotting with an antibody against GFP (indicating the presence of the receptor) or Streptavidin (indicating the presence of the ligand). The receptor was immunoprecipitated with GFP-trap agarose beads.

3.7 RLP32 forms a complex with SOBIR1, BAK1 and other SERK family members

As part of a common molecular activation mechanism, ligand binding of LRR receptor kinases like BRI1, FLS2 and EFR triggers rapid complex formation with a second type of LRR receptor kinase such as BAK1/SERK3 or another member of the SERK family (Chinchilla *et al.*, 2009). As a receptor like protein, RLP32 lacks any intracellular signaling domain. RLP32 requires co-receptors for the signal transduction into the cell after recognition of IF1 in the apoplast.

The LRR-RK SOBIR1, was shown to be involved in immune signaling mediated by LRR RLPs (Gust and Felix, 2014) or to interact with them in Arabidopsis, such as RLP1/REMAX and RLP42/RBPG1 (Jehle *et al.*, 2013; Zhang *et al.*, 2013; Zhang *et al.*, 2014), RLP23/nlp20 (Albert *et al.*, 2015) and RLP30/SCFE1 (Zhang *et al.*, 2013). The LRR-RK SERK3/BAK1 is a member of the subclass of subfamily II LRR-RKs with five closely related members and a well-known interactor of the LRR-RKs FLS2 and EFR, mediating immune signaling upon perception of bacterial flg22 or elf18 in Arabidopsis (Chinchilla *et al.*, 2007; Schwessinger *et al.*, 2011). RLP30-dependent signaling of SCFE1, (Zhang *et al.*, 2013) and RLP23-dependent signalling of nlp20 (Albert *et al.*, 2015) require both BAK1 and SOBIR1. Functional redundancy among members of the SERK protein family is a known phenomenon (Albrecht *et al.*, 2008); BAK1 and SERK4/BKK1 are involved in nlp20-induced signaling events (Albert *et al.*, 2015).

Dr. Li Fan treated SOBIR1-mutants, BAK1-mutants, BKK1-mutants as well as BAK1/BKK1-mutants of *A. thaliana* with IF1 (then RsE) (Fan, 2015). Ethylene production could be observed in BAK1 and BKK1- mutants, but not in the double mutant or SOBIR1-mutant (Figure 21 Supplement 1 B). This is a first indicator that RLP32 requires SOBIR1 and either BAK1 or BKK1 to successfully induce an immune response upon IF1 detection.

To investigate whether RLP32 forms stable complexes with these kinases all members of the SERK-family were included in a Co-immunoprecipitation experiment (Transient transformation of *N. benthamiana* (2.3.1.14, 2.3.1.15, 2.3.1.16). The C-terminal tagged proteins (SERK(1-5)-myc, SOBIR1-HA and RLP32-GFP) were overexpressed together in *N. benthamiana* for two days and pulled down using GFP-trap beads both in the absence and presence of the ligand IF1 (Figure 15). The presence of the proteins was detected via Western blots using tag-specific antisera.

SOBIR1 could be pulled down with RLP32 independent from the presence of the ligand, the same could be observed for SERK1 and 2. RLP32 and SERK3 only form a complex in the presence of IF1, as the band representing SERK3 is much stronger when the leaves were infiltrated with the ligand. Only weak bands are visible for SERK4 and 5, they did not form a complex with RLP32.

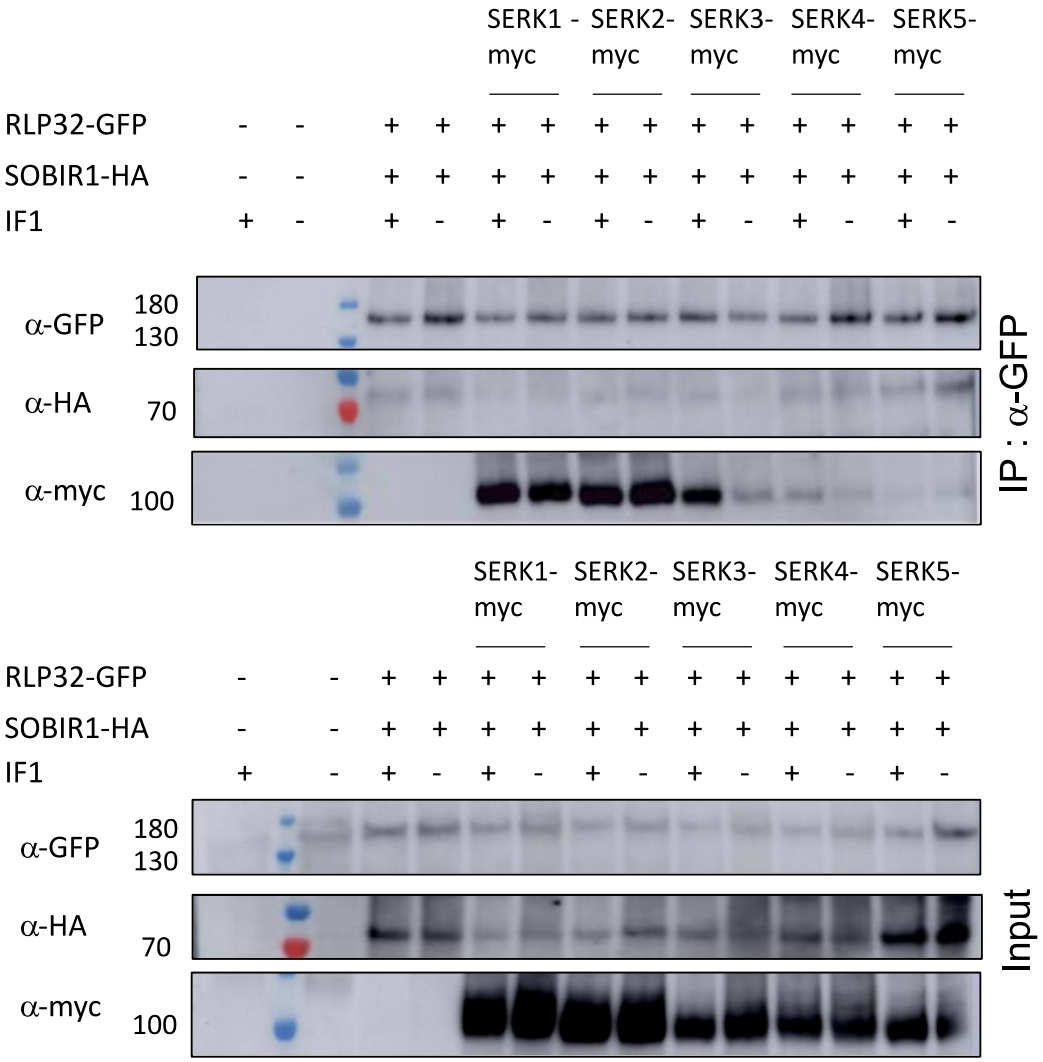

Figure 15: RLP32 interacts constitutively with SOBIR1 and, in an IF1-dependent manner, with BAK1 (SERK3)

Western Blot analysis with tag-specific antisera of Myc-tagged SERK1, SERK2, SERK3/BAK1, SERK4/BKK1 and SERK5 proteins transiently co-expressed with SOBIR1–HA and RLP23–GFP in *N. benthamiana* for 2 days and co-immunoprecipitated using GFP-trap beads. Leaf material was collected 5 minutes after infiltration with purified IF1 from lysed *E. coli* by Dr. Eric Melzer in a final dilution of 1:200 or 10mM $MgCl_2$ as a negative control. The experiment was performed three times with similar results.

3.8 Screening of various plant families for their ability to recognize lF1

Arabidopsis thaliana is able to detect lF1 through the receptor RLP32. To investigate how conserved lF1-surveillance is in different plant families, a collection of plants was tested for lF1-inducible ethylene production. (Figure 16 A). Leaf tissue was treated with 1 µM lF1, 1 µM flg22 (positive control), or 1 µM water (negative control).

A. thaliana is part of the *Brassicaceae* family, so other members of this family were tested, namely *Capsella rubella*, *Brassica napus*, *Brassica oleracea, Brassica oleracea var. botrytis, Arabis alpina, Thellungiella halophila* (Figure 16 B). Interestingly, no immune response to lF1 was triggered in the closest relative to *A. thaliana*, *Capsella rubella*. A low ethylene response was triggered by lF1 in *Brassica napus*. A close relative to *Brassica napus*, *Brassica oleracea*, showed the highest ethylene production after lF1 elicitation, but in *Brassica oleracea var. botrytis* no ethylene production was observed. *Brassica oleracea var. botrytis* is a cultivated variant of *Brassica oleracea* (Figure 16 A). The receptor might have been lost through mutation while breeding *Brassica oleracea var. botrytis*.

The only monocot plant in the collection, *Commelina communis*, did not produce ethylene after either lF1 or flg22 treatment. The same was also observed in *Solenostemon scutellarioides* (Figure 16 A).

In tomato, ethylene response was triggered by lF1 in the cultivated tomato *Solanum lycopersicum*, but not in the wild tomato *Solanum pennellii*. No other members of the solanaceous plants were lF1-sensitive (Figure 16 A).

The sensitivity to lF1 is not very conserved even in the *Brassicaceae* family, this suggests the presence of the receptor RLP32 is evolutionary young.

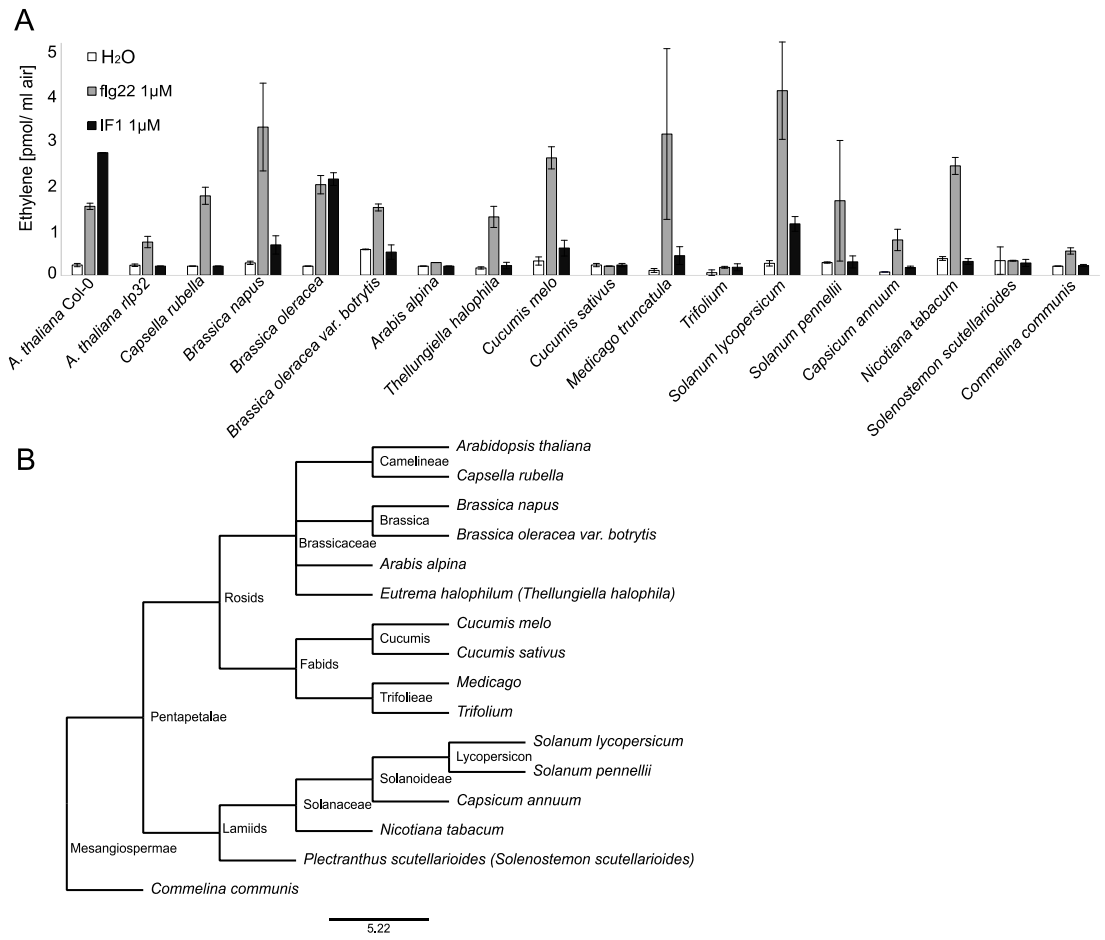

Figure 16: Identification of IF1-sensitive plants
A) Induction of ethylene biosynthesis in different plant species in response to 1 µM synthesized IF1, 1 µM flg22 (positive control) or MilliQ water (negative control). Leaf pieces from different plant species were treated for 4 h. Each bar represents the average value ±S.D. (n=3). The experiment was performed once. **B)** Common taxonomy tree (phylogenetic tree) of different plant species was created using the NCBI Taxonomy common tree tool.

3.8.1 Identification of the tomato chromosomal region encoding a putative IF1-recognizing receptor

The receptor RLP32, that is present in *A. thaliana* could not be found via BLASTp in the genome of either *S. lycopersicum* or *S. pennellii.* The plants were treated with different concentrations of synthesized IF1. The EC_{50} value of synthesized IF1 in *A. thaliana* is approximately 40 nM (Figure 6 B), but In *S. lycopersicum* ethylene response was triggered only with at least 1 µM. There might be an alternative receptor to RLP32 present in *S. lycopersicum. S. lycopersicum* and *S. pennellii* were crossed producing introgression lines that have insertions from *S. pennellii* in the genome of *S. lycopersicum* (Chitwood *et al.,* 2013). These introgression lines were sequenced identifying the positions of insertions from *S. pennellii* in the genome of *S. lycopersicum.* The introgression lines were screened for IF1 responsiveness to identify a region in the genome that can be mapped to IF1 sensitivity. Only the introgression lines 7-4 and 7-5 were not producing ethylene when treated with IF1 (Figure 17). Martin Boehme confirmed this result twice. The line 7-5 contains a 3.663 Mbp insertion of *S. pennellii* on the 7th chromosome which is also present in 7-4. There are 14 receptor candidates present in this region that could be candidates for the IF1 detecting receptors.

To find the receptor that recognizes IF1 in tomato, these receptor candidates could be transiently expressed in *N. benthamiana*, prior to elicitation of ethylene biosynthesis by IF1. The correct receptor could be transformed into *S. pennellii* to prove whether it would confer IF1 sensitivity to otherwise insensitive *S. pennellii.*

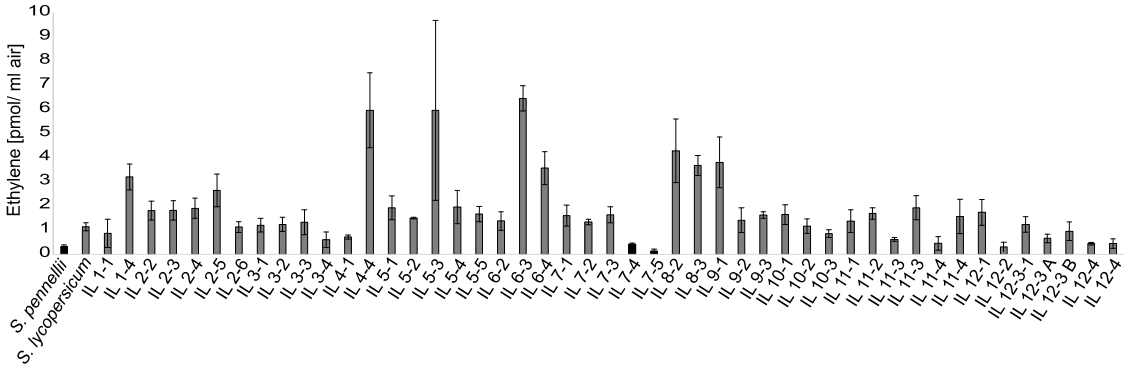

Figure 17: Screening of tomato introgression lines
Induction of ethylene biosynthesis in different plant species in response to 1 µM synthesized IF1. Each bar represents the average value ±S.D. (n=3). Leaf pieces from different tomato introgression lines and wildtype plants were treated with 1 µM IF1 for 4 h. The experiment was performed once. Martin Boehme repeated the experiment twice, only using the tomato lines IL7-4, 7-5, 11-4, 12-2 and 12-4

3.9 Complementation of insensitive plants with functional RLP32

Dr. Li Fan identified five *A. thaliana* ecotypes as IF1 insensitive, ICE21, ICE73, Mr-0, Dog4 and Yeg-1, in the ethylene induction assay. An early stop codon in RLP32 was detected in the ecotype Dog-4 and a truncated promoter region of RLP32 in ecotype ICE73 leads to a lowered expression of the receptor. She also identified *rlp32* mutants of *A. thaliana* to be insensitive to IF1.

To confirm that IF1 triggered immune response is RLP32-dependent, insensitive plants were transformed with either RLP32±GFP under the control of the endogenous promotor or the 35S-promotor. As a negative control, *rlp32* plants were transformed with only GFP under the control of the 35S-promotor (2.3.1.11.2, 2.3.1.12, 2.3.1.13). Successful expression of RLP32-GFP (Figure 18 B) and GFP (Figure 18 E) was confirmed in Western blots with GFP-specific antiserum. Overexpression (Figure 18 A) as well as native expression of RLP32 (Figure 18 C) in the insensitive ecotype ICE73 led to IF1-sensitivity. Ethylene synthesis was also induced by IF1 in *rlp32* plants expressing RLP32 under the control of the endogenous promotor (Figure 18 C).

Overexpression of GFP in *rlp32* plants did not lead to a gain in sensitivity (Figure 18 D).

N. benthamiana plants were transformed to stably express RLP32-GFP under the control of the 35S-promotor, in consequence *N. benthamiana* plants also gained sensitivity towards IF1 (Figure 20 B).

As positive control, all plants were treated either with 1 µM nlp20 or flg22; as a negative control they were treated with MilliQ water.

In summary, these observations suggest that RLP32 is required for IF1-specific recognition and immune activation in *A. thaliana* and confers sensitivity across genus boundaries.

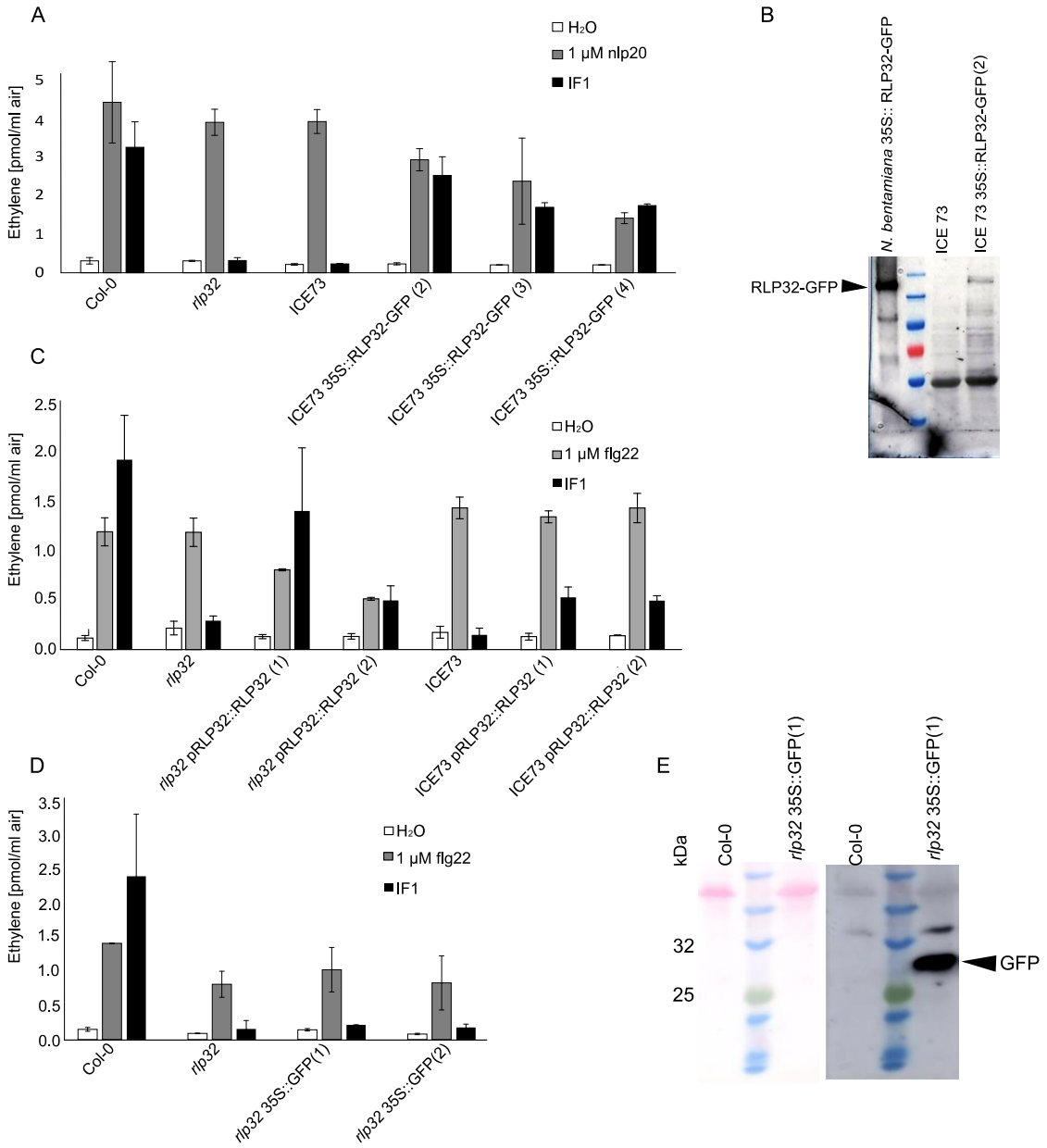

Figure 18: Complementation of IF1-insensitive plants with RLP32 restores responsiveness to IF1. **A) C) D)** Induction of ethylene biosynthesis in response to treatment with 1 µM flg22 (as positive control), MilliQ water (as negative control) and IF1 with unknown concentration purified from lysed *E. coli* by Dr. Eric Melzer. Each bar represents the average value ±S.D. (n=3) Leaf pieces from different plant species were treated for 4 h. The experiment was performed three times with similar results. **A)** *A. thaliana* ecotype ICE73 was stably transformed with 35S::RLP32-GFP. **B)** Western Blot stained with an antibody against GFP. RLP32-GFP was transiently expressed in *N. benthamiana.* RLP32-GFP was stably expressed in ICE73. **C)** *rlp32* and ICE73 were stably transformed with pRLP32::RLP32. **D)** *rlp32* was stably transformed with 35S::GFP. **E)** Ponceau stained membrane and Western Blot stained with an antibody against GFP. GFP was stably expressed in *rlp32.*

3.10 RLP32 is required for IF1-induced resistance against the bacterium Pseudomonas syringae pv. tomato DC3000

It is possible to enhance the immune response in plants by treating them with PAMPS inducing resistance before the actual microbial attack. This state of induced resistance is called priming (Conrath *et al.*, 2015). The receptor RLP32 is present in *A. thaliana* where it detects the bacterial protein IF1, inducing early immune response in the plant. To prove the hypothesis that RLP32 confers resistance against bacterial pathogens, *A. thaliana* ecotype Col-0 and two independent RLP32-knock-out mutant lines were primed with IF1, nlp20 or $MgCl_2$ one day prior to infection with *Pseudomonas syringae* pv. *tomato* DC3000 (*Pst*) (2.3.3.1, 2.3.3.2). $MgCl_2$ serves a negative control, whereas nlp20-priming was previously described to reduce *Pst*-growth in RLP23-expressing plants like *A. thaliana* (Albert *et al.*, 2015).

Three days after the infection the bacterial growth was significantly reduced in all plants primed with nlp20 compared to mock-treated plants as expected (Figure 4 Figure 19). After IF1 priming, significant growth reduction of *Pst* could be observed only in Col-0 plants but not in the RLP32 knock-out mutant plants compared to mock-treated plants (Figure 19) (2.3.5). This proves the hypothesis that RLP32 confers resistance *A. thaliana* against *P. syringae* which contain IF1.

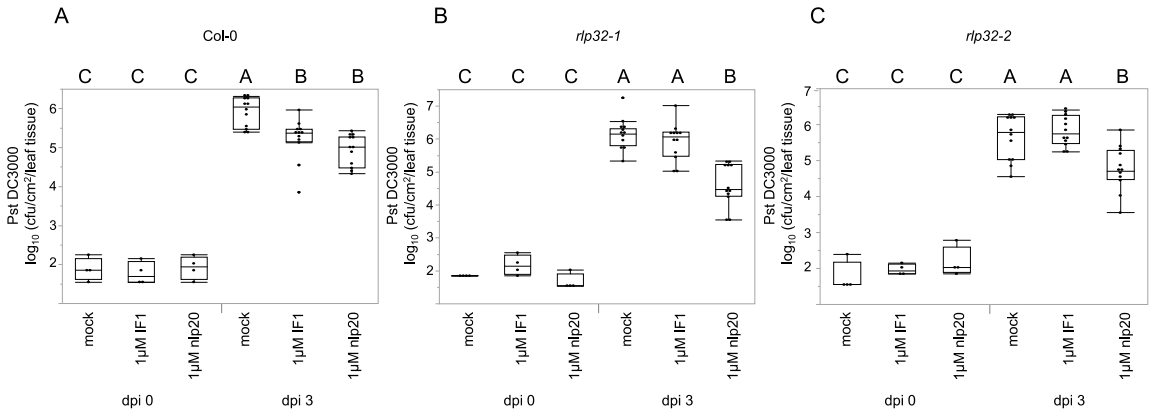

Figure 19: RLP32 -mediated priming of IF1 in *A. thaliana.*
Bacterial growth rates in *A. thaliana* Col-0 **A)** *rlp32-1* **B)** and *rlp32*-2 **C)** genotypes 0 and 3 dpi with *Pseudomonas syringae* pv. *tomato* DC3000. Priming of plants with 1 µM IF, 1 µM nlp20 (as positive control) or 10 mM $MgCl_2$ (as negative control) was performed 24 hours prior to inoculation with $1x10^4$ cfu/ml. Box plots show the minimum, first quartile, median, third quartile, and a maximum of log cfu/cm^2 (n=4 from 2 plants for 0 dpi n=12 from 6 plants for 3 dpi). Labels A-C indicate homogenous groups according to post-hoc comparisons following one-way ANOVA (Tukey's test multiple comparison analysis at a probability level of $p < 0.05$. The experiment was performed three times with similar results.

3.11 Stable expression of RLP32 in *N. benthamiana* confers enhanced resistance against *Pseudomonas syringae* pv. tomato hrcC-

There are several examples of host plants gaining resistance by transfer of immune receptors from other plants which are resistant to a pathogen. When EFR was transferred from *A. thaliana* into tomato, the plants gained resistance against a broad spectrum of bacterial infection in the field (Lacombe *et al.*, 2010). The interfamily transfer of immune receptors to create resistant plants is a possible tool for agriculture to decrease losses in harvest due to infection.

Nicotiana benthamiana lacks RLP32 and is susceptible to several proteobacterial pathogens like *P. syringae* pv. *tomato*. To investigate if *N. benthamiana* plants expressing RLP32 are able to resist the attack by Protobacteria such as *Pst,* transgenic plants (2.3.1.11.1) as well as *N. benthamiana* wild type plants were infected with *Pst* hrcC-.

The *N. benthamiana* plants were tested for functional RLP32 by eliciting the plants with 1 µM lF1 and measuring the ethylene production after 4h; as a positive control all plants were elicited with 1 µM flg22. In all *N. benthamiana* plants, ethylene production could be observed by flg22 elicitation, whereas ethylene production after lF1 elicitation could only be observed in *N. benthamiana* plants expressing RLP32 (Figure 20 B). Two transgenic RLP32-expressing lines with independent transformation events were chosen as a model system for the infection assay.

The leaves of 6-week-old *N. benthamiana* wild type plants and two independent RLP32-expressing lines were infected with *P. syringae* DC3000 hrcC-. This strain, which lacks the type lll secretion system, was chosen because the wild type strain, *Pst*, proliferated too quickly to detect a significant difference in bacterial growth between the wild type plants and the transgenic plants. Four days after the infection, the bacterial growth of *Pst* hrcC- was significantly reduced in both RLP32-expressing *N. benthamiana* lines compared to the wild type plants (Figure 20 A). This observation suggests that RLP32 might contribute to resistance to proteobacterial pathogens. RLP32 is thus a viable candidate to be transferred into crop plants to fend off proteobacterial pathogens in the field.

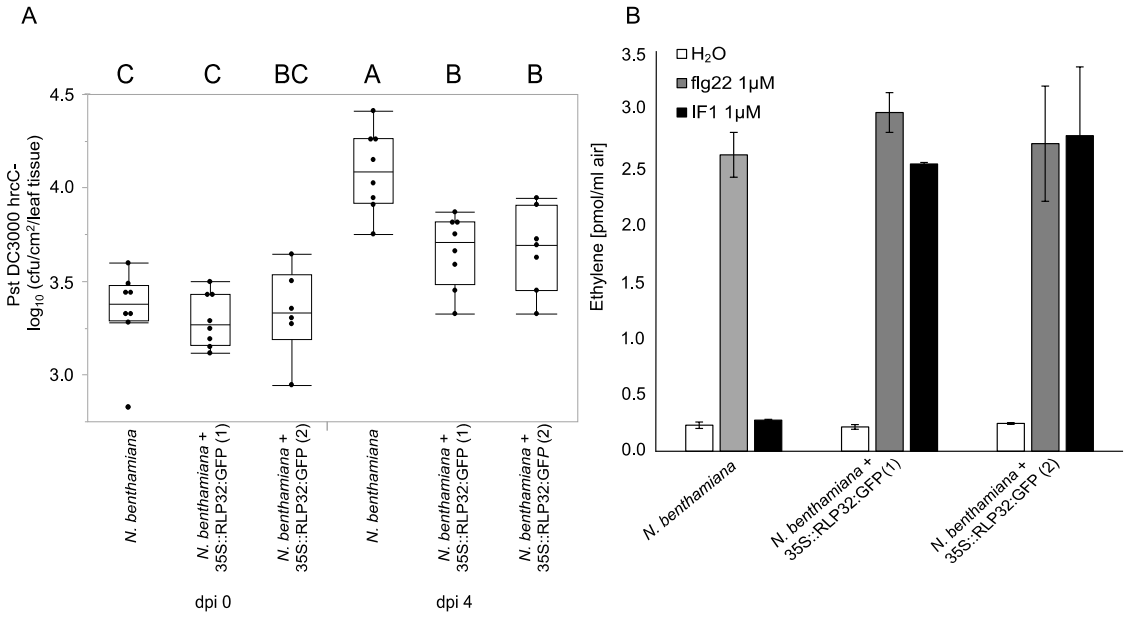

Figure 20: RLP32-mediated resistance in *N. benthamiana* plants
A) Bacterial growth of *Pseudomonas syringae* DC3000 pv. *tomato* hrcC- 0 and 4 days after inoculation of $2x10^4$ cfu/ml into *N. benthamiana* leaves of wild type plants as well as two independent RLP32-overexpressing lines. Box plots show the minimum, first quartile, median, third quartile, and a maximum of log cfu/cm^2 (n=8 from 4 plants for 0 dpi and 4 dpi). Labels A-C indicate homogenous groups according to post-hoc comparisons following one-way ANOVA (Tukey's test) multiple comparison analysis at a probability level of $p < 0.05$. The experiment was performed three times with similar results. **B)** Induction of ethylene biosynthesis in *N. benthamiana* wild type or RLP32-expressing plants in response to either water (as negative control), 1 µM flg22 (as positive control) or 1 µM IF1. Leaf pieces were treated for 4 h. Each bar represents the average value ±S.D. (n=3).

4 Discussion

Past approaches to identify immunogenic molecules derived from microbes relied almost exclusively on potentially time-consuming biochemical purification procedures (Felix *et al.*, 1999; Felix and Boller, 2003; Kunze *et al.*, 2004). Despite intense efforts remarkably few such structures have been identified so far. On the other hand, the sequencing of the *A. thaliana* genome led to the identification of numerous plant receptors, but the function of most of these receptors remains elusive (Kaul *et al.*, 2000; Wang *et al.*, 2008; Lehti-Shiu *et al.*, 2009; Kemmerling *et al.*, 2011). In recent years, several RLKs and RLPs were shown to confer disease resistance by detecting proteinaceous PAMPs derived from pathogenic microorganisms. To find a new receptor, that perceives a PAMP there are a variety of strategies. Most PRRs have been identified using forward genetics, but reverse genetics and biochemical properties have also been successfully used.

4.1 Approaches to identify new receptors

4.1.1 Biochemical approach

Biochemical purification has only been successful for identifying PEPR1 as the receptor for *At*Pep1, by photoaffinity labeling the ligand and subsequent purification of its binding receptor. Accompanying genetic evidence could verify PEPR1 as the *At*Pep1 receptor (Yamaguchi *et al.*, 2006). Affinity labeling also lead the discovery of *Os*CEBiP as a chitin binding protein (Ito *et al.*, 1997). *Os*CEBiP later proved to be important for chitin induced immune signaling in rice (Kaku *et al.*, 2006)

4.1.2 Reverse genetics approach

The genome of *A. thaliana* is sequenced and annotated. A library of receptor knock-out mutants can be screened for the loss of PAMP-sensitivity the find the receptor.

4.1.3 Forward genetic approaches

In forward genetic approaches, a gene responsible for a phenotype is investigated by screening of mutant organisms for a specific phenotype and subsequent identification of the mutated gene by mapping the locus via marker-based breeding or sequencing.

To identify the gene encoding a new receptor, a mutation collection, e.g. EMS mutants, can be screened for insensitivity to PAMP-treatment. Map based cloning or whole genome sequencing can be used to identify the mutated gene responsible for the insensitivity.

Complementation of the knock-out mutant resulting in gained sensitivity can be used to verify the candidate receptor.

4.1.3.1 Natural variation

The pattern recognition system of plants is redundant, with multiple PRRs contributing to the detection of a given type of pathogen. *A. thaliana* can detect the bacterial pathogen *Pst* DC3000 via PRRs with specificities for flagellin (Felix *et al.*, 1999), EF-Tu (Kunze *et al.*, 2004), medium-chain 3-hydroxy fatty acids (mc-3-OH-FAs) (Kutschera *et al.*, 2019) and peptidoglycan (Liu *et al.*, 2014). This redundancy of perception systems makes a plant less susceptible when a single PRR is lost during evolution or overcome by a pathogen. The redundancy of perception allows for the considerable natural variation observed between closely related species, accessions or even strains of plants with respect to the presence of individual PRRs.

Screening a collection of *A. thaliana* ecotypes for PAMP responsiveness, can reveal insensitive lines, which can be crossed with sensitive lines to create a mapping population to identify the locus involved in PAMP sensitivity.

Similarly, a collection of introgression lines derived from crossing of *S. lycopersicum* and *S. pennellii* (Chitwood *et al.*, 2013) has been a useful tool to identify candidate receptors in tomato.

4.1.3.2 GWAS of naturally occurring mutations in ecotype

The screening of different ecotypes of the same plant for PAMP sensitivity can provide information on the genome region of a receptor by GWAS analysis. SNPs of the ecotypes that show insensitivity can be compared to find mutations that are shared by these ecotypes, mapping PAMP-sensitivity to a certain region of the genome.

A novel receptor-ligand pair, RLP32-IF1, was characterized in this thesis following the results from two preceding dissertations from Dr. Li Fan and Dr. Eric Melzer.

Dr. Li Fan used purified bacterial extract from *Ralstonia solanacearum* to identify a new pattern recognition receptor in *A. thaliana*, RLP32, using a next generation sequencing (NGS) approach.

Dr. Eric Melzer purified the bacterial extracts of *R. solanacearum* and *E. coli* to isolate the molecule responsible for RLP32-dependent activation of the plant defense mechanisms. He was able to pin down the translation initiation factor 1 (IF1) as a candidate for the ligand that is recognized by RLP32.

In this thesis, the receptor RLP32 and its ligand IF1 were characterized. IF1 is highly conserved amongst *Proteobacteria*. The recognition of IF1 induces early immune responses, as well as resistance against pathogenic *Proteobacteria* in plants expressing RLP32. The receptor interacts constitutively with SOBIR1 and in a ligand dependent manner with BAK1 to transduce the signal from the apoplast into the plant cell where defense mechanisms are induced. Almost the entire IF1 protein is necessary to interact with RLP32. As RLP32 is only present in some Brassicaceae like *A. thaliana*, the introduction of RLP32 into crop plants can provide a new tool for disease resistance against pathogenic *Proteobacteria*.

4.2 IF1 is the ligand of the receptor RLP32

In the first part of this thesis, IF1 was confirmed to be the ligand of RLP32. IF1 preparations isolated from different origins (extraction of endogenous protein from *R. solanacearum* and *E. coli*, recombinant expression in *E. coli*, expression in *Pichia pastoris, in vitro* transcription and translation in a eukaryotic system, peptide synthesis) all induced RLP32-dependent ethylene biosynthesis.

RLP32 was expressed in plants that lack the receptor (*rlp32*, *A. thaliana* ecotype ICE73, *N. benthamiana*) that showed no ethylene response to IF1. After RLP32 was introduced into these plants, ethylene biosynthesis could be induced by IF1. RLP32-expressing plants (*A. thaliana* ecotype Col-0 and transgenic *N benthamiana*) are significantly more resistant to bacterial infection.

RLP32 specifically and physically interacts with IF1, as demonstrated in affinity-crosslinking experiments in which biotinylated IF1 was outcompeted by unlabeled IF1 *in*

planta. No interaction between lF1 and the structurally related LRR-RP RLP23 could be observed. The specific, physical interaction of a receptor and its ligand could also be shown for RLP23/nlp20 (Albert *et al.*, 2015) and SYR1/systemin (Wang *et al.*, 2018) in similar experiments. In conclusion, plants depend on the presence of RLP32 for lF1 perception.

4.3 A tertiary structure motif is required for lF1 immunogenicity

4.3.1 lF1 fulfills typical characteristics of a MAMP/PAMP

Like EF-Tu, lF1 is a highly conserved part of the prokaryotic translational apparatus (Sette *et al.*, 1997), and is critical for the viability of *E. coli* (Cummings and Hershey, 1994). Like EF-Tu, lF1 is another example for an immunogenically active protein, that is also part of the bacterial translation apparatus. EF-Tu is estimated to make up around 5% of the total protein. Although, lF1 protein abundance has not been estimated directly, the related translation initiation factor 3 (lF3), which is expected to function in a 1:1 molar ratio with lF1, is estimated to make up around 0.27% of the total bacterial protein (Howe and Hershey, 1983; Marintchev and Wagner, 2004). Nothing is known about the concentration of MAMPs in the apoplast, where it is detected by the plant. lF1, EF-Tu and the cold shock protein are strictly cytoplasmatic bacterial proteins. It is not clear yet, how these proteins reach the apoplast where they are detected. Small amounts of them are found in secretomes of bacteria (Song *et al.*, 2009). They could be released in a controlled process as such as general permeability changes occurring as part of osmotic adaptation in bacteria (Vázquez-Laslop *et al.*, 2001), they could be derived from dying bacteria in the plant surrounding or bacterial cells must be disrupted to facilitate release of cytoplasmatic proteins. In order to induce an immune response, the detection of lF1 must be very sensitive. The nature of the bioavailable immunogenic molecules and their apoplastic concentrations may have a big influence on their stability and motility within the apoplast. Also, the bioavailability of either the whole molecule or the epitope alone could impact their ability to interact with receptors leading to more complex signatures of infection. Flagellin monomers induce a non-host hypersensitive response in *Nicotiana benthamiana* whereas the flg22 peptide induces a basal immune response, demonstrating important differences in the immune eliciting potential of an isolated peptide versus an intact protein

(Taguchi *et al.*, 2003; Oh and Collmer, 2005; Hann and Rathjen, 2007; Nguyen *et al.*, 2010).

The EC_{50} of a ligand is the molar concentration producing 50% of the maximal possible stimulatory effect in a biological system (Neubig *et al.*, 2003). The EC_{50} of immunogenic ligands provides a relative measure of the concentration at which receptors become responsive to their respective ligands. Pathogen- or plant-derived ligands associated with defense tend to have relatively low EC_{50} values in the picomolar to nanomolar range, presumably because single cell detection and signal activation must induce a fast and robust defense response in the plant (Chivasa and Goodman, 2020).

The EC_{50} of IF1 that was recombinantly expressed in *E. coli* and purified is around 0.55 nM, which shows a high sensitivity.

4.3.2 The structure of IF1 plays a key role in the receptor binding

4.3.2.1 IF1 is heat sensitive

The native structure of globular proteins is determined by the primary structure. The secondary (alpha helix and beta sheet) and tertiary structure of proteins are formed by disulfide bonds between cysteines, ionic interaction between charged amino acids and hydrogen bonds forming between amino acids. Hydrophilic amino acids form hydrogen bonds with the surrounding water, whereas hydrophobic amino acids can be found in the core of the protein. The stable protein remains in a global minimum energy state. When proteins are heat or SDS-treated, they denature, because the secondary and tertiary structure resolves (Van Holde, 1977; Boye *et al.*, 1997). The unfolded state becomes more favorable while the initial state becomes increasingly destabilized upon heating (Potekhin and Kovrigin, 1998). For most proteinaceous PAMPS in the denatured state, the primary structure and the immunogenic epitope of the proteins are still available or even more accessible for receptor binding. Heat treatment of other PAMPs either did not affect the immunogenic activity or even increased the activity. Heat-denaturation by boiling of flagellin preparations resulted in increased activity and an EC_{50} of approximately 0.1 nM as compared to 0.5 nM for unboiled flagellin (Felix *et al.*, 1999). The immunogenic activity of EF-Tu in bacterial preparations was not affected by heating in SDS (1% [v/v], 95°C for 10 min) (Kunze *et al.*, 2004). A crude purification of cold shock protein was heat stable (Felix and Boller, 2003). Heat treatment of *Pp*NLP did not affect plant defense eliciting activity (Böhm *et al.*, 2014).

In contrast, when recombinantly expressed lF1 was SDS- and heat treated, the EC_{50} increased 10 to 40-fold. In the cases of flg22, elf18, csp22 and nlp20 secondary or tertiary structure are not important for receptor binding, as the linear epitope is still available after denaturation (Böhm *et al.*, 2014). For lF1, on the other hand, the secondary or tertiary seem to play a key role in binding to RLP32, as denaturation leads to lowered immunogenic activity. This means that in the case of lF1 a conformational epitope is recognized by the receptor.

In animals, antigen-specific membrane receptors on lymphocytes and secreted antibodies can recognize two different kinds of epitopes: epitopes composed of a few amino acids of the polypeptide chain in their linear order (linear epitopes), and those constituted by a few amino acids from different parts of the sequence, brought together by the folding of the polypeptide chain of the antigen into its native structure (conformational epitopes) (Barlow *et al.*, 1986; Goldsby *et al.*, 1999). The RLP Cf9 in tomato recognizes a 28 aa AVR9 peptide from *Cladosporium fulvum* which leads to hypersensitive response in the plant (van Kan *et al.*, 1991; Van den Ackerveken *et al.*, 1992; Van den Ackerveken *et al.*, 1993; Joosten *et al.*, 1994). The peptide consists of three antiparallel β–sheets and one extended loop. The structure is very stable and compact due to cysteine-bridges that are arranged in a cystine-knot (Vervoort *et al.*, 1997). Residues in the short connecting hydrophobic β–loop of the AVR9 peptide are essential for the elicitor activity (Kooman-Gersmann *et al.*, 1997). RLP32 could be one of the first plant receptors described in literature that binds a conformational epitope.

If a protein irreversibly remains in a denatured state or refolds after cooling depends on several transition parameters (kinetic and equilibrium). It is hard to predict how a protein behaves in different conditions only from the structural information. To predict if denaturation remains irreversible calorimetric studies of lF1 need to be conducted to gain information about its denaturing temperature, the refolding rate, the temperature of maximum stability and so forth. The interactions between the numerous amino-acid side groups of the protein and between the side groups and the solvent leads to some degree of ordered structure which is retained even after heat-denaturation (Tanford, 1970; Privalov *et al.*, 1989; Boye *et al.*, 1997).

It is possible, that lF1 can refold at least partially upon cooling. This would explain, why the immunogenic activity retains most of its activity after heat treatment. lF1 does not

contain any cysteines; therefore, post-transitional improper intramolecular disulfide bond formation, which would result in irreversible protein denaturation, is not possible. Circular dichroism could provide information on how the secondary and tertiary structure is influenced by heating and cooling.

Several examples of partial or total refolding of proteins upon cooling have been described. Slow cooling can lead to partial refolding to a non-native state through an intermediate state (Potekhin and Kovrigin), as observed for extracellular the endo-β-1,3-glucanase LamA (Koutsopoulos *et al.*, 2007). G-actin retained 60% of its original helical structure after it had been heated to more than 30°C above its denaturation temperature (Smith, 1994). After heat denaturation of β-Conglycinin, cooling induces refolding of the unfolded internal structure of dissociated monomers while the quaternary structure is not regained (Iwabuchi *et al.*, 1991). Slow cooling allowed heat-denatured ovalbumin to refold to its native structure (Tani *et al.*, 1997).

4.3.2.2 Almost the entire IF1 protein is needed for immune response elicitation

The EC_{50} value of IF1 is in a concentration range similar to other plant immune receptor elicitors like elf18 (0.2 nM) (Kunze *et al.*, 2004), csp22 (0.1 nM) (Felix and Boller, 2003), flg22 (30 pM) (Felix *et al.*, 1999) and nlp20 (2.77 nM) (Böhm *et al.*, 2014). All these ligands are shorter peptides of a full-length protein. The elf18 peptide is located in the N-terminus of EF-Tu (Kunze *et al.*, 2004); csp22 is located at the N-terminus of cold shock protein (Felix and Boller, 2003); flg22 is located in the N-terminus of flagellin (Felix *et al.*, 1999); nlp20 is located more in the center of Nep-like protein (Böhm *et al.*, 2014). In the case of IF1, the entire protein except for the first five amino acids at the N-terminus (A1-N5) is needed to elicit an immune response. These amino acids are not involved in the tertiary structure. Interestingly, the truncation of IF1 by last five amino acids at the C-terminus, which are also not involved in tertiary structure, yields an immunogenically inactive protein. Therefore, the C-terminus is crucial for the induction of the immune response.

4.3.2.3 IF1 has no linear epitope

Several strategies, that have been successfully used to identify epitopes, were employed in an effort to identify a linear epitope of IF1. The Nep1-like protein was discovered as a PAMP by analysis of gene orthology and variations in the primary sequences of the protein that has homologues in bacteria, fungi and oomycetes. The 20 aa epitope, nlp20, was

found through testing the immunogenic activity of nested synthetic peptides covering the entire *Pp*NLP protein sequence (Böhm *et al.*, 2014). An overlapping sequence shared by active peptides was gradually truncated at the N-terminus or the C-terminus to pin down the minimal epitope. Two motifs, A103-Y106 and K112D113, were important for the immunogenic activity. Alanine-scanning mutagenesis identified the amino acids, that are crucial for the induction of immune response.

In an attempt to identify a minimal epitope of IF1, 8 nested synthetic 30-aa-long peptides covering the entire sequence of IF1 were tested for induction of ethylene biosynthesis. None of the peptides showed immunogenic activity. Longer synthetic peptides covering the first and the second half of the full-length protein also failed to induce ethylene production. This strategy was not successful in finding an epitope in the primary sequence.

4.3.2.4 Shorter IF1 peptides have no inhibitory effects

It has been reported, that truncated inactive, structural analogs of immunogenic ligands can act as specific, competitive antagonist. A peptide comprising the N-terminal 8–11 amino acid residues of flg15 show no activity as agonists but act as specific, competitive antagonists (Felix *et al.*, 1999). The C-terminally truncated peptide elf12 has an antagonistic effect to the binding of elf18 (Kunze *et al.*, 2004) to EFR. In the case of systemin, a shorter peptide systemin 1-14 inhibited the binding to SYR1 completely. (Wang *et al.*, 2018). In the case of IF1, none of the shorter peptides had an antagonistic effect. This is another indicator that only folded full length or nearly full length IF1 can bind to the receptor.

4.3.2.5 IF1 orthologs from *Proteobacteria* show similar immunogenic activity, despite low sequence homology

Flg22 (Felix *et al.*, 1999), csp22 (Felix and Boller, 2003) and elf18 (Kunze *et al.*, 2004) were all identified through purification of the full-length protein (flagellin, cold shock protein and EF-Tu) from bacterial extract. Enzymatic cleavage with proteases of the elicitors abolished the immunogenic activity and identified the PAMPS as proteinaceous. Different cleavage sites of the proteases resulted in different peptides, which could be purified and tested for immunogenic activity. Important amino acids in the epitope could be identified by loss of immunogenic activity after protease digestion at specific cleavage sites. Active peptides could subsequently be identified via mass spectrometry, which helped to identify the proteins as well as the epitopes (Kunze *et al.*, 2004). In the case of EF-Tu, the reported

N-terminal acetylation of the full-length protein increased the elicitor activity of the minimal motif, elf18 (Kunze *et al.*, 2004).

The epitopes were further delineated through alignment of the proteins derived from different organisms. Often, a consensus sequence with a high similarity can be found as a good candidate for a potential immunogenic epitope (flg22, csp22). After an active peptide was found, the peptide was progressively shortened to find a minimal motif that could elicit the most sensitive immune response (Felix *et al.*, 1999; Felix and Boller, 2003).

A. tumefaciens, P. syringae and *E. coli* are three organisms which are not closely related but all belong to *Proteobacteria*. Comparison of the secondary and tertiary structure of IF1 derived these organisms by homology modeling reveals that the conservation of the 3D-structure is very high. The characteristic short alpha helix as well as the orientation of the beta sheets in the core globular structure can be found in all IF1-versions. Moreover, IF1 proteins from all three species show similar immunogenic activity and share a high homology over the entire aa sequence of the protein.

4.3.2.6 The 3D-structure of IF1 orthologs is very conserved

A similarity score analysis of the amino acids mapped onto the IF1 3D-structure reveals that the amino acids forming the alpha helix are very conserved, as well as parts of the beta sheets. Amino acids, that are in proximity due to secondary and tertiary structure can form a conformational epitope. It is very challenging to find the amino acids that form a conformational epitope by deletion of candidate amino acids, as the effects to the 3D-structure must be considered. Is the immunogenic activity lost, because an essential amino acid in the epitope is missing or was the conformational epitope disrupted due to a change in the 3D-structure? Co-crystallization of the apoplastic domain of RLP32 and IF1 could reveal the epitope as well as the active binding site in the receptor. FLS2 and flg22 have been successfully co-crystallized with BAK1 by Sun *et al.* (2013). Here it was revealed that the N-terminus of flg22 only binds to FLS2, whereas the C-terminal segment of flg22 bridges FLS2-LRR and BAK1-LRR and acts as a molecular glue to connect its receptor with a signaling partner. So far there are no X-ray crystallography data available elucidating the interaction of RLPs and BAK1, but in a serial deletion study it was revealed that LRR1 and LRR3 of *At*RLP23 are crucial for ligand binding required and thus for the recruitment of BAK1. For *At*FLS2 it has been reported that ligand binding also starts at LRR3 and stretches out to LRR16 (Sun *et al.*, 2013). Nlp20 might also act as a molecular glue for RLP23-BAK1 interaction (Albert *et al.*, 2019). In case of IF1 the last 5 amino acids

at the C-terminus are crucial for the immunogenic activity, but the mutation of arginine69, which is highly conserved amongst *Proteobacteria* did not abolish the activity. The C-terminus of IF1 could possibly act as a molecular glue between RLP32, SOBIR and BAK1.

In conclusion, the entire IF1 structure except for 5 amino acids at the N-terminus is required to induce an RLP32-dependent immune response. The structure of IF1 is likely critical for the formation of a conformational epitope which is recognized by RLP32.

4.4 IF1 is detected by some species in the *Brassicaceae* family

PAMP perception is not uniformly conserved between plant genera. Some PAMPs are only perceived by a narrow range of plant species, whereas others trigger defense responses in many species. For example, nlp20 perception is restricted to the *Brassicaceae* family (Böhm *et al.*, 2014). Perception of bacterial cold shock protein and EF-Tu seemed to be restricted to the orders of *Solanaceae* and *Brassicaceae*, respectively (Kunze *et al.*, 2004). Flagellin induces responses in plants belonging to many different orders (Felix *et al.*, 1999). In the case of IF1, the perception seems to be even more restricted. Not even all plants belonging to the *Brassicaceae* family can detect IF1. IF1 sensitivity must thus be a phylogenetically young trait.

Interestingly, *Solanum lycopersicum*, but not *Solanum pennellii*, is able to detect IF1. However, a much higher concentration of IF1 is required in *S. lycopersicum* as compared to *A. thaliana*. The closest homolog to RLP32 in the genome of *S. lycopersicum* is the RLP *Cf*9, but only 36% of the aa sequences are identical. This could be a hint that either *S. lycopersicum* developed a RLP32-independent perception mechanism for IF1 or a protein that shares similarity to IF1 is detected.

It has been reported that tomato, potato and pepper have developed another receptor that is distinct from FLS2. FLS3 also recognizes flagellin, but another epitope, flgII28 (Hind *et al.*, 2016).

4.5 RLP32 requires coreceptors to initiate plant defense response

The genome of *A. thaliana* encodes approximately 235 receptor-like kinases with extra cytoplasmic LRR domains which constitute the largest subfamily of RLKs (Lehti-Shiu *et al.*, 2009). They are composed of apoplastic ligand-binding domains that are linked to cytoplasmic serine/threonine protein kinase domains via transmembrane domains (Morillo and Tax, 2006). Additionally, there are 57 LRR-receptor like proteins (Wang *et al.*, 2008) present in *A. thaliana*. The intracellular protein kinase domain of RLKs is lacking in LRR-RLPs. Instead, LRR-RLPs interact with adaptor kinases such as SOBIR1 to form a heterodimeric receptor like kinase complex (Gust and Felix, 2014; Liebrand *et al.*, 2014; Domazakis *et al.*, 2018). Both RLKs and RLPs are involved in immunity and development (Jehle *et al.*, 2013; Liebrand *et al.*, 2013; Zhang *et al.*, 2013; Bi *et al.*, 2014; Zhang *et al.*, 2014; Ma and Borhan, 2015; Hegenauer *et al.*, 2016; Catanzariti *et al.*, 2017; Domazakis *et al.*, 2018; Wang *et al.*, 2018).

RLPs interact constitutively with SOBIR1 for downstream signaling after ligand binding (Gao *et al.*, 2009; Leslie *et al.*, 2010; Gust and Felix, 2014; Liebrand *et al.*, 2014). Both an active kinase domain and the SOBIR1 LRR ectodomain are required for signaling (Bi *et al.*, 2016; Albert *et al.*, 2019; Van Der Burgh *et al.*, 2019). Conserved GxxxG motifs in the trans-membrane regions of SOBIR1 and the RLPs *Sl*CF4, *Sl*Ve1 and *Sl*EIX2 are required for constitutive interaction (Russ and Engelman, 2000; Bi *et al.*, 2016). *At*RLP1 is the only RLP in *A. thaliana* that lacks the GxxxG motif, but the receptor has been reported to interact with SOBIR1 (Jehle *et al.*, 2013; Albert *et al.*, 2019). In addition to the GxxxG motif, ionic forces between oppositely charged regions in the extracellular juxta membrane domains (JM) of RLPs and SOBIR1 have been proposed to contribute to the formation of constitutive RLPs (Gust and Felix, 2014). In serial deletion studies, the role of both, the GxxxG motif and the charged patches in the JM, in the interaction of SOBIR1 and AtRLPs have been investigated. (Albert *et al.*, 2019). Both contribute in concert to the formation of the heteromeric complex (Albert *et al.*, 2019). The SOBIR1 LRR ectodomain and kinase domain are not required for interaction with RLPs, but are essential for signaling (Bi *et al.*, 2016; Albert *et al.*, 2019; Van Der Burgh *et al.*, 2019). Additionally, it has been reported that SOBIR1 stabilizes some RLPs and thus promotes their accumulation, as shown for Cf-4 and Ve1 (Liebrand *et al.*, 2013; Liebrand *et al.*, 2014). Genetic inactivation of *At*SOBIR1, on the other hand, had no detrimental effect on the protein levels of at least

three RLPs in a homologous plant background, contradicting the scaffolding function of SOBIR1 (Albert *et al.*, 2019).

As with RLKs, BAK1 is also recruited to two-component RLP/SOBIR1 complexes upon ligand recognition by the RLP involved. This has been demonstrated for RLP23 (Albert *et al.*, 2015); ELR (Domazakis *et al.*, 2018); Cf-4 (Postma *et al.*, 2016) and RLP30 (Zhang *et al.*, 2013). Initially it was reported that BAK1 is not recruited to RLP42 upon ligand perception (Zhang *et al.*, 2014), but more recent experiments reveal that BAK1 is recruited to RLP42 in a similar manner to other characterized RLPs (personal communication Dr. Lisha Zhang). As the constitutive interaction between RLPs and SOBIR1 and the ligand-dependent recruitment of BAK1 resembles the complex formation of RLKs and BAK1 it was hypothesized that the signal transduction also works in a similar manner. However, a recent comparative analysis of early signaling events and defense response patterns mediated through activation of either LRR RLK- or LRR-RLP has revealed significant differences (Wan *et al.*, 2019).

In co-immunoprecipitation experiments, RLP32 interacts constitutively with SOBIR1 and in a ligand-dependent manner with BAK1. RLP32 also interacts with SERK1 and SERK2 in a ligand-independent manner, but not with SERK4/BKK1. This partially contradicts the results of Dr. Li Fan (Fan, 2015). She observed induction of ethylene biosynthesis in *bak1* and *bkk1* plants but not in the double mutant plants *bak1/bkk1*. Based on this result, we would expect BAK1 and BKK1/SERK4 to interact with RLP32 interchangeably.

The lack of interaction between BKK1/SERK4 and RLP32 in coimmunoprecipitation assays is also distinct from other characterized elicitors. Ligand-dependent interaction with FLS2 or EFR was shown for SERK1-4 in transient expression assays in *N. benthamiana* (Schwessinger *et al.*, 2011). SERK1-4, but not SERK5 co-immunoprecipitated with RLP23 (Albert *et al.*, 2015). In this case, additional binding studies could clarify conflicting observations regarding the interaction of RLP/RLKs with the members of the SERK family. For example, spilt-YFP bimolecular fluorescence complementation assays (BIFC) could be performed in protoplasts from plants lacking SOBIR1, RLP32 and SERK1,2,3,4 and/or 5. In surface plasmon resonance experiments, purified RLP32, SOBIR1 and SERKs can be investigated as interaction partners. In vitro gel filtration experiments with recombinant ectodomains of RLP32 and SERKs could reveal if these proteins physically interact with each other in the presence of IF1. A similar experiment proved the physical interaction of RLP23 and BAK1 since co-migration and coelution occurred in the presence of nlp20

(Albert *et al.*, 2015). To reveal novel downstream signaling components of RLP32, quantitative phosphoproteomic analysis could be performed after elicitation of *A. thaliana* with lF1.

4.6 RLP32 confers resistance to *Proteobacteria*

Estimates of average global losses of crop plants to diseases and pests range from 11–30% (Oerke and Dehne, 2004; Savary *et al.*, 2019). In 2012, Mansfield *et al.* published a top ten list of the most important bacterial pathogens. All of these bacteria belong to *Proteobacteria*, with *P. syringae* taking first and *R. solanacearum* taking second place (Mansfield *et al.*, 2012). Fungal pathogens are controlled mostly using fungicides, but there are few effective strategies for fighting bacterial pathogens in the field. To make matters worse, some pesticides are rapidly losing efficacy due to pathogen evolution, and their use faces increasingly strict regulations to minimize unwanted side effects (Geiger *et al.*, 2010; Bolton *et al.*, 2012; Wieczorek *et al.*, 2015; Godoy *et al.*, 2016; Lamichhane *et al.*, 2016). Resistance breeding of crop plants is very time-consuming and expensive, and some crop plants also are very hard to breed. Genetic modification of crop plants provides a promising tool for crop protection. Indeed, different strategies for bioengineering crop plants have already proven to be successful in the field. Here different layers of the plant defense have been the focus of creating disease resistance. For example, susceptible plants can gain novel recognition specificity by introducing receptors from other plants. EFR has been introduced to various crop plants like tomato (Kunwar *et al.*, 2018), wheat (Schoonbeek *et al.*, 2015), rice (Lu *et al.*, 2015; Schwessinger *et al.*, 2015) and potato (Boschi *et al.*, 2017) resulting in broad spectrum bacterial resistant crops with no yield reduction. Use of R genes focuses on another layer of innate immunity, effector recognition. Stacking three late blight resistance genes from wild species (*RB*, *Rpi-blb2* and *Rpi-vnt1.1*) directly into susceptible potato varieties confers complete field resistance to late blight (Ghislain *et al.*, 2019). Plant pathogens are highly adaptable and have much faster life cycles than their plant hosts. Host specific microbial effectors can be quickly mutated as microbes do not rely on them for their survival. Introducing NLRs recognizing bacterial effectors can be overcome by pathogens rather quickly due to selective pressure. MAMPs on the other hand are highly conserved and crucial for the viability of the microbes. A combination of apoplastic receptors recognizing external immune signals or a combination of PRRs and NLRs covering both layers of plant defense, could provide a more stable and sustainable resistance. Transgenic tomatoes expressing a PRR (EFR) from *A. thaliana* and a resistance gene (Bs2) from pepper showed resistance to both bacterial spot and bacterial wilt (Kunwar *et al.*, 2018).

To test the effect that a PRR has on the resistance of a plant, infection assays can be conducted on PRR-expressing and PRR-lacking plants. The progression of the infection can be tracked over time. Either direct infection or infection after priming have been used to show the effect on the resistance of single PRRs in the past.

Priming is an adaptive strategy that improves the defensive capacity of plants. Priming can be induced by molecules from microbes (both pathogenic and symbiotic), as well as chemicals and abiotic cues. Upon stimulus perception, changes may occur in the plant at the physiological, transcriptional, metabolic, and epigenetic levels. When a pathogenic attack occurs after priming the defense response can occur faster and stronger (Mauch-Mani *et al.*, 2017). Foliar application as well as bioengineering the genes encoding proteinaceous PAMPs such as harpins (Chen *et al.*, 2008; Choi *et al.*, 2012), elicitins (Keller *et al.*, 1999; Mohamed *et al.*, 2007), and flagellins (Takakura *et al.*, 2008) have been successfully applied for disease control in crop plants.

Two different infection assays showed that the presence of RLP32 in plants leads to significantly increased resistance to *P. syringae*. *N. benthamiana* plants expressing RLP32 were more resistant to *P. syringae hrcC*- than wild-type plants. Priming of *A. thaliana* Col-0 plants and *rlp32* mutant plants with lF1 one day prior to infection with *P. syringae* DC3000 significantly reduced bacterial growth in an RLP32 dependent manner. Direct infection of *N. benthamiana* and *A. thaliana* with *P. syringae* DC3000 without priming showed no significant difference in bacterial growth between RLP32-expressing and plants lacking RLP32. RLP32-related immunity might be suppressed by effectors secreted by *P. syringae* during the infection. *P. syringae hrcC*- mutants are not able to inject effectors into the plant cells as the type III secretion system is nonfunctional. Under natural conditions *Hyaloperonospora arabidopsidis* can establish an infection on Arabidopsis, as *H. arabidopsidis* probably suppresses the plant immune response with its effectors. Nlp24 derived from HaNLP3 can induce a strong priming effect in *Arabidopsis* leading to drastically reduced growth of *H. arabidopsidis* (Oome *et al.*, 2014).

The resistance conferred by RLP32 against *Proteobacteria* makes the receptor another interesting candidate to be introduced into crop plants. It would be interesting to observe the degree of resistance in RLP32-expressing plants in the field, as EFR expression in crop plants showed impressive results. Transgenic expression of RLP32 in combination with receptors like RLP23, EFR and RLP30, could lead to a broad-spectrum and durable resistance against bacteria, oomycetes and fungi in crop plants.

A combination of the best technologies and practices can be used in an integrated approach to address some of the challenges in agriculture, making plants more resilient to abiotic and biotic stresses and thus enhancing sustainable crop production. Genetic modification is one approach to produce plants, that are more resilient and produce higher yields. Indeed, the use of genetically modified plants (GMOs) have delivered net benefits for farmers, both small and large scale; and consumers, in the countries where cultivation has been permitted (Brookes and Barfoot, 2016). A series of extensive and long-term research studies have shown that the benefits of growing genetically modified crops in the fight against global food shortages and hunger have been significant (Herring, 2013). Despite all the benefits, GMOs must be handled with care. A fundamental understanding of the physiological changes in the plant is necessary to assess unwanted side effects on the environment, human health and to keep control over the new crop plants.

5 Summary

Plants can detect pathogens via pattern recognition receptors (PRRs) that bind pathogen-associated molecular patterns (PAMPs), thereby inducing PAMP triggered immunity (PTI). Prior to this study, the translation initiation factor IF1 was purified from bacterial extract and was shown to trigger early immune responses in *A. thaliana*. The receptor-like protein RLP32 was identified as the putative pattern recognition receptor of IF1 in *A. thaliana.*

In this study, RLP32 was confirmed as the IF1 receptor using a variety of biochemical and immunological analyses. RLP32 is only present in some members of the *Brassicaceae* family. Complementation of IF1-insensitive plants with the RLP32 conferred the plants with the ability to respond to IF1. IF1 and RLP32 were further shown to directly and specifically interact *in planta.* Co-immunoprecipitation experiments showed constitutive interaction of RLP32 with the adaptor kinase SOBIR1. The RLP32/SOBIR1 complex interacts with the coreceptor BAK1/SERK3 in an IF1 dependent manner, analogous to what is reported for other PRR/ligand systems.

IF1 was confirmed to be the ligand of RLP32. IF1 is conserved among *Proteobacteria*. IF1 derived from different *Proteobacteria* showed similar immunogenic activity. Deletion construct analysis revealed that virtually the entire IF1 protein (or its tertiary structure fold) are required for its immunogenic activity.

Solanaceous crops lack an RLP32-homolog and are susceptible towards many pathogenic *Proteobacteria*. After stable transformation of *N. benthamiana* with RLP32, immune responses are induced when elicited with IF1. *N. benthamiana* expressing RLP32 showed enhanced resistance after infection with the hrcC- mutant strain of *Pseudomonas syringae*, indicating that *N. benthamiana* gained responsiveness to pathogenic proteobacteria. IF1 successfully primed immunity in *A. thaliana* leading to an enhanced resistance to *P. syringae*. In contrast, pretreatment with IF1 did not protect *rlp32* knock-out mutant genotypes.

The discovery of the new receptor-ligand pair RLP32/IF1 can be implemented in modern breeding techniques in crop plants to potentially improve resistance against proteobacterial pathogens.

6 Zusammenfassung

Pflanzen besitzen Immunrezeptoren, sogenannte pattern recognition receptors (PRRs), über die molekulare Muster von Pathogenen erkannt werden (pathogen-associated molecular patterns (PAMPs)). Durch die Erkennung von Pathogenen werden in der Pflanze Abwehrmechanismen (PAMP triggered immunity (PTI)) induziert. Vor Beginn dieser Doktorarbeit wurde der Translationsinitiationsfaktor 1 (IF1) aus bakteriellem Extrakt aufgereinigt. IF1initiiert frühe Immunreaktionen in *A. thaliana.* Das Rezeptorprotein RLP32 wurde als möglicher IF1-Rezeptor in *A. thaliana* identifiziert.

In dieser Arbeit konnte RLP32 als Rezeptor von IF1 durch biochemische und immunologische Analysen bestätigt werden. RLP32 ist nur in einigen Mitgliedern der *Brassicaceae*-Familie zu finden. Die Komplementation von IF1-insensitiven Pflanzen mit RLP32 verhalf den Pflanzen dazu auf IF1 zu reagieren. Ebenso konnte gezeigt werden, dass IF1 und RLP32 *in planta* direkt und spezifisch miteinander interagieren. Ko-Immunopräzipitationsexperimente zeigten, dass RLP32 konstitutiv mit der Adapterkinase SOBIR1 interagiert. Der RLP32/SOBIR1-Komplex interagiert IF1-abhängig mit dem Ko-Rezeptor BAK1/SERK3, so wie es bereits für andere PRR/ Ligandensysteme beschrieben wurde.

IF1 konnte als Ligand von RLP32 bestätigt werden. IF1 ist in Proteobakterien konserviert. IF1 aus verschiedenen *Proteobacteria* wiesen ähnliche immunologische Aktivitäten auf. Die Analyse von Deletionskonstrukten ergab, dass fast das ganze IF1-Protein (oder dessen Tertiärstrukturfaltung) nötig sind, für dessen immunologische Aktivität ist.

Kulturpflanzen, die zu den *Solanaceae* gehören, verfügen nicht über ein RLP32-Homolog. Sie sind anfällig gegenüber proteobakeriellen Pathogenen. Nachdem RLP32 stabil in *N. benthamiana* transformiert wurde, konnte eine Immunantwort durch IF1 induziert werden. *N. benthamiana,* die RLP32 exprimieren, zeigten eine erhöhte Resistenz nach Infektion mit dem *Pseudomonas syringae* hrcC- Mutanten-Stamm, was darauf schließen lässt, dass *N. benthamiana* Reaktionsfähigkeit auf pathogene Proteobakterien erlangte. IF1 konnte erfolgreich das Immunsystem in *A. thaliana* primen, was zu einer erhöhten Resistenz gegenüber *P. syringae* führte. Im Gegensatz dazu führte eine Vorbehandlung von *rlp32-knock-out* Mutanten mit IF1 nicht zu Resistenz gegenüber *P. syringae*.

Die Entdeckung des neuen Rezeptor-Liganden-Paares RLP32/IF1 kann in modernen Züchtungsmethoden impliziert werden, um Kulturpflanzen zu entwickeln, die gegenüber proteobakteriellen Pathogenen resistent sind.

7 Supplement

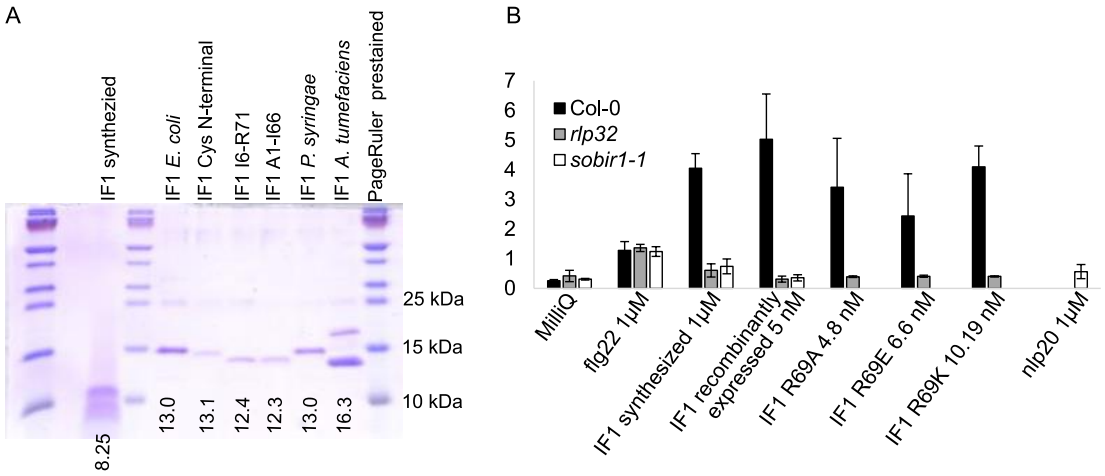

Figure 21: Supplement 1

A) Coomassie-stained 16% tricine gel of synthesized native IF1, recombinantly expressed and purified IF1-6xHis-tag, IF1-6xHis-tag+N-terminal cysteine, IF1 (I6-R71)-6xHis-tag, IF1 (I6-R71)-6xHis-tag derived from *E. coli;* recombinantly expressed and purified IF1-6xHis-tag of *A. tumefaciens* and *P. syringae.* The numbers in the rows indicate the molecular weight of each version of purified IF1. **B)** Induction of ethylene biosynthesis in Col-0, *rlp32* and *sobir1-1* in response to either MilliQ water (as negative control), 1 µM flg22 (as positive control) or native or R69A/E/K IF1-6xHis recombinantly expressed. Leaf pieces were treated for 4 h. Each bar represents the average value ±S.D. (n=4).

8 Abbreviations

30S IC	30S initiation complex
30S PIC	30S preinitiation complex
70S IC	70S initiation complex
aa	amino acid
aIF1A	archaeal IF1 homologues
APS	ammonium persulfate
ATP	Adenosine triphosphate
AtPEPR1	AtPEP RECEPTOR
AtRLP/ReMAX	receptor of eMAX
AtWAK1	WALL-ASSOCIATED KINASE 1
Ave1	Avirulence on Ve1
Avr4/Avr9	Avirulence 4/9
BAK1	BRI1-associated kinase 1
BGAL1	b-glactosidase
BIK1	*Botrytis*-induced kinase 1
BIR1/2/3	BAK1-INTERACTING RECEPTOR-LIKE KINASE 1/2/3
BKK1	BAK1-like kinase 1
BR	brassinosteroid
BRI1	brassinosteroid insensitive 1
BSA	Bovine serum albumin
CDPK	calcium-dependent protein kinase
CERK1	CHITIN ELICITOR RECEPTOR KINASE 1
Cf	*Cladosporium fulvum*
Cf4/9	Cladosporium fulvum resistance genes 4/9
CLV2	CLAVATA2

CNGC2	cyclic nucleotide-gated channel
CORE	COLD SHOCK PROTEIN RECEPTOR
CSIR	cell surface immune receptor
CuRe1	CUSCUTA RECEPTOR 1
CV	column volumes
Da	Dalton
DAMP	damage associated molecular pattern
DMSO	Dimethylsulfoxide
DORN1	DOESN'T RESPOND TO NUCLEOTIDES
E. coli	*Escherichia coli*
EC_{50}	half-maximal response
EDTA	Ethylenediaminetetraacetic acid
EFR	ELONGATION FACTOR (EF)-Tu RECEPTOR
EF-TU	ELONGATION FACTOR-Tu
EGF	epidermal growth factor
eIF1A	eukaryotic IF1 homologues
Eix1/2	ethylene-inducing xylanase
ELR	ELICITIN RESPONSE protein
eMAX	enigmatic PAMP from *Xanthomonas* spp.
ETI	effector-triggered immunity
ETS	effector-triggered susceptibility
EVR	EVERSHED
FER	FERONIA
FLS2/3	FLAGELLIN-SENSING 2/3
g	gram
GlcNAc	N-acetylglucosamine

GPI	glycophosphatidylinositol
HAMP	herbivore associated molecular pattern
HR	hypersensitive response
Ig	Immonoglobulin
IIR	intracellular immune receptor
IL	Interleukin
INF1	*Phytophthora infestans* elicitin *1*
IP	invasion pattern
IPR	IP receptor
LB	lysogeny broth
LLG1	LORELEI-LIKE GPI-ANCHORED PROTEIN 1
LORE	LIPOOLIGOSACCHARIDE-SPECIFIC REDUCED ELICITATION
LRR	leucine-rich repeat
LYK	LysM CONTAINING RECEPTOR-LIKE KINASE
LysM	lysin motif
m	milli
M	Molar
MAMP	pathogen-associated molecular pattern
MAP3K	MAP kinase kinase
MAPK	mitogen-activated protein kinase
$MgCl_2$	Magnesium chloride
MKK	MAPK kinase
mL	Milliliter
Mr	Molekulargewicht
mRNA	messenger RNA
MTI	MAMP-triggered immunity

NAMP	nematode associated molecular pattern
NaOH	Sodium hydroxide
*Nb*CSPR	RECEPTOR-LIKE PROTEIN REQUIRED FOR CSP22 RESPONSIVENESS
NLP	Nep1-like protein
NLR	nucleotide-binding leucine-rich repeat
nm	Nanometer
N-Terminus	Amino-Terminus
OB	oligo-nucleotide binding
OG	oligogalacturonide
PAGE	Polyacrylamid-Gelelektrophorese
PAMP	pathogen-associated molecular pattern
ParAMP	parasitic plant associated molecular pattern
PBL1	PBS1-like kinase 1
PBS	phosphate buffered saline
PEPR1	PEP1 RECEPTOR1
PGN	peptidoglycan
PM	plasma membrane
PRR	pattern recognition receptor
PTI	PAMP-triggered immunity
P. syringae	*Pseudomonas syringae*
R	resistance
RALF	rapid alkalization factor
RbohD	RESPIRATORY BURST OXIDASE HOMOLOG PROTEIN D
RGS1	Regulator of G protein signaling 1
RLCK	receptor-like cytoplasmic kinase
RLK	receptor like kinase

RLP	receptor like protein
ROS	reactive oxygen species
rpm	revolutions per minute
RT	Raumtemperatur
S	Svedberg
SAR	systemic defense signaling
SCFE1	*sclerotinia* culture filtrate elicitor1
SD	standard deviation
SDS	sodium dodecyl sulfate
SERK3	somatic embryogenesis receptor 3
SOBIR1	SUPPRESSOR OF BIR1 (BAK1-INTERACTING RECEPTOR-LIKE KINASE 1)
SPP motif	serine and proline rich region
SYR1	SYSTEMIN RECEPTOR 1
TBS	Tris-buffered saline
TEMED	Tetramethylenediamine
TF	transcriptional factor
TIR	an intracellular Toll-IL-1 receptor
TLR	Toll-like receptor
TLR	Toll-like receptor
TM	transmembrane region
Tris	Tris(hydroxymethyl)-aminomethan
U	Unit
VT	virulence target
WT	Wildtype
µm	Mikrometer

9 Acknowledgment

I want to take this opportunity to thank…

…Prof. Dr. Thorsten Nürnberger for providing such a fascinating research topic, for being my first referee, for his excellent mentorship through scientific discussions, giving me the freedom to develop my own ideas and supervision of my PhD and career advice.

…Prof. Dr. Georg Felix for being the second referee of my thesis, for challenging me in scientific discussions, for all the protein purification advice, for entertaining and thought-provoking lunch conversations and for being a second mentor to me.

…Prof. Dr. Claudia Oecking, Prof. Dr. Thomas Lahaye for examining me.

Thank you to my colleagues from the central facilities for their excellent service I could always rely on.

I want to thank all my colleagues of the plant biochemistry department, both present and absent, for giving me advice when experiments were especially tough and celebrating my successes with me. Thank you for your companionship, entertaining coffee breaks, lunch breaks, happy hours, retreats, jogging rounds, hiking trips, barbecues, carnivals, dinner parties and so on. I call myself lucky to have worked in such an uplifting environment and for becoming not only colleagues but friends with so many of you guys.

Special thanks to Dr. Rory Pruitt for your comments on my thesis. Thank you for your time and patience, for your friendship, support, scientific discussions and advice, for movie nights, thanksgivings, baking so much delicious pastry and burning of the calories with tennis matches, bike tours and jogging rounds. Thank you for keeping me calm. You are the best desk partner and friend a girl could ask for.

Dr. Maria Schlöffel, thank you for your friendship, scientific discussions and advice, for lending me a helping hand in the Pst assay. Thanks to our first baking date, you made me feel welcome in Tübingen from the start. I enjoyed every moment we spent together ever since, especially our vacations.

Finally, I want to thank my parents, my boyfriend Lasse and my friends for their continued support and unconditional love.

10 References

Aderem A, Ulevitch RJ (2000) Toll-like receptors in the induction of the innate immune response. Nature **406:** 782-787

Ailloud F, Lowe T, Cellier G, Roche D, Allen C, Prior P (2015) Comparative genomic analysis of Ralstonia solanacearum reveals candidate genes for host specificity. BMC genomics **16:** 270

Albert I, Böhm H, Albert M, Feiler CE, Imkampe J, Wallmeroth N, Brancato C, Raaymakers TM, Oome S, Zhang H (2015) An RLP23–SOBIR1–BAK1 complex mediates NLP-triggered immunity. Nature plants **1:** 15140

Albert I, Hua C, Nurnberger T, Pruitt R, Zhang L (2020) Surface sensor systems in plant immunity. Plant Physiology

Albert I, Zhang L, Bemm H, Nürnberger T (2019) Structure-Function Analysis of Immune Receptor At RLP23 with its Ligand nlp20 and Coreceptors At SOBIR1 and At BAK1. Molecular Plant-Microbe Interactions**:** MPMI-09-18-0263-R

Albert M, Jehle AK, Fürst U, Chinchilla D, Boller T, Felix G (2013) A two-hybrid-receptor assay demonstrates heteromer formation as switch-on for plant immune receptors. Plant physiology **163:** 1504-1509

Albert M, Jehle AK, Mueller K, Eisele C, Lipschis M, Felix G (2010) Arabidopsis thaliana pattern recognition receptors for bacterial elongation factor Tu and flagellin can be combined to form functional chimeric receptors. Journal of Biological Chemistry **285:** 19035-19042

Albrecht C, Russinova E, Kemmerling B, Kwaaitaal M, de Vries SC (2008) Arabidopsis SOMATIC EMBRYOGENESIS RECEPTOR KINASE proteins serve brassinosteroid-dependent and-independent signaling pathways. Plant physiology **148:** 611-619

Asai T, Tena G, Plotnikova J, Willmann MR, Chiu W-L, Gomez-Gomez L, Boller T, Ausubel FM, Sheen J (2002) MAP kinase signalling cascade in Arabidopsis innate immunity. Nature **415:** 977-983

Ausubel FM (2005) Are innate immune signaling pathways in plants and animals conserved? Nature immunology **6:** 973-979

Banchereau J, Pascual V, O'garra A (2012) From IL-2 to IL-37: the expanding spectrum of anti-inflammatory cytokines. Nature immunology **13:** 925

Barik SK (2013) FLORAL DIP: A SIMPLE AND EFFICIENT AGROBACTERIUM MEDIATED TRANSFORMATION METHOD IS USED IN A MODEL PLANT ARABIDOPSIS THALIANA.

Barlow D, Edwards M, Thornton J (1986) Continuous and discontinuous protein antigenic determinants. Nature **322:** 747-748

Battiste JL, Pestova TV, Hellen CU, Wagner G (2000) The eIF1A solution structure reveals a large RNA-binding surface important for scanning function. Molecular cell **5:** 109-119

Bauer Z, Gómez-Gómez L, Boller T, Felix G (2001) Sensitivity of different ecotypes and mutants ofArabidopsis thaliana toward the bacterial elicitor flagellin correlates with the presence of receptor-binding sites. Journal of Biological Chemistry **276:** 45669-45676

Belkhadir Y, Yang L, Hetzel J, Dangl JL, Chory J (2014) The growth–defense pivot: crisis management in plants mediated by LRR-RK surface receptors. Trends in biochemical sciences **39:** 447-456

Bell JK, Mullen GE, Leifer CA, Mazzoni A, Davies DR, Segal DM (2003) Leucine-rich repeats and pathogen recognition in Toll-like receptors. Trends in immunology **24:** 528-533

Bent AF, Mackey D (2007) Elicitors, effectors, and R genes: the new paradigm and a lifetime supply of questions. Annu. Rev. Phytopathol. **45:** 399-436

Bi G, Liebrand TW, Bye RR, Postma J, van der Burgh AM, Robatzek S, Xu X, Joosten MH (2016) SOBIR1 requires the GxxxG dimerization motif in its transmembrane domain to form constitutive complexes with receptor-like proteins. Molecular plant pathology **17:** 96-107

Bi G, Liebrand TW, Cordewener JH, America AH, Xu X, Joosten MH (2014) Arabidopsis thaliana receptor-like protein At RLP23 associates with the receptor-like kinase At SOBIR1. Plant signaling & behavior **9:** e27937

Bloemberg GV, Lugtenberg BJ (2001) Molecular basis of plant growth promotion and biocontrol by rhizobacteria. Current opinion in plant biology **4:** 343-350

Blume B, Nürnberger T, Nass N, Scheel D (2000) Receptor-mediated increase in cytoplasmic free calcium required for activation of pathogen defense in parsley. Plant Cell **12:** 1425-1440

Boelens R, Gualerzi C (2002) Structure and function of bacterial initiation factors. Current protein & peptide science **3:** 107-119

Böhm H, Albert I, Fan L, Reinhard A, Nürnberger T (2014) Immune receptor complexes at the plant cell surface. Current opinion in plant biology **20:** 47-54

Böhm H, Albert I, Oome S, Raaymakers TM, Van den Ackerveken G, Nürnberger T (2014) A conserved peptide pattern from a widespread microbial virulence factor triggers pattern-induced immunity in Arabidopsis. PLoS Pathog **10:** e1004491

Boller T, Felix G (2009) A renaissance of elicitors: perception of microbe-associated molecular patterns and danger signals by pattern-recognition receptors. Annual review of plant biology **60:** 379-406

Bolton MD, Rivera-Varas V, del Río Mendoza LE, Khan MF, Secor GA (2012) Efficacy of variable tetraconazole rates against Cercospora beticola isolates with differing in vitro sensitivities to DMI fungicides. Plant disease **96:** 1749-1756

Boschi F, Schvartzman C, Murchio S, Ferreira V, Siri MI, Galván GA, Smoker M, Stransfeld L, Zipfel C, Vilaró FL (2017) Enhanced bacterial wilt resistance in potato through expression of Arabidopsis EFR and introgression of quantitative resistance from Solanum commersonii. Frontiers in plant science **8:** 1642

Boutrot F, Zipfel C (2017) Function, discovery, and exploitation of plant pattern recognition receptors for broad-spectrum disease resistance. Annual review of Phytopathology **55:** 257-286

Boye J, Ma C-Y, Harwalkar V (1997) Thermal denaturation and coagulation of proteins. *In* Food proteins and their applications. CRC Press, pp 25-56

Brookes G, Barfoot P (2016) GM crops: global socio-economic and environmental impacts 1996–2014. Dorchester, UK: PG Economics

Brutus A, Sicilia F, Macone A, Cervone F, De Lorenzo G (2010) A domain swap approach reveals a role of the plant wall-associated kinase 1 (WAK1) as a receptor of oligogalacturonides. Proceedings of the National Academy of Sciences **107:** 9452-9457

Buscaill P, Chandrasekar B, Sanguankiattichai N, Kourelis J, Kaschani F, Thomas EL, Morimoto K, Kaiser M, Preston GM, Ichinose Y (2019) Glycosidase and glycan polymorphism control hydrolytic release of immunogenic flagellin peptides. Science **364:** eaav0748

Bycroft M, Hubbard TJ, Proctor M, Freund SM, Murzin AG (1997) The solution structure of the S1 RNA binding domain: a member of an ancient nucleic acid–binding fold. Cell **88:** 235-242

Cao Y, Liang Y, Tanaka K, Nguyen CT, Jedrzejczak RP, Joachimiak A, Stacey G (2014) The kinase LYK5 is a major chitin receptor in Arabidopsis and forms a chitin-induced complex with related kinase CERK1. elife **3:** e03766

Carter AP, Clemons WM, Brodersen DE, Morgan-Warren RJ, Hartsch T, Wimberly BT, Ramakrishnan V (2001) Crystal structure of an initiation factor bound to the 30S ribosomal subunit. Science **291:** 498-501

Catanzariti AM, Do HT, Bru P, de Sain M, Thatcher LF, Rep M, Jones DA (2017) The tomato I gene for Fusarium wilt resistance encodes an atypical leucine-rich repeat receptor-like protein whose function is nevertheless dependent on SOBIR 1 and SERK 3/BAK 1. The Plant Journal **89:** 1195-1209

Cesari S, Bernoux M, Moncuquet P, Kroj T, Dodds P (2014) A novel conserved mechanism for plant NLR protein pairs: the 'integrated decoy' hypothesis. Frontiers in Plant Science **5**

Chang X, Nick P (2012) Defence signalling triggered by Flg22 and Harpin is integrated into a different stilbene output in Vitis cells. PLoS One **7**

Chen GY, Nuñez G (2010) Sterile inflammation: sensing and reacting to damage. Nature Reviews Immunology **10:** 826-837

Chen L, Zhang S-J, Zhang S-S, Qu S, Ren X, Long J, Yin Q, Qian J, Sun F, Zhang C (2008) A fragment of the Xanthomonas oryzae pv. oryzicola harpin HpaGXooc reduces disease and increases yield of rice in extensive grower plantings. Phytopathology **98:** 792-802

Chinchilla D, Bauer Z, Regenass M, Boller T, Felix G (2006) The Arabidopsis receptor kinase FLS2 binds flg22 and determines the specificity of flagellin perception. The Plant Cell **18:** 465-476

Chinchilla D, Shan L, He P, de Vries S, Kemmerling B (2009) One for all: the receptor-associated kinase BAK1. Trends in plant science **14:** 535-541

Chinchilla D, Zipfel C, Robatzek S, Kemmerling B, Nürnberger T, Jones JD, Felix G, Boller T (2007) A flagellin-induced complex of the receptor FLS2 and BAK1 initiates plant defence. Nature **448:** 497-500

Chitwood DH, Kumar R, Headland LR, Ranjan A, Covington MF, Ichihashi Y, Fulop D, Jiménez-Gómez JM, Peng J, Maloof JN (2013) A quantitative genetic basis for leaf morphology in a set of precisely defined tomato introgression lines. The Plant Cell**:** tpc. 113.112391

Chivasa S, Goodman HL (2020) Stress-adaptive gene discovery by exploiting collective decision-making of decentralized plant response systems. New Phytologist **225:** 2307-2313

Choi J, Tanaka K, Cao Y, Qi Y, Qiu J, Liang Y, Lee SY, Stacey G (2014) Identification of a plant receptor for extracellular ATP. Science **343:** 290-294

Choi J, Tanaka K, Liang Y, Cao Y, Lee SY, Stacey G (2014) Extracellular ATP, a danger signal, is recognized by DORN1 in Arabidopsis. Biochemical Journal **463:** 429-437

Choi M-S, Heu S, Paek N-C, Koh H-J, Lee J-S, Oh C-S (2012) Expression of hpa1 gene encoding a bacterial harpin protein in Xanthomonas oryzae pv. oryzae enhances disease resistance to both fungal and bacterial pathogens in rice and Arabidopsis. The Plant Pathology Journal **28:** 364-372

Choi M-S, Kim W, Lee C, Oh C-S (2013) Harpins, multifunctional proteins secreted by gram-negative plant-pathogenic bacteria. Molecular plant-microbe interactions **26:** 1115-1122

Conrath U, Beckers GJ, Langenbach CJ, Jaskiewicz MR (2015) Priming for enhanced defense. Annual review of phytopathology **53**

Cook DE, Mesarich CH, Thomma BP (2015) Understanding plant immunity as a surveillance system to detect invasion. Annual review of phytopathology **53:** 541-563

Cook DN, Pisetsky DS, Schwartz DA (2004) Toll-like receptors in the pathogenesis of human disease. Nature immunology **5:** 975-979

Couto D, Zipfel C (2016) Regulation of pattern recognition receptor signalling in plants. Nature Reviews Immunology **16:** 537

Cummings HS, Hershey J (1994) Translation initiation factor IF1 is essential for cell viability in Escherichia coli. Journal of bacteriology **176:** 198-205

Davis P, Williams S (1998) Protein modification by thermal processing. Allergy **53:** 102-105

de Azevedo Souza C, Li S, Lin AZ, Boutrot F, Grossmann G, Zipfel C, Somerville SC (2017) Cellulose-derived oligomers act as damage-associated molecular patterns and trigger defense-like responses. Plant physiology **173:** 2383-2398

de Jonge R, van Esse HP, Maruthachalam K, Bolton MD, Santhanam P, Saber MK, Zhang Z, Usami T, Lievens B, Subbarao KV (2012) Tomato immune receptor Ve1 recognizes effector of multiple fungal pathogens uncovered by genome and RNA sequencing. Proceedings of the National Academy of Sciences **109:** 5110-5115

de Torres Zabala M, Zhai B, Jayaraman S, Eleftheriadou G, Winsbury R, Yang R, Truman W, Tang S, Smirnoff N, Grant M (2016) Novel JAZ co-operativity and unexpected JA dynamics underpin A rabidopsis defence responses to P seudomonas syringae infection. New Phytologist **209:** 1120-1134

Dodds PN, Rathjen JP (2010) Plant immunity: towards an integrated view of plant–pathogen interactions. Nature Reviews Genetics **11:** 539-548

Domazakis E, Wouters D, Visser RG, Kamoun S, Joosten MH, Vleeshouwers VG (2018) The ELR-SOBIR1 complex functions as a two-component receptor-like kinase to mount defense against Phytophthora infestans. Molecular Plant-Microbe Interactions **31:** 795-802

Du J, Verzaux E, Chaparro-Garcia A, Bijsterbosch G, Keizer LP, Zhou J, Liebrand TW, Xie C, Govers F, Robatzek S (2015) Elicitin recognition confers enhanced resistance to Phytophthora infestans in potato. Nature plants **1:** 1-5

Dunwell J (2013) Global population growth, food security and food and farming for the future. Successful Agricultural Innovation in Emerging Economies: New Genetic Technologies for Global Food Production **100:** 23

Edwards A, Civitello A, Hammond HA, Caskey CT (1991) DNA typing and genetic mapping with trimeric and tetrameric tandem repeats. American journal of human genetics **49:** 746

Ellinger D, Voigt CA (2014) Callose biosynthesis in Arabidopsis with a focus on pathogen response: what we have learned within the last decade. Annals of botany **114:** 1349-1358

Fan L (2015) Identification of a novel receptor of bacterial PAMP RsE in Arabidopsis using genomic tools.

Felix G, Boller T (2003) Molecular Sensing of Bacteria in Plants the highly conserved RNA-binding motif rnp-1 of bacterial cold shock proteins is recognized as an elicitor signal in tobacco. Journal of Biological Chemistry **278:** 6201-6208

Felix G, Duran JD, Volko S, Boller T (1999) Plants have a sensitive perception system for the most conserved domain of bacterial flagellin. The Plant Journal **18:** 265-276

Freeman BC, Beattie GA (2008) An overview of plant defenses against pathogens and herbivores. The Plant Health Instructor

Gao M, Wang X, Wang D, Xu F, Ding X, Zhang Z, Bi D, Cheng YT, Chen S, Li X (2009) Regulation of cell death and innate immunity by two receptor-like kinases in Arabidopsis. Cell host & microbe **6:** 34-44

Garcia-Brugger A, Lamotte O, Vandelle E, Bourque S, Lecourieux D, Poinssot B, Wendehenne D, Pugin A (2006) Early signaling events induced by elicitors of plant defenses. Molecular plant-microbe interactions **19:** 711-724

Geiger F, Bengtsson J, Berendse F, Weisser WW, Emmerson M, Morales MB, Ceryngier P, Liira J, Tscharntke T, Winqvist C (2010) Persistent negative effects of pesticides on biodiversity and biological control potential on European farmland. Basic and Applied Ecology **11:** 97-105

Ghislain M, Byarugaba AA, Magembe E, Njoroge A, Rivera C, Román ML, Tovar JC, Gamboa S, Forbes GA, Kreuze JF (2019) Stacking three late blight resistance genes from wild species directly into African highland potato varieties confers complete field resistance to local blight races. Plant biotechnology journal **17:** 1119-1129

Girardin SE, Sansonetti PJ, Philpott DJ (2002) Intracellular vs extracellular recognition of pathogens–common concepts in mammals and flies. Trends in microbiology **10:** 193-199

Glawischnig E (2007) Camalexin. Phytochemistry **68:** 401-406

Godoy CV, Seixas CDS, Soares RM, Marcelino-Guimarães FC, Meyer MC, Costamilan LM (2016) Asian soybean rust in Brazil: past, present, and future. Pesquisa Agropecuária Brasileira **51:** 407-421

Goldsby RA, Kindt TJ, Osborne BA (1999) Immunology 4e. *In*. W.H. Freeman & Company

Gómez-Gómez L, Boller T (2000) FLS2: an LRR receptor–like kinase involved in the perception of the bacterial elicitor flagellin in Arabidopsis. Molecular cell **5:** 1003-1011

Gómez-Gómez L, Felix G, Boller T (1999) A single locus determines sensitivity to bacterial flagellin in Arabidopsis thaliana. The Plant Journal **18:** 277-284

Grigoriadou C, Marzi S, Kirillov S, Gualerzi CO, Cooperman BS (2007) A quantitative kinetic scheme for 70 S translation initiation complex formation. Journal of molecular biology **373:** 562-572

Gualerzi C, Risuleo G, Pon CL (1977) Initial rate kinetic analysis of the mechanism of initiation complex formation and the role of initiation factor IF-3. Biochemistry **16:** 1684-1689

Gualerzi CO, Pon CL (1990) Initiation of mRNA translation in prokaryotes. Biochemistry **29:** 5881-5889

Gust AA, Felix G (2014) Receptor like proteins associate with SOBIR1-type of adaptors to form bimolecular receptor kinases. Current opinion in plant biology **21:** 104-111

Gust AA, Pruitt R, Nürnberger T (2017) Sensing Danger: Key to Activating Plant Immunity. Trends in Plant Science **22:** 779-791

Halter T, Imkampe J, Blaum BS, Stehle T, Kemmerling B (2014) BIR2 affects complex formation of BAK1 with ligand binding receptors in plant defense. Plant Signal Behav **9**

Halter T, Imkampe J, Mazzotta S, Wierzba M, Postel S, Bücherl C, Kiefer C, Stahl M, Chinchilla D, Wang X (2014) The leucine-rich repeat receptor kinase BIR2 is a negative regulator of BAK1 in plant immunity. Current Biology **24:** 134-143

Hann DR, Rathjen JP (2007) Early events in the pathogenicity of Pseudomonas syringae on Nicotiana benthamiana. The Plant Journal **49:** 607-618

Harrison SJ, Mott EK, Parsley K, Aspinall S, Gray JC, Cottage A (2006) A rapid and robust method of identifying transformed Arabidopsis thaliana seedlings following floral dip transformation. Plant methods **2:** 19

He P, Shan L, Sheen J (2007) Elicitation and suppression of microbe-associated molecular pattern-triggered immunity in plant–microbe interactions. Cellular microbiology **9:** 1385-1396

Heese A, Hann DR, Gimenez-Ibanez S, Jones AM, He K, Li J, Schroeder JI, Peck SC, Rathjen JP (2007) The receptor-like kinase SERK3/BAK1 is a central regulator of innate immunity in plants. Proceedings of the National Academy of Sciences **104:** 12217-12222

Hegenauer V, Fürst U, Kaiser B, Smoker M, Zipfel C, Felix G, Stahl M, Albert M (2016) Detection of the plant parasite Cuscuta reflexa by a tomato cell surface receptor. Science **353:** 478-481

Herring RJ (2013) Transgenics and the poor: Biotechnology in development studies. Routledge

Hind SR, Strickler SR, Boyle PC, Dunham DM, Bao Z, O'Doherty IM, Baccile JA, Hoki JS, Viox EG, Clarke CR (2016) Tomato receptor FLAGELLIN-SENSING 3 binds flgII-28 and activates the plant immune system. Nature plants **2:** 1-8

Howe JG, Hershey J (1983) Initiation factor and ribosome levels are coordinately controlled in Escherichia coli growing at different rates. Journal of Biological Chemistry **258:** 1954-1959

Hrabak EM, Chan CW, Gribskov M, Harper JF, Choi JH, Halford N, Kudla J, Luan S, Nimmo HG, Sussman MR (2003) The Arabidopsis CDPK-SnRK superfamily of protein kinases. Plant physiology **132:** 666-680

Imkampe J, Halter T, Huang S, Schulze S, Mazzotta S, Schmidt N, Manstretta R, Postel S, Wierzba M, Yang Y (2017) The Arabidopsis leucine-rich repeat receptor kinase BIR3 negatively regulates BAK1 receptor complex formation and stabilizes BAK1. The Plant Cell **29:** 2285-2303

Inoue H, Nojima H, Okayama H (1990) High efficiency transformation of Escherichia coli with plasmids. Gene **96:** 23-28

Ito Y, Kaku H, Shibuya N (1997) Identification of a high-affinity binding protein for N-acetylchitooligosaccharide elicitor in the plasma membrane of suspension-cultured rice cells by affinity labeling. The Plant Journal **12:** 347-356

Iwabuchi S, Watanabe H, Yamauchi F (1991) Thermal denaturation of. beta.-conglycinin. Kinetic resolution of reaction mechanism. Journal of Agricultural and Food chemistry **39:** 27-33

Iwasaki A, Medzhitov R (2015) Control of adaptive immunity by the innate immune system. Nature immunology **16:** 343

Jabs T, Tschöpe M, Colling C, Hahlbrock K, Scheel D (1997) Elicitor-stimulated ion fluxes and O2− from the oxidative burst are essential components in triggering defense gene activation and phytoalexin synthesis in parsley. Proceedings of the National Academy of Sciences **94:** 4800-4805

Jackson RW (2009) Plant pathogenic bacteria: genomics and molecular biology. Caister Academic Press

Jehle AK, Lipschis M, Albert M, Fallahzadeh-Mamaghani V, Fürst U, Mueller K, Felix G (2013) The receptor-like protein ReMAX of Arabidopsis detects the microbe-associated molecular pattern eMax from Xanthomonas. The Plant Cell **25:** 2330-2340

Jones JD, Dangl JL (2006) The plant immune system. nature **444:** 323-329

Joosten MH, Cozijnsen TJ, De Wit PJ (1994) Host resistance to a fungal tomato pathogen lost by a single base-pair change in an avirulence gene. Nature **367:** 384-386

Kadota Y, Sklenar J, Derbyshire P, Stransfeld L, Asai S, Ntoukakis V, Jones JD, Shirasu K, Menke F, Jones A (2014) Direct regulation of the NADPH oxidase RBOHD by the PRR-associated kinase BIK1 during plant immunity. Molecular cell **54:** 43-55

Kaiser B, Vogg G, Fürst UB, Albert M (2015) Parasitic plants of the genus Cuscuta and their interaction with susceptible and resistant host plants. Frontiers in plant science **6:** 45

Kaku H, Nishizawa Y, Ishii-Minami N, Akimoto-Tomiyama C, Dohmae N, Takio K, Minami E, Shibuya N (2006) Plant cells recognize chitin fragments for defense signaling through a plasma membrane receptor. Proceedings of the National Academy of Sciences **103:** 11086-11091

Kanyuka K, Rudd JJ (2019) Cell surface immune receptors: the guardians of the plant's extracellular spaces. Current opinion in plant biology **50:** 1-8

Karimi M, Inzé D, Depicker A (2002) GATEWAY™ vectors for Agrobacterium-mediated plant transformation. Trends in plant science **7:** 193-195

Kaul S, Koo HL, Jenkins J, Rizzo M, Rooney T, Tallon LJ, Feldblyum T, Nierman W, Benito MI, Lin X (2000) Analysis of the genome sequence of the flowering plant Arabidopsis thaliana. nature **408:** 796-815

Kawchuk LM, Hachey J, Lynch DR, Kulcsar F, Van Rooijen G, Waterer DR, Robertson A, Kokko E, Byers R, Howard RJ (2001) Tomato Ve disease resistance genes encode cell surface-like receptors. Proceedings of the National Academy of Sciences **98:** 6511-6515

Keller H, Pamboukdjian N, Ponchet M, Poupet A, Delon R, Verrier J-L, Roby D, Ricci P (1999) Pathogen-induced elicitin production in transgenic tobacco generates a hypersensitive response and nonspecific disease resistance. The Plant Cell **11:** 223-235

Kemmerling B, Halter T, Mazzotta S, Mosher S, Nürnberger T (2011) A genome-wide survey for Arabidopsis leucine-rich repeat receptor kinases implicated in plant immunity. Front Plant Sci **2:** 88

Kemmerling B, Schwedt A, Rodriguez P, Mazzotta S, Frank M, Qamar SA, Mengiste T, Betsuyaku S, Parker JE, Mussig C, Thomma BP, Albrecht C, de Vries SC, Hirt H, Nürnberger T (2007) The BRI1-associated kinase 1, BAK1, has a brassinolide-independent role in plant cell-death control. Curr Biol **17:** 1116-1122

Kinoshita T, Caño-Delgado A, Seto H, Hiranuma S, Fujioka S, Yoshida S, Chory J (2005) Binding of brassinosteroids to the extracellular domain of plant receptor kinase BRI1. Nature **433:** 167-171

Kooman-Gersmann M, Vogelsang R, Hoogendijk EC, De Wit PJ (1997) Assignment of amino acid residues of the AVR9 peptide of Cladosporium fulvum that determine elicitor activity. Molecular plant-microbe interactions **10:** 821-829

Koutsopoulos S, van der Oost J, Norde W (2007) Kinetically controlled refolding of a heat-denatured hyperthermostable protein. The FEBS Journal **274:** 5915-5923

Krol E, Mentzel T, Chinchilla D, Boller T, Felix G, Kemmerling B, Postel S, Arents M, Jeworutzki E, Al-Rasheid KA (2010) Perception of the Arabidopsis danger signal peptide 1 involves the pattern recognition receptor AtPEPR1 and its close homologue AtPEPR2. Journal of Biological Chemistry **285:** 13471-13479

Kunwar S, Iriarte F, Fan Q, Evaristo da Silva E, Ritchie L, Nguyen NS, Freeman JH, Stall RE, Jones JB, Minsavage GV (2018) Transgenic expression of EFR and

Bs2 genes for field management of bacterial wilt and bacterial spot of tomato. Phytopathology **108:** 1402-1411

Kunze G, Zipfel C, Robatzek S, Niehaus K, Boller T, Felix G (2004) The N terminus of bacterial elongation factor Tu elicits innate immunity in Arabidopsis plants. The Plant Cell **16:** 3496-3507

Kutschera A, Dawid C, Gisch N, Schmid C, Raasch L, Gerster T, Schäffer M, Smakowska-Luzan E, Belkhadir Y, Vlot ACJS (2019) Bacterial medium-chain 3-hydroxy fatty acid metabolites trigger immunity in Arabidopsis plants. **364:** 178-181

Lacombe S, Rougon-Cardoso A, Sherwood E, Peeters N, Dahlbeck D, van Esse HP, Smoker M, Rallapalli G, Thomma BP, Staskawicz B, Jones JD, Zipfel C (2010) Interfamily transfer of a plant pattern-recognition receptor confers broad-spectrum bacterial resistance. Nat Biotechnol **28:** 365-369

Laemmli UK (1970) Cleavage of structural proteins during the assembly of the head of bacteriophage T4. nature **227:** 680-685

Lal NK, Nagalakshmi U, Hurlburt NK, Flores R, Bak A, Sone P, Ma X, Song G, Walley J, Shan L (2018) The receptor-like cytoplasmic kinase BIK1 localizes to the nucleus and regulates defense hormone expression during plant innate immunity. Cell host & microbe **23:** 485-497. e485

Lamichhane JR, Dachbrodt-Saaydeh S, Kudsk P, Messéan A (2016) Toward a reduced reliance on conventional pesticides in European agriculture. Plant Disease **100:** 10-24

Laursen BS, Sørensen HP, Mortensen KK, Sperling-Petersen HU (2005) Initiation of protein synthesis in bacteria. Microbiol. Mol. Biol. Rev. **69:** 101-123

Lehti-Shiu MD, Zou C, Hanada K, Shiu S-H (2009) Evolutionary history and stress regulation of plant receptor-like kinase/pelle genes. Plant Physiology **150:** 12-26

Lenarčič T, Albert I, Böhm H, Hodnik V, Pirc K, Zavec AB, Podobnik M, Pahovnik D, Žagar E, Pruitt R (2017) Eudicot plant-specific sphingolipids determine host selectivity of microbial NLP cytolysins. Science **358:** 1431-1434

Leslie ME, Lewis MW, Youn J-Y, Daniels MJ, Liljegren SJ (2010) The EVERSHED receptor-like kinase modulates floral organ shedding in Arabidopsis. Development **137:** 467-476

Li J (2010) Multi-tasking of somatic embryogenesis receptor-like protein kinases. Current opinion in plant biology **13:** 509-514

Li J, Wen J, Lease KA, Doke JT, Tax FE, Walker JC (2002) BAK1, an Arabidopsis LRR receptor-like protein kinase, interacts with BRI1 and modulates brassinosteroid signaling. Cell **110:** 213-222

Li L, Li M, Yu L, Zhou Z, Liang X, Liu Z, Cai G, Gao L, Zhang X, Wang Y (2014) The FLS2-associated kinase BIK1 directly phosphorylates the NADPH oxidase RbohD to control plant immunity. Cell host & microbe **15:** 329-338

Liang X, Ma M, Zhou Z, Wang J, Yang X, Rao S, Bi G, Li L, Zhang X, Chai J (2018) Ligand-triggered de-repression of Arabidopsis heterotrimeric G proteins coupled to immune receptor kinases. Cell research **28:** 529-543

Liebrand TW, van den Berg GC, Zhang Z, Smit P, Cordewener JH, America AH, Sklenar J, Jones AM, Tameling WI, Robatzek S (2013) Receptor-like kinase SOBIR1/EVR interacts with receptor-like proteins in plant immunity against fungal infection. Proceedings of the National Academy of Sciences **110:** 10010-10015

Liebrand TW, van den Burg HA, Joosten MH (2014) Two for all: receptor-associated kinases SOBIR1 and BAK1. Trends in plant science **19:** 123-132

Liu X, Grabherr HM, Willmann R, Kolb D, Brunner F, Bertsche U, Kuhner D, Franz-Wachtel M, Amin B, Felix G, Ongena M, Nürnberger T, Gust AA (2014) Host-

induced bacterial cell wall decomposition mediates pattern-triggered immunity in Arabidopsis. Elife **3**

Lu D, Wu S, Gao X, Zhang Y, Shan L, He P (2010) A receptor-like cytoplasmic kinase, BIK1, associates with a flagellin receptor complex to initiate plant innate immunity. Proceedings of the National Academy of Sciences **107:** 496-501

Lu F, Wang H, Wang S, Jiang W, Shan C, Li B, Yang J, Zhang S, Sun W (2015) Enhancement of innate immune system in monocot rice by transferring the dicotyledonous elongation factor Tu receptor EFR. Journal of integrative plant biology **57:** 641-652

Ma L, Borhan MH (2015) The receptor-like kinase SOBIR1 interacts with Brassica napus LepR3 and is required for Leptosphaeria maculans AvrLm1-triggered immunity. Frontiers in plant science **6:** 933

Malinovsky FG, Fangel JU, Willats WG (2014) The role of the cell wall in plant immunity. Frontiers in plant science **5:** 178

Manosalva P, Manohar M, Von Reuss SH, Chen S, Koch A, Kaplan F, Choe A, Micikas RJ, Wang X, Kogel K-H (2015) Conserved nematode signalling molecules elicit plant defenses and pathogen resistance. Nature communications **6:** 7795

Mansfield J, Genin S, Magori S, Citovsky V, Sriariyanum M, Ronald P, Dow M, Verdier V, Beer SV, Machado MA (2012) Top 10 plant pathogenic bacteria in molecular plant pathology. Molecular plant pathology **13:** 614-629

Mao G, Meng X, Liu Y, Zheng Z, Chen Z, Zhang S (2011) Phosphorylation of a WRKY transcription factor by two pathogen-responsive MAPKs drives phytoalexin biosynthesis in Arabidopsis. The Plant Cell **23:** 1639-1653

Marintchev A, Wagner G (2004) Translation initiation: structures, mechanisms and evolution. Quarterly reviews of biophysics **37:** 197-284

Mauch-Mani B, Baccelli I, Luna E, Flors V (2017) Defense priming: an adaptive part of induced resistance. Annual Review of Plant Biology **68:** 485-512

McGurl B, Pearce G, Orozco-Cardenas M, Ryan CA (1992) Structure, expression, and antisense inhibition of the systemin precursor gene. Science **255:** 1570-1573

Medzhitov R, Janeway CA (1997) Innate immunity: the virtues of a nonclonal system of recognition. Cell **91:** 295-298

Medzhitov R, Janeway CA (2002) Decoding the patterns of self and nonself by the innate immune system. Science **296:** 298-300

Meindl T, Boller T, Felix G (2000) The bacterial elicitor flagellin activates its receptor in tomato cells according to the address–message concept. The Plant Cell **12:** 1783-1794

Melotto M, Underwood W, He SY (2008) Role of stomata in plant innate immunity and foliar bacterial diseases. Annu. Rev. Phytopathol. **46:** 101-122

Melotto M, Underwood W, Koczan J, Nomura K, He SY (2006) Plant stomata function in innate immunity against bacterial invasion. Cell **126:** 969-980

Melzer E (2013) Charakterisierung eines neuen bakteriellen Elicitors von Ralstonia solanacearum in Arabidopsis thaliana. Dissertation 1–139

Miedes E, Vanholme R, Boerjan W, Molina A (2014) The role of the secondary cell wall in plant resistance to pathogens. Frontiers in plant science **5:** 358

Milon P, Carotti M, Konevega AL, Wintermeyer W, Rodnina MV, Gualerzi CO (2010) The ribosome-bound initiation factor 2 recruits initiator tRNA to the 30S initiation complex. EMBO reports **11:** 312-316

Milon P, Konevega AL, Gualerzi CO, Rodnina MV (2008) Kinetic checkpoint at a late step in translation initiation. Molecular cell **30:** 712-720

Milón P, Maracci C, Filonava L, Gualerzi CO, Rodnina MV (2012) Real-time assembly landscape of bacterial 30S translation initiation complex. Nature structural & molecular biology **19:** 609-615

Mithöfer A, Boland W (2008) Recognition of herbivory-associated molecular patterns. Plant Physiology **146:** 825-831

Miya A, Albert P, Shinya T, Desaki Y, Ichimura K, Shirasu K, Narusaka Y, Kawakami N, Kaku H, Shibuya N (2007) CERK1, a LysM receptor kinase, is essential for chitin elicitor signaling in Arabidopsis. Proceedings of the National Academy of Sciences **104:** 19613-19618

Mogensen TH (2009) Pathogen recognition and inflammatory signaling in innate immune defenses. Clinical microbiology reviews **22:** 240-273

Mohamed N, Lherminier J, Farmer M-J, Fromentin J, Béno N, Houot V, Milat M-L, Blein J-P (2007) Defense responses in grapevine leaves against Botrytis cinerea induced by application of a Pythium oligandrum strain or its elicitin, oligandrin, to roots. Phytopathology **97:** 611-620

Monaghan J, Zipfel C (2012) Plant pattern recognition receptor complexes at the plasma membrane. Current opinion in plant biology **15:** 349-357

Morillo SA, Tax FE (2006) Functional analysis of receptor-like kinases in monocots and dicots. Current opinion in plant biology **9:** 460-469

Morrissey JP, Osbourn AE (1999) Fungal resistance to plant antibiotics as a mechanism of pathogenesis. Microbiol. Mol. Biol. Rev. **63:** 708-724

Mott GA, Middleton MA, Desveaux D, Guttman DS (2014) Peptides and small molecules of the plant-pathogen apoplastic arena. Frontiers in plant science **5:** 677

Myasnikov AG, Marzi S, Simonetti A, Giuliodori AM, Gualerzi CO, Yusupova G, Yusupov M, Klaholz BP (2005) Conformational transition of initiation factor 2 from the GTP-to GDP-bound state visualized on the ribosome. Nature structural & molecular biology **12:** 1145-1149

Nam KH, Li J (2002) BRI1/BAK1, a receptor kinase pair mediating brassinosteroid signaling. Cell **110:** 203-212

Navarro L, Dunoyer P, Jay F, Arnold B, Dharmasiri N, Estelle M, Voinnet O, Jones JD (2006) A plant miRNA contributes to antibacterial resistance by repressing auxin signaling. Science **312:** 436-439

Neubig RR, Spedding M, Kenakin T, Christopoulos A (2003) International Union of Pharmacology Committee on Receptor Nomenclature and Drug Classification. XXXVIII. Update on terms and symbols in quantitative pharmacology. Pharmacological reviews **55:** 597-606

Nguyen HP, Chakravarthy S, Velásquez AC, McLane HL, Zeng L, Nakayashiki H, Park D-H, Collmer A, Martin GB (2010) Methods to study PAMP-triggered immunity using tomato and Nicotiana benthamiana. Molecular Plant-Microbe Interactions **23:** 991-999

Noman A, Aqeel M, Lou Y (2019) PRRs and NB-LRRs: from signal perception to activation of plant innate immunity. International journal of molecular sciences **20:** 1882

Nühse TS, Peck SC, Hirt H, Boller T (2000) Microbial elicitors induce activation and dual phosphorylation of the Arabidopsis thaliana MAPK 6. Journal of Biological Chemistry **275:** 7521-7526

Nürnberger T, Brunner F (2002) Innate immunity in plants and animals: emerging parallels between the recognition of general elicitors and pathogen-associated molecular patterns. Curr Opin Plant Biol **5:** 318-324

Nürnberger T, Brunner F, Kemmerling B, Piater L (2004) Innate immunity in plants and animals: striking similarities and obvious differences. Immunol Rev **198:** 249-266

O'Neill LA, Bowie AG (2007) The family of five: TIR-domain-containing adaptors in Toll-like receptor signalling. Nature Reviews Immunology **7:** 353-364

OECD, Food, Nations AOotU (2019) OECD-FAO Agricultural Outlook 2019-2028,

Oerke E-C, Dehne H-W (2004) Safeguarding production—losses in major crops and the role of crop protection. Crop protection **23:** 275-285

Oh HS, Collmer A (2005) Basal resistance against bacteria in Nicotiana benthamiana leaves is accompanied by reduced vascular staining and suppressed by multiple Pseudomonas syringae type III secretion system effector proteins. The Plant Journal **44:** 348-359

Oh M-H, Wang X, Kota U, Goshe MB, Clouse SD, Huber SC (2009) Tyrosine phosphorylation of the BRI1 receptor kinase emerges as a component of brassinosteroid signaling in Arabidopsis. Proceedings of the National Academy of Sciences **106:** 658-663

Oh M-H, Wang X, Wu X, Zhao Y, Clouse SD, Huber SC (2010) Autophosphorylation of Tyr-610 in the receptor kinase BAK1 plays a role in brassinosteroid signaling and basal defense gene expression. Proceedings of the National Academy of Sciences **107:** 17827-17832

Oome S, Raaymakers TM, Cabral A, Samwel S, Bohm H, Albert I, Nürnberger T, Van den Ackerveken G (2014) Nep1-like proteins from three kingdoms of life act as a microbe-associated molecular pattern in Arabidopsis. Proc Natl Acad Sci U S A **111:** 16955-16960

Ottmann C, Luberacki B, Kufner I, Koch W, Brunner F, Weyand M, Mattinen L, Pirhonen M, Anderluh G, Seitz HU, Nürnberger T, Oecking C (2009) A common toxin fold mediates microbial attack and plant defense. Proc Natl Acad Sci U S A **106:** 10359-10364

Pearce G, Strydom D, Johnson S, Ryan CA (1991) A polypeptide from tomato leaves induces wound-inducible proteinase inhibitor proteins. Science **253:** 895-897

Postma J, Liebrand TW, Bi G, Evrard A, Bye RR, Mbengue M, Kuhn H, Joosten MH, Robatzek S (2016) Avr4 promotes Cf-4 receptor-like protein association with the BAK1/SERK3 receptor-like kinase to initiate receptor endocytosis and plant immunity. New Phytologist **210:** 627-642

Potekhin SA, Kovrigin EL (1998) Folding under inequilibrium conditions as a possible reason for partial irreversibility of heat-denatured proteins: computer simulation study. Biophysical chemistry **73:** 241-248

Privalov P, Tiktopulo E, Venyaminov SY, Griko YV, Makhatadze G, Khechinashvili N (1989) Heat capacity and conformation of proteins in the denatured state. Journal of molecular biology **205:** 737-750

Pruitt RN, Schwessinger B, Joe A, Thomas N, Liu F, Albert M, Robinson MR, Chan LJG, Luu DD, Chen H (2015) The rice immune receptor XA21 recognizes a tyrosine-sulfated protein from a Gram-negative bacterium. Science Advances **1:** e1500245

Raaijmakers JM, Paulitz TC, Steinberg C, Alabouvette C, Moënne-Loccoz Y (2009) The rhizosphere: a playground and battlefield for soilborne pathogens and beneficial microorganisms. Plant and soil **321:** 341-361

Rivas S, Thomas CM (2005) Molecular interactions between tomato and the leaf mold pathogen Cladosporium fulvum. Annu. Rev. Phytopathol. **43:** 395-436

Romeis T, Herde M (2014) From local to global: CDPKs in systemic defense signaling upon microbial and herbivore attack. Current opinion in plant biology **20:** 1-10

Ron M, Avni A (2004) The receptor for the fungal elicitor ethylene-inducing xylanase is a member of a resistance-like gene family in tomato. The Plant Cell **16:** 1604-1615

Rubartelli A, Lotze MT (2007) Inside, outside, upside down: damage-associated molecular-pattern molecules (DAMPs) and redox. Trends in immunology **28:** 429-436

Russ WP, Engelman DM (2000) The GxxxG motif: a framework for transmembrane helix-helix association. Journal of molecular biology **296:** 911-919

Saijo Y, Loo EPi, Yasuda S (2018) Pattern recognition receptors and signaling in plant–microbe interactions. The Plant Journal **93:** 592-613

Sambrook J, Russell DW (2001) Molecular Cloning-Sambrook & Russel-Vol. 1, 2, 3. Cold Spring Harb Lab Press

Santiago J, Henzler C, Hothorn M (2013) Molecular mechanism for plant steroid receptor activation by somatic embryogenesis co-receptor kinases. Science **341:** 889-892

Saur IM, Kadota Y, Sklenar J, Holton NJ, Smakowska E, Belkhadir Y, Zipfel C, Rathjen JP (2016) NbCSPR underlies age-dependent immune responses to bacterial cold shock protein in Nicotiana benthamiana. Proceedings of the National Academy of Sciences **113:** 3389-3394

Savary S, Willocquet L, Pethybridge SJ, Esker P, McRoberts N, Nelson A (2019) The global burden of pathogens and pests on major food crops. Nature ecology & evolution **3:** 430-439

Schlöffel MA, Käsbauer C, Gust AA (2019) Interplay of plant glycan hydrolases and LysM proteins in plant–bacteria interactions. International Journal of Medical Microbiology

Schoonbeek Hj, Wang HH, Stefanato FL, Craze M, Bowden S, Wallington E, Zipfel C, Ridout CJ (2015) Arabidopsis EF-Tu receptor enhances bacterial disease resistance in transgenic wheat. New Phytologist **206:** 606-613

Schulze B, Mentzel T, Jehle AK, Mueller K, Beeler S, Boller T, Felix G, Chinchilla D (2010) Rapid heteromerization and phosphorylation of ligand-activated plant transmembrane receptors and their associated kinase BAK1. Journal of Biological Chemistry **285:** 9444-9451

Schwessinger B, Bahar O, Thomas N, Holton N, Nekrasov V, Ruan D, Canlas PE, Daudi A, Petzold CJ, Singan VR (2015) Transgenic expression of the dicotyledonous pattern recognition receptor EFR in rice leads to ligand-dependent activation of defense responses. PLoS Pathog **11:** e1004809

Schwessinger B, Roux M, Kadota Y, Ntoukakis V, Sklenar J, Jones A, Zipfel C (2011) Phosphorylation-dependent differential regulation of plant growth, cell death, and innate immunity by the regulatory receptor-like kinase BAK1. PLoS genetics **7**

Serrano M, Coluccia F, Torres M, L'Haridon F, Métraux J-P (2014) The cuticle and plant defense to pathogens. Frontiers in plant science **5:** 274

Sette M, van Tilborg P, Spurio R, Kaptein R, Paci M, Gualerzi CO, Boelens R (1997) The structure of the translational initiation factor IF1 from E. coli contains an oligomer-binding motif. The EMBO Journal **16:** 1436-1443

Shiu S-H, Bleecker AB (2003) Expansion of the receptor-like kinase/Pelle gene family and receptor-like proteins in Arabidopsis. Plant physiology **132:** 530-543

Smakowska E, Kong J, Busch W, Belkhadir Y (2016) Organ-specific regulation of growth-defense tradeoffs by plants. Current opinion in plant biology **29:** 129-137

Smith DM (1994) Protein interactions in gels: protein-protein interactions. Marcel Dekker, New York

Smith MF, Mitchell A, Li G, Ding S, Fitzmaurice AM, Ryan K, Crowe S, Goldberg JB (2003) Toll-like receptor (TLR) 2 and TLR5, but not TLR4, are required for Helicobacter pylori-induced NF-κB activation and chemokine expression by epithelial cells. Journal of Biological Chemistry **278:** 32552-32560

Song C, Kumar A, Saleh M (2009) Bioinformatic comparison of bacterial secretomes. Genomics, proteomics & bioinformatics **7:** 37-46

Stegmann M, Monaghan J, Smakowska-Luzan E, Rovenich H, Lehner A, Holton N, Belkhadir Y, Zipfel C (2017) The receptor kinase FER is a RALF-regulated scaffold controlling plant immune signaling. Science **355:** 287-289

Sun Y, Li L, Macho AP, Han Z, Hu Z, Zipfel C, Zhou J-M, Chai J (2013) Structural basis for flg22-induced activation of the Arabidopsis FLS2-BAK1 immune complex. Science **342:** 624-628

Taguchi F, Shimizu R, Nakajima R, Toyoda K, Shiraishi T, Ichinose Y (2003) Differential effects of flagellins from Pseudomonas syringae pv. tabaci, tomato and glycinea on plant defense response. Plant Physiology and Biochemistry **41:** 165-174

Takakura Y, CHE FS, Ishida Y, Tsutsumi F, KUROTANI KI, Usami S, Isogai A, Imaseki H (2008) Expression of a bacterial flagellin gene triggers plant immune responses and confers disease resistance in transgenic rice plants. Molecular plant pathology **9:** 525-529

Tampakaki AP, Panopoulos NJ (2000) Elicitation of hypersensitive cell death by extracellularly targeted HrpZPsph produced in planta. Molecular plant-microbe interactions **13:** 1366-1374

Tanford C (1970) Protein denaturation. Adv. Protein Chem **24:** 95

Tani F, Shirai N, Venelle F, Yasumoto K, Onishi T, Doi E (1997) Temperature control for kinetic refolding of heat-denatured ovalbumin. Protein Science **6:** 1491-1502

Tao Y, Xie Z, Chen W, Glazebrook J, Chang H-S, Han B, Zhu T, Zou G, Katagiri F (2003) Quantitative nature of Arabidopsis responses during compatible and incompatible interactions with the bacterial pathogen Pseudomonas syringae. The Plant Cell **15:** 317-330

Teixeira PJP, Colaianni NR, Fitzpatrick CR, Dangl JL (2019) Beyond pathogens: microbiota interactions with the plant immune system. Current opinion in microbiology **49:** 7-17

Tena G, Boudsocq M, Sheen J (2011) Protein kinase signaling networks in plant innate immunity. Current opinion in plant biology **14:** 519-529

Thomma BP, Nürnberger T, Joosten MH (2011) Of PAMPs and effectors: the blurred PTI-ETI dichotomy. Plant Cell **23:** 4-15

Tian W, Hou C, Ren Z, Wang C, Zhao F, Dahlbeck D, Hu S, Zhang L, Niu Q, Li L (2019) A calmodulin-gated calcium channel links pathogen patterns to plant immunity. Nature **572:** 131-135

Torres MA, Jones JD, Dangl JL (2006) Reactive oxygen species signaling in response to pathogens. Plant physiology **141:** 373-378

Tsuda K, Katagiri F (2010) Comparing signaling mechanisms engaged in pattern-triggered and effector-triggered immunity. Current opinion in plant biology **13:** 459-465

Underhill DM, Ozinsky A (2002) Toll-like receptors: key mediators of microbe detection. Current opinion in immunology **14:** 103-110

Van den Ackerveken GF, Van Kan JA, De Wit PJ (1992) Molecular analysis of the avirulence gene avr9 of the fungal tomato pathogen Cladosporium fulvum fully supports the gene-for-gene hypothesis. The Plant Journal **2:** 359-366

Van den Ackerveken GF, Vossen P, De Wit J (1993) The AVR9 race-specific elicitor of Cladosporium fulvum is processed by endogenous and plant proteases. Plant Physiology **103:** 91-96

Van Der Burgh AM, Postma J, Robatzek S, Joosten MH (2019) Kinase activity of SOBIR1 and BAK1 is required for immune signalling. Molecular plant pathology **20:** 410-422

van der Hoorn RA, Kamoun S (2008) From guard to decoy: a new model for perception of plant pathogen effectors. The Plant Cell **20:** 2009-2017

Van Holde K (1977) Effects of amino acid composition and microenvironment on protein structure.

van Kan JA, Van den Ackerveken G, De Wit P (1991) Cloning and characterization of cDNA of avirulence gene avr9 of the fungal pathogen Cladosporium fulvum, causal agent of tomato leaf mold. Mol. Plant-Microbe Interact **4:** 52-59

Vázquez-Laslop N, Lee H, Hu R, Neyfakh AA (2001) Molecular sieve mechanism of selective release of cytoplasmic proteins by osmotically shocked Escherichia coli. Journal of Bacteriology **183:** 2399-2404

Vervoort J, van den Hooven HW, Berg A, Vossen P, Vogelsang R, Joosten MH, de Wit PJ (1997) The race-specific elicitor AVR9 of the tomato pathogen Cladosporium fulvum: a cystine knot protein: sequence-specific 1H NMR assignments, secondary structure and global fold of the protein. FEBS letters **404:** 153-158

Voet D, Voet JG, Pratt CW (2013) Fundamentals of biochemistry: life at the molecular level,

Vorwerk S, Somerville S, Somerville C (2004) The role of plant cell wall polysaccharide composition in disease resistance. Trends in plant science **9:** 203-209

Wan W-L, Fröhlich K, Pruitt RN, Nürnberger T, Zhang LJCOiPB (2019) Plant cell surface immune receptor complex signaling. **50:** 18-28

Wan WL, Zhang L, Pruitt R, Zaidem M, Brugman R, Ma X, Krol E, Perraki A, Kilian J, Grossmann G (2019) Comparing Arabidopsis receptor kinase and receptor protein-mediated immune signaling reveals BIK1-dependent differences. New Phytologist **221:** 2080-2095

Wang G, Ellendorff U, Kemp B, Mansfield JW, Forsyth A, Mitchell K, Bastas K, Liu C-M, Woods-Tör A, Zipfel C (2008) A genome-wide functional investigation into the roles of receptor-like proteins in Arabidopsis. Plant Physiology **147:** 503-517

Wang L, Albert M, Einig E, Fürst U, Krust D, Felix G (2016) The pattern-recognition receptor CORE of Solanaceae detects bacterial cold-shock protein. Nature plants **2:** 16185

Wang L, Einig E, Almeida-Trapp M, Albert M, Fliegmann J, Mithöfer A, Kalbacher H, Felix G (2018) The systemin receptor SYR1 enhances resistance of tomato against herbivorous insects. Nature plants **4:** 152-156

Wang X, Kota U, He K, Blackburn K, Li J, Goshe MB, Huber SC, Clouse SD (2008) Sequential transphosphorylation of the BRI1/BAK1 receptor kinase complex impacts early events in brassinosteroid signaling. Developmental cell **15:** 220-235

Wang X, Li X, Meisenhelder J, Hunter T, Yoshida S, Asami T, Chory J (2005) Autoregulation and homodimerization are involved in the activation of the plant steroid receptor BRI1. Developmental cell **8:** 855-865

Wang Y, Dang F, Liu Z, Wang X, Eulgem T, Lai Y, Yu L, She J, Shi Y, Lin J (2013) C a WRKY 58, encoding a group I WRKY transcription factor of C apsicum annuum, negatively regulates resistance to R alstonia solanacearum infection. Molecular plant pathology **14:** 131-144

Weber MH, Beckering CL, Marahiel MA (2001) Complementation of cold shock proteins by translation initiation factor IF1 in vivo. Journal of bacteriology **183:** 7381-7386

Weller DM, Raaijmakers JM, Gardener BBM, Thomashow LS (2002) Microbial populations responsible for specific soil suppressiveness to plant pathogens. Annual review of phytopathology **40:** 309-348

Wendehenne D, Lamotte O, Frachisse J-M, Barbier-Brygoo H, Pugin A (2002) Nitrate efflux is an essential component of the cryptogein signaling pathway leading to defense responses and hypersensitive cell death in tobacco. The Plant Cell **14:** 1937-1951

Whippo CW, Hangarter RP (2005) A brassinosteroid-hypersensitive mutant of BAK1 indicates that a convergence of photomorphogenic and hormonal signaling modulates phototropism. Plant Physiology **139:** 448-457

Wieczorek TM, Berg G, Semaškienė R, Mehl A, Sierotzki H, Stammler G, Justesen AF, Jørgensen LN (2015) Impact of DMI and SDHI fungicides on disease control and CYP51 mutations in populations of Zymoseptoria tritici from Northern Europe. European Journal of Plant Pathology **143:** 861-871

Willmann R, Lajunen HM, Erbs G, Newman MA, Kolb D, Tsuda K, Katagiri F, Fliegmann J, Bono JJ, Cullimore JV, Jehle AK, Gotz F, Kulik A, Molinaro A, Lipka V, Gust AA, Nürnberger T (2011) Arabidopsis lysin-motif proteins LYM1 LYM3 CERK1 mediate bacterial peptidoglycan sensing and immunity to bacterial infection. Proc Natl Acad Sci U S A **108:** 19824-19829

Xiao Y, Stegmann M, Han Z, DeFalco TA, Parys K, Xu L, Belkhadir Y, Zipfel C, Chai J (2019) Mechanisms of RALF peptide perception by a heterotypic receptor complex. Nature **572:** 270-274

Xue DX, Li CL, Xie ZP, Staehelin C (2019) LYK4 is a component of a tripartite chitin receptor complex in Arabidopsis thaliana. Journal of Experimental Botany **70:** 5507-5516

Yamaguchi Y, Huffaker A (2011) Endogenous peptide elicitors in higher plants. Current opinion in plant biology **14:** 351-357

Yamaguchi Y, Huffaker A, Bryan AC, Tax FE, Ryan CA (2010) PEPR2 is a second receptor for the Pep1 and Pep2 peptides and contributes to defense responses in Arabidopsis. The Plant Cell **22:** 508-522

Yamaguchi Y, Pearce G, Ryan CA (2006) The cell surface leucine-rich repeat receptor for AtPep1, an endogenous peptide elicitor in Arabidopsis, is functional in transgenic tobacco cells. Proceedings of the National Academy of Sciences **103:** 10104-10109

Zhang J, Zhou J-M (2010) Plant immunity triggered by microbial molecular signatures. Molecular Plant **3:** 783-793

Zhang L, Kars I, Essenstam B, Liebrand TW, Wagemakers L, Elberse J, Tagkalaki P, Tjoitang D, van den Ackerveken G, van Kan JA (2014) Fungal endopolygalacturonases are recognized as microbe-associated molecular patterns by the Arabidopsis receptor-like protein RESPONSIVENESS TO BOTRYTIS POLYGALACTURONASES1. Plant Physiology **164:** 352-364

Zhang LX, Foxman B, Gilsdorf JR, Marrs CF (2005) Bacterial genomic DNA isolation using sonication for microarray analysis. Biotechniques **39:** 640-+

Zhang W, Fraiture M, Kolb D, Loffelhardt B, Desaki Y, Boutrot FF, Tor M, Zipfel C, Gust AA, Brunner F (2013) Arabidopsis receptor-like protein30 and receptor-like kinase suppressor of BIR1-1/EVERSHED mediate innate immunity to necrotrophic fungi. Plant Cell **25:** 4227-4241

Zhang W, Fraiture M, Kolb D, Löffelhardt B, Desaki Y, Boutrot FF, Tör M, Zipfel C, Gust AA, Brunner F (2013) Arabidopsis receptor-like protein30 and receptor-like kinase suppressor of BIR1-1/EVERSHED mediate innate immunity to necrotrophic fungi. The Plant Cell **25:** 4227-4241

Zheng X-y, Zhou M, Yoo H, Pruneda-Paz JL, Spivey NW, Kay SA, Dong X (2015) Spatial and temporal regulation of biosynthesis of the plant immune signal salicylic acid. Proceedings of the National Academy of Sciences **112:** 9166-9173

Zimmermann S, Nürnberger T, Frachisse JM, Wirtz W, Guern J, Hedrich R, Scheel D (1997) Receptor-mediated activation of a plant Ca2+-permeable ion channel involved in pathogen defense. Proc Natl Acad Sci U S A **94:** 2751-2755

Zipfel C, Felix G (2005) Plants and animals: a different taste for microbes? Current opinion in plant biology **8:** 353-360

Zipfel C, Kunze G, Chinchilla D, Caniard A, Jones JD, Boller T, Felix G (2006) Perception of the bacterial PAMP EF-Tu by the receptor EFR restricts Agrobacterium-mediated transformation. Cell **125:** 749-760

Zipfel C, Robatzek S, Navarro L, Oakeley EJ, Jones JD, Felix G, Boller T (2004) Bacterial disease resistance in Arabidopsis through flagellin perception. Nature **428:** 764-767